CHAPTER

10

Mass Transfer

Mass transfer occurs in mixtures containing concentration variations. For example, when dye is dropped into a pail of water, mass transfer processes are responsible for the movement of dye molecules through the water until equilibrium is established and the concentration is uniform. Mass is transferred from one location to another under the influence of a concentration difference or concentration gradient in the system. There are many situations in bioprocessing where the concentrations of compounds are not uniform; we rely on mechanisms of mass transfer to transport material from regions of high concentration to regions where the concentration is initially low.

An important example of mass transfer in bioprocessing is the supply of oxygen in fermenters for aerobic culture. The concentration of oxygen at the surface of air bubbles is high compared with that in the bulk of the liquid; this concentration gradient promotes oxygen transfer from the bubbles into the medium. Another example is the extraction of penicillin from fermentation liquor using organic solvents such as butyl acetate. When solvent is added to the broth, the relatively high concentration of penicillin in the aqueous phase and low concentration in the organic phase causes mass transfer of penicillin into the solvent. Solvent extraction is an effective downstream processing technique because it selectively removes the desired product from the fermentation fluid.

Mass transfer plays a vital role in many reaction systems. As the distance between the reactants and the site of reaction becomes greater, the rate of mass transfer is more likely to influence or control the conversion rate. Taking again the example of oxygen in aerobic cultures, if mass transfer of oxygen from the bubbles is slow, the rate of cell metabolism will become dependent on the rate of oxygen supply from the gas phase. Because oxygen is a critical component of aerobic fermentations and is so sparingly soluble in aqueous solutions, much of our interest in mass transfer lies with the transfer of oxygen across gas–liquid interfaces. However, liquid–solid mass transfer can also be important in systems containing clumps, pellets, flocs, or films of cells or enzymes. In these cases, nutrients

in the liquid phase must be transported into the solid before they can be utilised in reaction. Unless mass transfer is rapid, the supply of nutrients will limit the rate of biological conversion.

In solids and quiescent fluids, mass transfer occurs as a result of molecular diffusion. However, most mass transfer systems contain moving fluid so that mass transfer by molecular motion is supplemented by convective transfer. There is an enormous variety of circumstances in which convective mass transfer takes place. In this chapter, we will consider the theory of mass transfer with applications relevant to bioprocessing.

10.1 MOLECULAR DIFFUSION

Molecular diffusion is the movement of component molecules in a mixture under the influence of a concentration difference in the system. Diffusion of molecules occurs in the direction required to destroy the concentration gradient, that is, from regions of high concentration to regions of low concentration. If the gradient is maintained by constantly supplying material to the region of high concentration and removing it from the region of low concentration, diffusion will be continuous. This situation is often exploited in mass transfer operations and reaction systems.

10.1.1 Diffusion Theory

In this text, we confine our discussion of diffusion to *binary mixtures*—that is, mixtures or solutions containing only two components. Consider a closed system containing molecular components A and B. Initially, the concentration of A in the system is not uniform; as indicated in Figure 10.1, concentration C_A varies from C_{A1} to C_{A2} as a function of distance

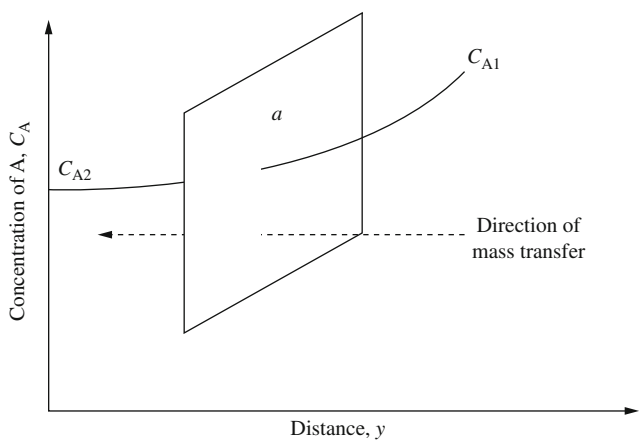

FIGURE 10.1 Concentration gradient of component A inducing mass transfer across area a.

y. In response to this concentration gradient, molecules of A will diffuse away from the region of high concentration until eventually the whole system acquires uniform composition. If there is no large-scale fluid motion in the system (e.g., due to stirring), mixing occurs solely by molecular movement.

Assume that mass transfer of A occurs across area a perpendicular to the direction of diffusion. In single-phase systems, the rate of mass transfer due to molecular diffusion is given by *Fick's law of diffusion*, which states that the mass flux is proportional to the concentration gradient:

$$J_A = \frac{N_A}{a} = -\mathscr{D}_{AB}\frac{dC_A}{dy} \tag{10.1}$$

In Eq. (10.1), J_A is the *mass flux* of component A, N_A is the *rate of mass transfer* of component A, a is the area across which mass transfer occurs, $\mathscr{D}_{AB}$ is the *binary diffusion coefficient* or *diffusivity* of component A in a mixture of A and B, C_A is the concentration of component A, and y is distance. dC_A/dy is the *concentration gradient*, or change in concentration of A with distance.

As indicated in Eq. (10.1), mass flux is defined as the rate of mass transfer per unit area perpendicular to the direction of movement; typical units for J_A are gmol $s^{-1}\,m^{-2}$. Corresponding units for N_A are gmol s^{-1}, for C_A gmol m^{-3}, and for $\mathscr{D}_{AB}$ $m^2\,s^{-1}$. Mass rather than mole units may be used for J_A, N_A, and C_A; Eq. (10.1) holds in either case. Equation (10.1) indicates that the rate of diffusion can be enhanced by increasing the area available for mass transfer, the concentration gradient in the system, or the magnitude of the diffusion coefficient. The negative sign in Eq. (10.1) indicates that the direction of mass transfer is always from high concentration to low concentration, opposite to the direction of the concentration gradient. In other words, if the slope of C_A versus y is positive as in Figure 10.1, the direction of mass transfer is in the negative y-direction, and vice versa.

The diffusion coefficient $\mathscr{D}_{AB}$ is a property of materials. Values can be found in handbooks. $\mathscr{D}_{AB}$ reflects the ease with which diffusion takes place. Its value depends on both components of the mixture; for example, the diffusivity of carbon dioxide in water will be different from the diffusivity of carbon dioxide in another solvent such as ethanol. The value of $\mathscr{D}_{AB}$ is also dependent on temperature. The diffusivity of gases varies with pressure; for liquids there is an approximate linear dependence on concentration. Diffusivities are several orders of magnitude smaller for diffusion in liquids than in gases. For example, $\mathscr{D}_{AB}$ for oxygen in air at 25°C and 1 atm is $2.1 \times 10^{-5}\,m^2\,s^{-1}$, whereas $\mathscr{D}_{AB}$ for oxygen in water at 25°C and 1 atm is $2.5 \times 10^{-9}\,m^2\,s^{-1}$. For dilute concentrations of glucose in water at 25°C, $\mathscr{D}_{AB}$ is $6.9 \times 10^{-10}\,m^2\,s^{-1}$.

When diffusivity values are not available for the materials, temperature, or pressure of interest, $\mathscr{D}_{AB}$ can be estimated using equations. Relationships for calculating diffusivities are available from other references [1–3]. The theory of diffusion in liquids is not as well advanced as diffusion in gases; there are also fewer experimental data available for liquid systems.

10.1.2 Analogy between Mass, Heat, and Momentum Transfer

There is a close similarity between the processes of mass, heat, and momentum transfer occurring as a result of molecular motion. This is suggested by the form of the equations for mass, heat, and momentum fluxes:

$$J_A = -\mathscr{D}_{AB}\frac{dC_A}{dy} \tag{10.2}$$

$$\hat{q} = -k\frac{dT}{dy} \tag{9.2}$$

and

$$\tau = -\mu\frac{dv}{dy} \tag{7.6}$$

The three processes represented above are quite different at the molecular level, but the basic equations have the same form. In each case, flux in the y-direction is directly proportional to the driving force (either dC_A/dy, dT/dy, or dv/dy), with the proportionality constant ($\mathscr{D}_{AB}$, k, or μ) a physical property of the material. The negative signs in Eqs. (10.2), (9.2), and (7.6) indicate that transfer of mass, heat, or momentum is always in the direction opposite to that of increasing concentration, temperature, or velocity. The similarity in the form of the three rate equations makes it possible in some situations to apply an analysis of one process to either of the other two.

The analogy of Eqs. (10.2), (9.2), and (7.6) is valid for transport of mass, heat, and momentum resulting from motion or vibration of molecules. Extension of the analogy to turbulent flow is generally valid for heat and mass transfer; however the analogy with momentum transfer presents a number of difficulties. Several analogy theories have been proposed in the chemical engineering literature to describe simultaneous transport phenomena in turbulent systems. Details are presented elsewhere [3, 4].

10.2 ROLE OF DIFFUSION IN BIOPROCESSING

Fluid mixing is carried out in most industrial processes where mass transfer takes place. Bulk fluid motion results in more rapid large-scale mixing than does molecular diffusion: why then is diffusive transport still important? These are some areas of bioprocessing where diffusion plays a major role.

- *Scale of mixing*. As discussed in Section 8.9, turbulence in fluids produces bulk mixing on a scale equal to the smallest eddy size. Within the smallest eddies, flow is largely streamline so that further mixing must occur by diffusion of the fluid components. Mixing on a molecular scale therefore relies on diffusion as the final step in the mixing process.
- *Solid-phase reaction*. In biological systems, reactions are sometimes mediated by catalysts in solid form (e.g., clumps, flocs, and films of cells) and by immobilised enzyme and cell particles. When cells or enzymes are clumped together into a solid particle,

substrates must be transported into the solid before reaction can take place. Mass transfer within solid particles is usually unassisted by bulk fluid convection; therefore, the only mechanism for intraparticle mass transfer is molecular diffusion. As the reaction proceeds, diffusion is also responsible for the removal of product molecules away from the site of reaction. As discussed more fully in Chapter 13, when reaction is coupled with diffusion, the overall reaction rate can be reduced significantly if diffusion is slow.

- *Mass transfer across phase boundaries*. Mass transfer between phases occurs often in bioprocessing. Oxygen transfer from gas bubbles to fermentation broth, penicillin recovery from aqueous to organic liquid, and glucose uptake from liquid medium into mould pellets are typical examples. When different phases come into contact, the fluid velocity near the phase interface is decreased significantly and diffusion becomes crucial for mass transfer. This is discussed further in the next section.

10.3 FILM THEORY

The *two-film theory* is a useful model for mass transfer between phases. Mass transfer of solute from one phase to another involves transport from the bulk of one phase to the *phase boundary* or *interface*, then movement from the interface into the bulk of the second phase. The film theory is based on the idea that a fluid film or *mass transfer boundary layer* forms wherever there is contact between two phases.

Let us consider mass transfer of component A across the phase boundary represented in Figure 10.2. Assume that the phases are two immiscible liquids such as water and chloroform, and that A is initially at higher concentration in the aqueous phase than in the

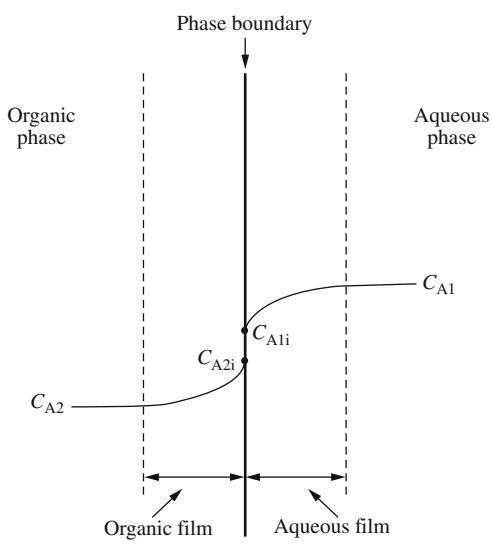

FIGURE 10.2 Film resistance to mass transfer between two immiscible liquids.

organic phase. Each phase is well mixed and in turbulent flow. The concentration of A in the bulk aqueous phase is C_{A1}; the concentration of A in the bulk organic phase is C_{A2}.

According to the film theory, turbulence in each fluid dies out at the phase boundary. A thin film of relatively stagnant fluid exists on either side of the interface; mass transfer through this film is effected solely by molecular diffusion. The concentration of A changes near the interface as indicated in Figure 10.2; C_{A1i} is the interfacial concentration of A in the aqueous phase; C_{A2i} is the interfacial concentration of A in the organic phase. Most of the resistance to mass transfer resides in the liquid films rather than in the bulk liquid. For practical purposes it is generally assumed that there is negligible resistance to transport at the interface itself; this is equivalent to assuming that the phases are in equilibrium at the plane of contact. The difference between C_{A1i} and C_{A2i} at the interface accounts for the possibility that, at equilibrium, A may be more soluble in one phase than in the other. For example, if A were acetic acid in contact at the interface with both water and chloroform, the equilibrium concentration in water would be greater than in chloroform by a factor of between 5 and 10. C_{A1i} would then be significantly higher than C_{A2i}.

Even though the bulk liquids in Figure 10.2 may be well mixed, diffusion of component A is crucial for mass transfer because the local fluid velocities approach zero at the interface. The film theory as described above is applied extensively in analysis of mass transfer, although it is a greatly simplified representation. There are other models of mass transfer in fluids that lead to more realistic mathematical outcomes than the film theory [1, 4]. Nevertheless, irrespective of how mass transfer is visualised, diffusion is always an important mechanism of mass transfer close to the interface between fluids.

10.4 CONVECTIVE MASS TRANSFER

The term *convective mass transfer* refers to mass transfer occurring in the presence of bulk fluid motion. Molecular diffusion will occur whenever there is a concentration gradient; however if the bulk fluid is also moving, the overall rate of mass transfer will be higher due to the contribution of convective currents. Analysis of mass transfer is most important in multiphase systems where interfacial boundary layers provide significant mass transfer resistance. Let us develop an expression for the rate of mass transfer that is applicable to mass transfer boundary layers.

The rate of mass transfer is directly proportional to the area available for transfer and the driving force for the transfer process. This can be expressed as:

$$\text{Transfer rate} \propto \text{transfer area} \times \text{driving force} \tag{10.3}$$

The proportionality coefficient in this equation is called the *mass transfer coefficient*, so that:

$$\text{Transfer rate} = \text{mass transfer coefficient} \times \text{transfer area} \times \text{driving force} \tag{10.4}$$

For each fluid at a phase boundary, the driving force for mass transfer of component A through the boundary layer can be expressed in terms of the concentration difference of

A across the fluid film. Therefore, the rate of mass transfer from the bulk fluid through the boundary layer to the interface is:

$$N_A = ka\,\Delta C_A = ka\,(C_{Ab} - C_{Ai}) \tag{10.5}$$

where N_A is the rate of mass transfer of component A, k is the mass transfer coefficient, a is the area available for mass transfer, C_{Ab} is the bulk concentration of component A away from the phase boundary, and C_{Ai} is the concentration of A at the interface. Equation (10.5) is usually used to represent the *volumetric rate of mass transfer*, so units of N_A are, for example, gmol $m^{-3}\,s^{-1}$.

Consistent with this representation, a is the interfacial area per unit volume with dimensions L^{-1} and units of, for example, $m^2\,m^{-3}$ or m^{-1}. The dimensions of the mass transfer coefficient k are LT^{-1}; the SI units for k are m s^{-1}. Equation (10.5) indicates that the rate of convective mass transfer can be enhanced by increasing the area available for mass transfer, the concentration difference between the bulk fluid and the interface, and the magnitude of the mass transfer coefficient. By analogy with Eq. (9.11) for heat transfer, Eq. (10.5) can also be written in the form:

$$N_A = \frac{\Delta C_A}{R_m} \tag{10.6}$$

where R_m is the resistance to mass transfer:

$$R_m = \frac{1}{k\,a} \tag{10.7}$$

Mass transfer coupled with fluid flow is a more complicated process than diffusive mass transfer. The value of the mass transfer coefficient k reflects the contribution to mass transfer from all the processes in the system that influence the boundary layer. Like the heat transfer coefficient in Chapter 9, k depends on the combined effects of the flow velocity, the geometry of the mass transfer system, and fluid properties such as viscosity and diffusivity. Because the hydrodynamics of most practical systems are not easily characterised, k cannot be calculated reliably from first principles. Instead, it is measured experimentally or estimated using correlations available from the literature. In general, reducing the thickness of the boundary layer or increasing the diffusion coefficient in the film will enhance the value of k, thus improving the rate of mass transfer.

In bioprocessing, three mass transfer situations that involve multiple phases are *liquid–solid mass transfer*, *liquid–liquid mass transfer* between immiscible solutions, and *gas–liquid mass transfer*. Use of Eq. (10.5) to determine the rate of mass transfer in these systems is discussed in the following sections.

10.4.1 Liquid–Solid Mass Transfer

Mass transfer between a moving liquid and a solid is important in biological processing in a variety of applications. Transport of substrates to solid-phase cell or enzyme catalysts has already been mentioned. Adsorption of molecules onto surfaces, such as in chromatography, requires transport from the liquid phase to a solid; liquid–solid mass transfer is

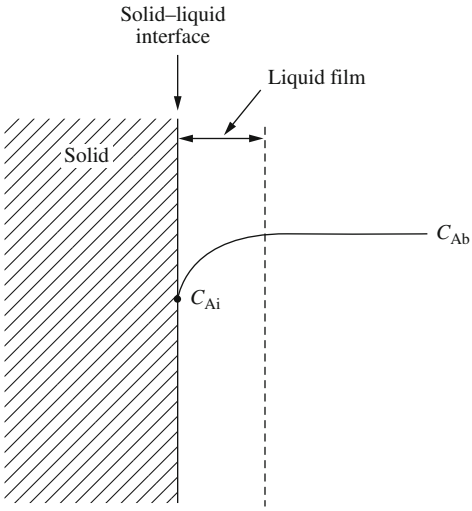

FIGURE 10.3 Concentration gradient for liquid–solid mass transfer.

also important in crystallisation as molecules move from the liquid to the face of the growing crystal. Conversely, the process of dissolving a solid in liquid requires liquid–solid mass transfer directed away from the solid surface.

Let us assume that component A is required for reaction at the surface of a solid. The situation at the interface between flowing liquid containing A and the solid is illustrated in Figure 10.3. Near the interface, the fluid velocity is reduced and a boundary layer develops. As A is consumed by reaction at the surface, the local concentration of A decreases and a concentration gradient is established through the film. The concentration difference between the bulk liquid and the phase interface drives mass transfer of A from the liquid to the solid, allowing the reaction to continue. If the solid is nonporous, A does not penetrate further than the surface. The concentration of A at the phase boundary is C_{Ai}; the concentration of A in the bulk liquid outside the film is C_{Ab}. If a is the liquid–solid interfacial area per unit volume, the volumetric rate of mass transfer can be determined from Eq. (10.5) as:

$$N_A = k_L a (C_{Ab} - C_{Ai}) \tag{10.8}$$

where k_L is the *liquid-phase mass transfer coefficient*.

Application of Eq. (10.8) requires knowledge of the mass transfer coefficient, the interfacial area between the phases, the bulk concentration of A, and the concentration of A at the interface. The value of the mass transfer coefficient is either measured or calculated using published correlations. In most cases, the area a can be determined from the shape and size of the solid. Bulk concentrations are generally easy to measure; however, estimation of the interfacial concentration C_{Ai} is much more difficult, as measuring compositions at phase boundaries is not straightforward experimentally. To overcome this problem, we must consider the processes in the system that occur in conjunction with mass transfer. In

the example of Figure 10.3, transport of A is linked to reaction at the surface of the solid, so C_{Ai} will depend on the rate of consumption of A at the interface. In practice, we can calculate the rate of mass transfer of A in this situation only if we have information about the rate of reaction at the solid surface. Simultaneous reaction and mass transfer occur in many bioprocesses as outlined in more detail in Chapter 13.

10.4.2 Liquid–Liquid Mass Transfer

Liquid–liquid mass transfer between immiscible solvents is most often encountered in the product recovery stages of bioprocessing. Organic solvents are used to isolate antibiotics, steroids, and alkaloids from fermentation broths; two-phase aqueous systems are useful for protein purification. Liquid–liquid mass transfer is also important when hydrocarbons are used as substrates in fermentation, for example, to produce microbial biomass for single-cell protein. Water-immiscible organic solvents are of increasing interest for enzyme and whole-cell biocatalysis: two-phase reaction systems can be used to overcome problems with poor substrate solubility and product toxicity, and can shift chemical equilibria for enhanced yields and selectivity in metabolic reactions.

The situation at the interface between two immiscible liquids is shown in Figure 10.2. Component A is present at bulk concentration C_{A1} in one phase; this concentration falls to C_{A1i} at the interface. In the other liquid, the concentration of A falls from C_{A2i} at the interface to C_{A2} in the bulk. The rate of mass transfer N_A in each liquid phase is expressed using Eq. (10.5):

$$N_{A1} = k_{L1}\, a\, (C_{A1} - C_{A1i}) \tag{10.9}$$

and

$$N_{A2} = k_{L2}\, a\, (C_{A2i} - C_{A2}) \tag{10.10}$$

where k_L is the liquid-phase mass transfer coefficient, and subscripts 1 and 2 refer to the two liquid phases. Application of Eqs. (10.9) and (10.10) is difficult because interfacial concentrations are not measured easily, as mentioned in Section 10.4.1. However, in this case, C_{A1i} and C_{A2i} can be eliminated by considering the physical situation at the interface and manipulating the equations.

First, let us recognise that at steady state, because there can be no accumulation of A at the interface or anywhere else in the system, any A transported through liquid 1 must also be transported through liquid 2. This means that N_{A1} in Eq. (10.9) must be equal to N_{A2} in Eq. (10.10) so that $N_{A1} = N_{A2} = N_A$. We can then rearrange Eqs. (10.9) and (10.10):

$$\frac{N_A}{k_{L1}\, a} = C_{A1} - C_{A1i} \tag{10.11}$$

and

$$\frac{N_A}{k_{L2}\, a} = C_{A2i} - C_{A2} \tag{10.12}$$

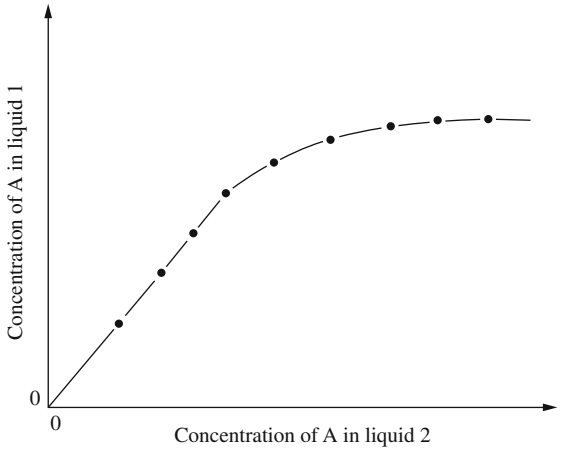

FIGURE 10.4 Equilibrium curve for solute A in two immiscible solvents 1 and 2.

Normally, it can be assumed that there is negligible resistance to mass transfer at the actual interface—that is, within distances corresponding to molecular free paths on either side of the phase boundary. This is equivalent to assuming that the phases are in equilibrium *at the interface*; therefore, C_{A1i} and C_{A2i} are equilibrium concentrations.

The assumption of phase-boundary equilibrium has been subjected to many tests. As a result, it is known that there are special circumstances, such as when there is adsorption of material at the interface, for which the assumption is invalid. However, in ordinary situations, the evidence is that equilibrium does exist at the interface between phases. Note that we are not proposing to relate bulk concentrations C_{A1} and C_{A2} using equilibrium relationships, only C_{A1i} and C_{A2i}. If the bulk liquids were in equilibrium, no net mass transfer would take place.

A typical equilibrium curve relating the concentrations of solute A in two immiscible liquid phases is shown in Figure 10.4. The points making up the curve are obtained readily from experiments; alternatively, equilibrium data can be found in handbooks. The equilibrium distribution of one solute between two phases can be described using the *distribution law*. At equilibrium, the ratio of the solute concentrations in the two phases is equal to the *distribution coefficient* or *partition coefficient*, m. As shown in Figure 10.4, when the concentration of A is low, the equilibrium curve is approximately a straight line so that m is constant. The distribution law is accurate only if both solvents are immiscible and there is no chemical reaction.

If C_{A1i} and C_{A2i} are equilibrium concentrations, they can be related using the distribution coefficient m:

$$m = \frac{C_{A1i}}{C_{A2i}} \tag{10.13}$$

such that

$$C_{A1i} = m\, C_{A2i} \tag{10.14}$$

and

$$C_{A2i} = \frac{C_{A1i}}{m} \tag{10.15}$$

Equations (10.14) and (10.15) can now be used to eliminate the interfacial concentrations from Eqs. (10.11) and (10.12). First, we make a direct substitution:

$$\frac{N_A}{k_{L1}\,a} = C_{A1} - m\,C_{A2i} \tag{10.16}$$

and

$$\frac{N_A}{k_{L2}\,a} = \frac{C_{A1i}}{m} - C_{A2} \tag{10.17}$$

If we now multiply Eq. (10.12) by m:

$$\frac{m\,N_A}{k_{L2}\,a} = m\,C_{A2i} - m\,C_{A2} \tag{10.18}$$

and divide Eq. (10.11) by m:

$$\frac{N_A}{m\,k_{L1}\,a} = \frac{C_{A1}}{m} - \frac{C_{A1i}}{m} \tag{10.19}$$

and add Eq. (10.16) to Eq. (10.18), and Eq. (10.17) to Eq. (10.19), we eliminate the interfacial concentration terms completely:

$$N_A\left(\frac{1}{k_{L1}\,a} + \frac{m}{k_{L2}\,a}\right) = C_{A1} - m\,C_{A2} \tag{10.20}$$

$$N_A\left(\frac{1}{m\,k_{L1}\,a} + \frac{1}{k_{L2}\,a}\right) = \frac{C_{A1}}{m} - C_{A2} \tag{10.21}$$

Equations (10.20) and (10.21) combine the mass transfer resistances in the two liquid films, and relate the rate of mass transfer N_A to the bulk fluid concentrations C_{A1} and C_{A2}. The bracketed expressions for the combined mass transfer coefficients are used to define the *overall liquid-phase mass transfer coefficient*, K_L. Depending on the terms used to represent the concentration difference, we can define two overall mass transfer coefficients:

$$\frac{1}{K_{L1}\,a} = \frac{1}{k_{L1}\,a} + \frac{m}{k_{L2}\,a} \tag{10.22}$$

and

$$\frac{1}{K_{L2}\,a} = \frac{1}{m\,k_{L1}\,a} + \frac{1}{k_{L2}\,a} \tag{10.23}$$

where K_{L1} is the overall mass transfer coefficient based on the bulk concentration in liquid 1, and K_{L2} is the overall mass transfer coefficient based on the bulk concentration in liquid 2.

We can now summarise the results to obtain two equations for the mass transfer rate at the interfacial boundary in liquid–liquid systems:

$$N_A = K_{L1}\,a\,(C_{A1} - m\,C_{A2}) \tag{10.24}$$

and

$$N_A = K_{L2}\,a\left(\frac{C_{A1}}{m} - C_{A2}\right) \tag{10.25}$$

where K_{L1} and K_{L2} are given by Eqs. (10.22) and (10.23). Use of either of these two equations requires knowledge of the concentrations of A in the bulk fluids, the partition coefficient m, the interfacial area a between the two liquid phases, and the value of either K_{L1} or K_{L2}. C_{A1} and C_{A2} are generally easy to measure. m can also be measured or is found in handbooks of physical properties. The overall mass transfer coefficients can be measured experimentally or are estimated from published correlations for k_{L1} and k_{L2} in the literature. The only remaining parameter is the interfacial area, a. In many applications of liquid–liquid mass transfer, it may be difficult to know how much interfacial area is available between the phases. For example, liquid–liquid extraction is often carried out in stirred tanks where an impeller is used to disperse and mix droplets of one phase through the other. The interfacial area in these circumstances will depend on the size, shape, and number of the droplets, which depend in turn on the intensity of agitation and properties of the fluid. Because these factors also affect the value of k_L, correlations for mass transfer coefficients in liquid–liquid systems are often given in terms of k_La as a combined parameter. For convenience, the combined term k_La is then referred to as the mass transfer coefficient.

Equations (10.24) and (10.25) indicate that the rate of mass transfer between two liquid phases is not dependent simply on the concentration difference: the equilibrium relationship is also an important factor. According to Eq. (10.24), the driving force for transfer of A from liquid 1 to liquid 2 is the difference between the bulk concentration C_{A1} and *the concentration of A in liquid 1 that would be in equilibrium with bulk concentration* C_{A2} *in liquid 2*. Similarly, the driving force for mass transfer according to Eq. (10.25) is the difference between C_{A2} and the concentration of A in liquid 2 that would be in equilibrium with C_{A1} in liquid 1.

10.4.3 Gas–Liquid Mass Transfer

Gas–liquid mass transfer is of great importance in bioprocessing because of the requirement for oxygen in aerobic cell cultures. Transfer of a solute such as oxygen from gas to liquid is analysed in a similar way to that presented previously for liquid–solid and liquid–liquid mass transfer.

Figure 10.5 shows the situation at an interface between gas and liquid phases containing component A. Let us assume that A is transferred from the gas phase into the liquid. The concentration of A in the liquid is C_{AL} in the bulk and C_{ALi} at the interface. In the gas, the concentration is C_{AG} in the bulk and C_{AGi} at the interface.

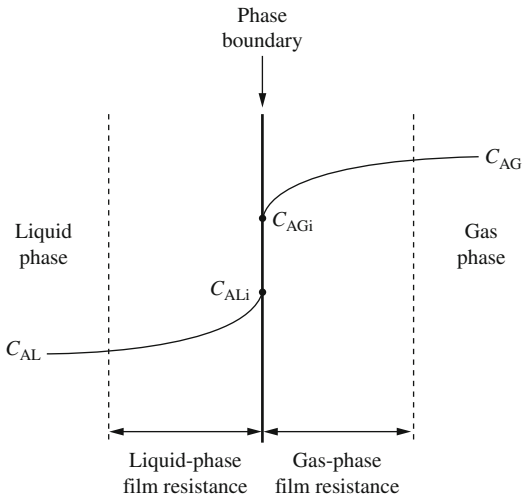

FIGURE 10.5 Concentration gradients for gas–liquid mass transfer.

From Eq. (10.5), the rate of mass transfer of A through the gas boundary layer is:

$$N_{AG} = k_G a (C_{AG} - C_{AGi}) \tag{10.26}$$

and the rate of mass transfer of A through the liquid boundary layer is:

$$N_{AL} = k_L a (C_{ALi} - C_{AL}) \tag{10.27}$$

where k_G is the gas-phase mass transfer coefficient and k_L is the liquid-phase mass transfer coefficient. To eliminate C_{AGi} and C_{ALi}, we must manipulate the equations as discussed in Section 10.4.2.

If we assume that equilibrium exists at the interface, C_{AGi} and C_{ALi} can be related. For dilute concentrations of most gases and for a wide range of concentration for some gases, the equilibrium concentration in the gas phase is a linear function of liquid concentration. Therefore, we can write:

$$C_{AGi} = m\, C_{ALi} \tag{10.28}$$

or, alternatively:

$$C_{ALi} = \frac{C_{AGi}}{m} \tag{10.29}$$

where m is the distribution factor. These equilibrium relationships can be incorporated into Eqs. (10.26) and (10.27) at steady state using procedures that parallel those applied already for liquid–liquid mass transfer. The results are also similar to Eqs. (10.20) and (10.21):

$$N_A \left(\frac{1}{k_G a} + \frac{m}{k_L a} \right) = C_{AG} - m\, C_{AL} \tag{10.30}$$

$$N_A\left(\frac{1}{m\,k_G\,a}+\frac{1}{k_L\,a}\right)=\frac{C_{AG}}{m}-C_{AL} \tag{10.31}$$

The combined mass transfer coefficients in Eqs. (10.30) and (10.31) can be used to define overall mass transfer coefficients. The *overall gas-phase mass transfer coefficient* K_G is defined by the equation:

$$\frac{1}{K_G\,a}=\frac{1}{k_G\,a}+\frac{m}{k_L\,a} \tag{10.32}$$

and the *overall liquid-phase mass transfer coefficient* K_L is defined as:

$$\frac{1}{K_L\,a}=\frac{1}{m\,k_G\,a}+\frac{1}{k_L\,a} \tag{10.33}$$

The rate of mass transfer in gas−liquid systems can therefore be expressed using either of two equations:

$$N_A=K_G\,a\,(C_{AG}-m\,C_{AL}) \tag{10.34}$$

or

$$N_A=K_L\,a\left(\frac{C_{AG}}{m}-C_{AL}\right) \tag{10.35}$$

Equations (10.34) and (10.35) are usually expressed using equilibrium concentrations. mC_{AL} is equal to C^*_{AG}, the gas-phase concentration of A in equilibrium with C_{AL}, and C_{AG}/m is equal to C^*_{AL}, the liquid-phase concentration of A in equilibrium with C_{AG}. Equations (10.34) and (10.35) become:

$$N_A=K_G\,a\,(C_{AG}-C^*_{AG}) \tag{10.36}$$

and

$$N_A=K_L\,a\,(C^*_{AL}-C_{AL}) \tag{10.37}$$

Equations (10.36) and (10.37) can be simplified for systems in which most of the resistance to mass transfer lies in either the gas-phase interfacial film or the liquid-phase interfacial film. When solute A is very soluble in the liquid, for example in transfer of ammonia to water, the liquid-side resistance is small compared with that posed by the gas interfacial film. From Eq. (10.7), if the liquid-side resistance is small, $k_L\,a$ must be relatively large. From Eq. (10.32), $K_G a$ is then approximately equal to $k_G a$. Using this result in Eq. (10.36) gives:

$$N_A=k_G\,a\,(C_{AG}-C^*_{AG}) \tag{10.38}$$

Conversely, if A is poorly soluble in the liquid (e.g., oxygen in aqueous solution), the liquid-phase mass transfer resistance dominates and $k_G a$ is much larger than $k_L a$. From

Eq. (10.33), this means that $K_L a$ is approximately equal to $k_L a$ and Eq. (10.37) can be simplified to:

$$N_A = k_L a (C^*_{AL} - C_{AL}) \tag{10.39}$$

Because gas–liquid oxygen transfer plays a crucial role in many bioprocesses, we will make further use of Eq. (10.39) in subsequent sections of this chapter. In practical applications, obtaining the values of C_{AL} and C^*_{AL} for use in Eq. (10.39) is reasonably straightforward. However, as described in relation to liquid–liquid mass transfer in Section 10.4.2, it is generally difficult to estimate the interfacial area a. When gas is sparged through a liquid, the interfacial area will depend on the size and number of bubbles present, which in turn depend on many other factors such as medium composition, stirrer speed, and gas flow rate. Because k_L is also affected by these parameters, k_L and a are usually combined together and the combined term $k_L a$ referred to as the mass transfer coefficient.

10.5 OXYGEN UPTAKE IN CELL CULTURES

Cells in aerobic culture take up oxygen from the liquid phase. The rate of oxygen transfer from gas to liquid is therefore of prime importance, especially in dense cell cultures where the demand for dissolved oxygen is high. An expression for the rate of oxygen transfer from gas to liquid is given by Eq. (10.39): N_A is the rate of oxygen transfer per unit volume of fluid (gmol m^{-3} s^{-1}), k_L is the liquid-phase mass transfer coefficient (m s^{-1}), a is the gas–liquid interfacial area per unit volume of fluid (m^2 m^{-3}), C_{AL} is the oxygen concentration in the broth (gmol m^{-3}), and C^*_{AL} is the oxygen concentration in the broth in equilibrium with the gas phase (gmol m^{-3}). The equilibrium concentration C^*_{AL} is also known as the *saturation concentration* or *solubility* of oxygen in the broth. C^*_{AL} represents the maximum possible oxygen concentration that can occur in the liquid under the prevailing gas-phase composition, temperature, and pressure. The difference ($C^*_{AL} - C_{AL}$) between the maximum possible and actual oxygen concentrations in the liquid represents the *concentration-difference driving force* for mass transfer.

The solubility of oxygen in aqueous solutions at ambient temperature and pressure is less than 10 ppm. This amount of oxygen is quickly consumed in aerobic cultures and must be replaced constantly by sparging. An actively respiring cell population can consume the entire oxygen content of a culture broth within a few seconds; therefore, the maximum amount of oxygen that can be dissolved in the medium must be transferred from the gas phase 10 to 15 times per minute. This is not an easy task because the low solubility of oxygen guarantees that the concentration difference ($C^*_{AL} - C_{AL}$) is always very small. Design of fermenters for aerobic culture must take these factors into account and provide optimum mass transfer conditions.

10.5.1 Factors Affecting Cellular Oxygen Demand

The rate at which oxygen is consumed by cells in fermenters determines the rate at which oxygen must be transferred from the gas phase to the liquid phase. Many factors

influence oxygen demand: the most important of these are cell species, culture growth phase, and the nature of the carbon source provided in the medium. In batch culture, the rate of oxygen uptake varies with time. The reasons for this are twofold. First, the concentration of cells increases during the course of batch culture and the total rate of oxygen uptake is proportional to the number of cells present. In addition, the rate of oxygen consumption per cell, known as the *specific oxygen uptake rate*, also varies, often reaching a maximum during the early stages of cell growth. If Q_O is the oxygen uptake rate per volume of broth and q_O is the specific oxygen uptake rate:

$$Q_O = q_O x \tag{10.40}$$

where x is cell concentration. Typical units for q_O are gmol $g^{-1}\,s^{-1}$, and for Q_O, gmol $l^{-1}\,s^{-1}$. Typical profiles of Q_O, q_O, and x during batch culture of microbial, plant, and animal cells are shown in Figure 10.6.

The inherent demand of an organism for oxygen (q_O) depends primarily on the biochemical nature of the cell and its nutritional environment. However, when the level of dissolved oxygen in the medium falls below a certain point, the specific rate of oxygen uptake is also dependent on the oxygen concentration in the liquid, C_{AL}. The dependence of q_O on C_{AL} is shown in Figure 10.7. If C_{AL} is above the *critical oxygen concentration* C_{crit}, q_O is a constant maximum and independent of C_{AL}. If C_{AL} is below C_{crit}, q_O is approximately linearly dependent on oxygen concentration.

To eliminate oxygen limitations and allow cell metabolism to function at its fastest, the dissolved oxygen concentration at every point in the fermenter must be above C_{crit}. The exact value of C_{crit} depends on the organism, but usually falls between 5% and 10% of air saturation under average operating conditions. For cells with relatively high C_{crit} levels, the task of transferring sufficient oxygen to maintain $C_{AL} > C_{crit}$ is more challenging than for cultures with low C_{crit} values.

The choice of substrate used in the fermentation medium can also affect the oxygen demand. Because glucose is generally consumed more rapidly than other sugars, rates of oxygen uptake are often higher when glucose is used. For example, maximum oxygen consumption rates of 5.5, 6.1, and 12 mmol $l^{-1}\,h^{-1}$ have been observed for *Penicillium* mould growing on lactose, sucrose, and glucose, respectively [5]. As discussed in Section 4.6, oxygen requirements for cell growth and product formation also depend on the degree of reduction of the substrate. From electron balance considerations, the specific oxygen demand is greater when carbon substrates with a high degree of reduction are used. Therefore, specific oxygen uptake rates tend to be higher in cultures growing on alcohol or alkane hydrocarbons compared with carbohydrates.

Typical maximum q_O and Q_O values observed during batch culture of various organisms are listed in Table 10.1. Although specific oxygen uptake rates depend on the medium and culture conditions, plant and animal cells generally have significantly lower oxygen requirements than microbial cells.

10.5.2 Oxygen Transfer from Gas Bubble to Cell

In aerobic cultures, oxygen molecules must overcome a series of transport resistances before being utilised by the cells. Eight mass transfer steps involved in transport of oxygen

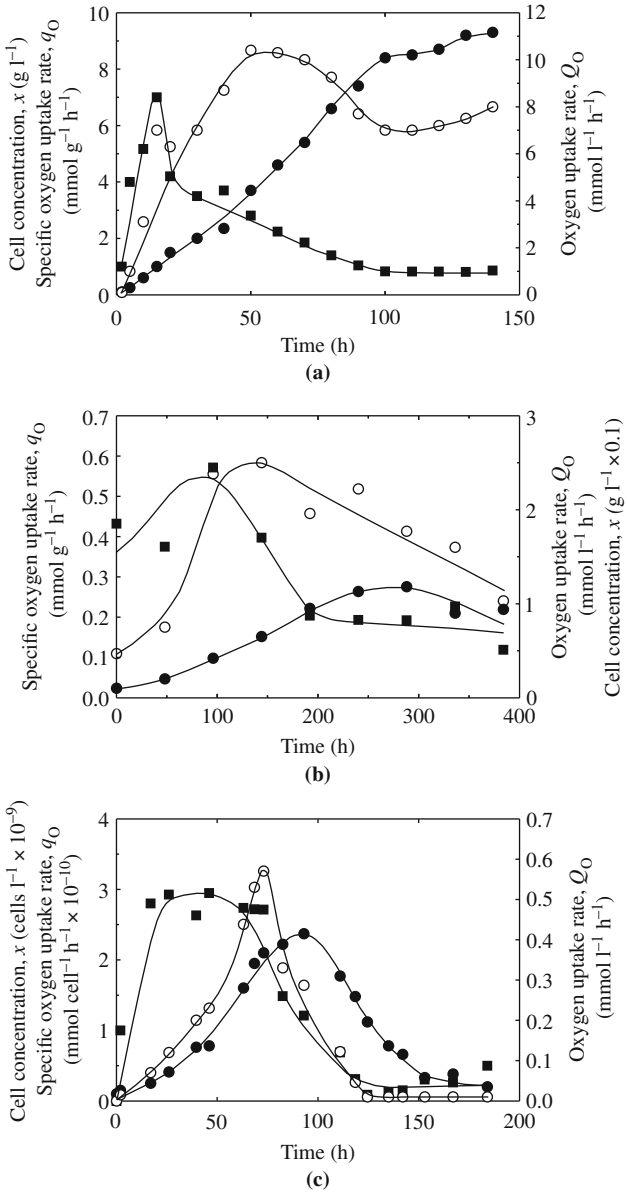

FIGURE 10.6 Variations in the oxygen uptake rate Q_O (○), the specific oxygen uptake rate q_O (■), and the cell concentration x (●) during batch culture of microbial, plant, and animal cells.
(a) Streptomyces aureofaciens. *Data from A.L. Jensen, J.S. Schultz, and P. Shu, 1966, Scale-up of antibiotic fermentations by control of oxygen utilization.* Biotechnol. Bioeng. *8, 525–537.*
(b) *Catharanthus roseus. Data from J.B. Snape, N.H. Thomas, and J.A. Callow, 1989, How suspension cultures of* Catharanthus roseus *respond to oxygen limitation: small-scale tests with applications to large-scale cultures.* Biotechnol. Bioeng. *34, 1058–1062.*
(c) Mouse–mouse hybridoma cells. *Data from S. Tatiraju, M. Soroush, and R. Mutharasan, 1999, Multi-rate nonlinear state and parameter estimation in a bioreactor.* Biotechnol. Bioeng. *63, 22–32.*

from the interior of gas bubbles to the site of intracellular reaction are represented diagrammatically in Figure 10.8. They are:

1. Transfer from the interior of the bubble to the gas–liquid interface
2. Movement across the gas–liquid interface
3. Diffusion through the relatively stagnant liquid film surrounding the bubble
4. Transport through the bulk liquid

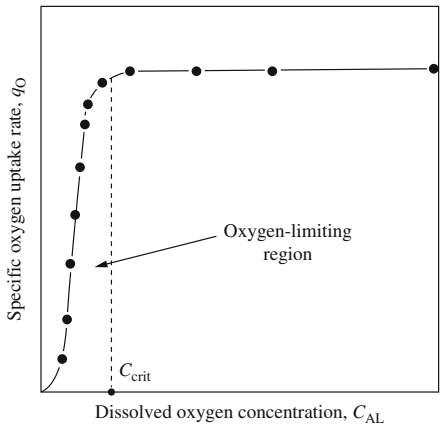

FIGURE 10.7 Relationship between the specific rate of oxygen consumption by cells and dissolved oxygen concentration.

TABLE 10.1 Typical Oxygen Uptake Rates in Different Cell Cultures

Type of cell culture	Carbon source	Maximum specific oxygen uptake rate, q_O (mmol g^{-1} dry weight h^{-1})	Maximum specific oxygen uptake rate, q_O (mmol $cell^{-1}$ h^{-1})	Maximum volumetric oxygen uptake rate, Q_O (mmol l^{-1} h^{-1})	Reference
MICROBIAL					
Aerobacter aerogenes	Peptone	–	3.2×10^{-11}	7.4	[6]
Aspergillus niger	Glucose	1.6	–	8.8	[7]
Bacillus subtilis	Peptone	–	1.5×10^{-10}	–	[8]
Beneckea natriegens	*n*-Propanol	12	–	6.0	[9]
Escherichia coli	Peptone	–	3.2×10^{-11}	5.0	[6]
Penicillium chrysogenum	Lactose	1.2	–	30	[10]
Saccharomyces cerevisiae	Ethanol	10	–	40	[11]
Streptomyces aureofaciens	Corn starch	7.0	–	10	[12]
Streptomyces coelicolor	Glucose	7.4	–	5.5	[13]
Streptomyces griseus	Meat extract	4.1	–	16	[14]
Xanthomonas campestris	Glucose	4.5	–	11	[15]
PLANT					
Catharanthus roseus	Sucrose	0.45	–	2.7	[16]
Nicotiana tabacum	Sucrose	0.90	–	1.0	[17]
ANIMAL					
Chinese hamster ovary (CHO)	Glucose/glutamine	–	2.9×10^{-10}	0.60	[18]
Hybridoma	Glucose/glutamine	–	2.9×10^{-10}	0.57	[19]

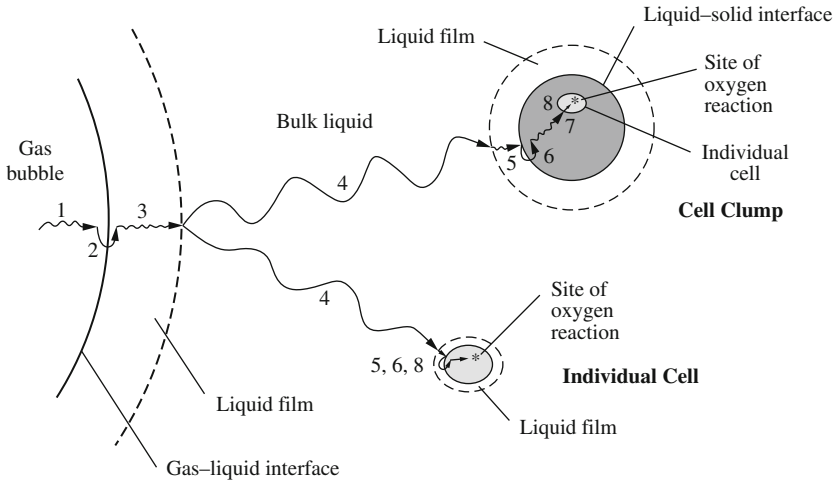

FIGURE 10.8 Steps for transfer of oxygen from gas bubble to cell.

5. Diffusion through the relatively stagnant liquid film surrounding the cells
6. Movement across the liquid–cell interface
7. If the cells are in a floc, clump, or solid particle, diffusion through the solid to the individual cell
8. Transport through the cytoplasm to the site of reaction

Note that resistance due to the gas boundary layer on the inside of the bubble has been neglected; because of the low solubility of oxygen in aqueous solutions, we can assume that the liquid-film resistance dominates gas–liquid mass transfer (see Section 10.4.3). If the cells are individually suspended in liquid rather than in a clump, step (7) disappears.

The relative magnitudes of the various mass transfer resistances depend on the composition and rheological properties of the liquid, the mixing intensity, the size of the bubbles, the size of any cell clumps, interfacial adsorption characteristics, and other factors. However, for most bioreactors the following analysis is valid.

1. Transfer through the bulk gas phase in the bubble is relatively fast.
2. The gas–liquid interface itself contributes negligible resistance.
3. The liquid film around the bubbles is a major resistance to oxygen transfer.
4. In a well-mixed fermenter, concentration gradients in the bulk liquid are minimised and mass transfer resistance in this region is small. However, rapid mixing can be difficult to achieve in viscous fermentation broths; if this is the case, oxygen transfer resistance in the bulk liquid may be important.
5. Because single cells are much smaller than gas bubbles, the liquid film surrounding each cell is much thinner than that around the bubbles. The effect of the cell liquid film on mass transfer can generally be neglected. On the other hand, if the cells form large clumps, the liquid-film resistance around the clumps can be significant.
6. Resistance at the liquid–cell interface is negligible.

7. When the cells are in clumps, intraparticle resistance is likely to be significant as oxygen has to diffuse through the solid pellet to reach the cells in the interior. The magnitude of this resistance depends on the size and properties of the cell clumps.
8. Intracellular oxygen transfer resistance is negligible because of the small distances involved.

When cells are dispersed in the liquid and the bulk fermentation broth is well mixed, *the major resistance to oxygen transfer is the liquid film surrounding the gas bubbles*. Transport through this film becomes the rate-limiting step in the complete process, and controls the overall mass transfer rate. Consequently, the rate of oxygen transfer from the bubbles all the way to the cells is dominated by the rate of step (3). The mass transfer rate for this step is represented by Eq. (10.39).

At steady state there can be no accumulation of oxygen at any location in the fermenter; therefore, the rate of oxygen transfer from the bubbles must be equal to the rate of oxygen consumption by the cells. If we make N_A in Eq. (10.39) equal to Q_O in Eq. (10.40) we obtain the following equation:

$$k_L a\,(C^*_{AL} - C_{AL}) = q_O\,x \tag{10.41}$$

The mass transfer coefficient $k_L a$ is used to characterise the oxygen transfer capability of fermenters. If $k_L a$ for a particular system is small, the ability of the reactor to deliver oxygen to the cells is limited. We can predict the response of the system to changes in mass transfer conditions using Eq. (10.41). For example, if the rate of cell metabolism remains unchanged but $k_L a$ is increased (e.g., by raising the stirrer speed to reduce the thickness of the boundary layer around the bubbles), the dissolved oxygen concentration C_{AL} must rise in order for the left side of Eq. (10.41) to remain equal to the right side. Similarly, if the rate of oxygen consumption by the cells accelerates while $k_L a$ is unaffected, C_{AL} must decrease.

We can use Eq. (10.41) to deduce some important relationships for fermenters. First, let us estimate the maximum cell concentration that can be supported by the fermenter's oxygen transfer system. For a given set of operating conditions, the maximum rate of oxygen transfer occurs when the concentration-difference driving force $(C^*_{AL} - C_{AL})$ is highest—that is, when the concentration of dissolved oxygen C_{AL} is zero. Therefore from Eq. (10.41), the maximum cell concentration that can be supported by oxygen transfer in the fermenter is:

$$x_{max} = \frac{k_L a\;\; C^*_{AL}}{q_O} \tag{10.42}$$

It is generally undesirable for cell density to be limited by the rate of mass transfer. Therefore, if x_{max} estimated using Eq. (10.42) is lower than the cell concentration required in the fermentation process, $k_L a$ must be improved. Note that the cell concentration in Eq. (10.42) is a theoretical maximum corresponding to operation of the system at its maximum oxygen transfer rate. Cell concentrations approaching x_{max} will be achieved only if all other culture conditions are favourable and if sufficient time and substrates are provided.

Comparison of x_{max} values evaluated using Eqs. (9.54) and (10.42) can be used to gauge the relative effectiveness of heat and mass transfer in aerobic fermentation. For example, if

x_{max} from Eq. (10.42) is small while x_{max} calculated from heat transfer considerations is large, we would know that mass transfer is more likely to limit biomass growth than heat transfer. If both x_{max} values are greater than that desired for the process, heat and mass transfer can be considered adequate.

Eq. (10.42) is a useful hypothetical relationship; however, as indicated in Figure 10.7, operation of culture systems at a dissolved oxygen concentration of zero is not advisable because the specific oxygen uptake rate depends on oxygen concentration. Accordingly, another important parameter is the minimum k_La required to maintain $C_{AL} > C_{crit}$ in the fermenter. This can be determined from Eq. (10.41) as:

$$(k_La)_{crit} = \frac{q_O x}{(C^*_{AL} - C_{crit})} \tag{10.43}$$

EXAMPLE 10.1 CELL CONCENTRATION IN AEROBIC CULTURE

A strain of *Azotobacter vinelandii* is cultured in a 15-m^3 stirred fermenter for alginate production. Under current operating conditions, k_La is 0.17 s^{-1}. The solubility of oxygen in the broth is approximately 8×10^{-3} kg m^{-3}.

(a) The specific rate of oxygen uptake is 12.5 mmol g^{-1} h^{-1}. What is the maximum cell concentration supported by oxygen transfer in the fermenter?

(b) The bacteria suffer growth inhibition after copper sulphate is accidentally added to the fermentation broth just after the start of the culture. This causes a reduction in the oxygen uptake rate to 3 mmol g^{-1} h^{-1}. What maximum cell concentration can now be supported by oxygen transfer in the fermenter?

Solution

(a) From Eq. (10.42):

$$x_{max} = \frac{0.17\ \text{s}^{-1}\,(8 \times 10^{-3}\ \text{kg m}^{-3})}{\dfrac{12.5\ \text{mmol}}{\text{g h}} \cdot \left|\dfrac{1\ \text{h}}{3600\ \text{s}}\right| \cdot \left|\dfrac{1\ \text{gmol}}{1000\ \text{mmol}}\right| \cdot \left|\dfrac{32\ \text{g}}{1\ \text{gmol}}\right| \cdot \left|\dfrac{1\ \text{kg}}{1000\ \text{g}}\right|}$$

$$x_{max} = 1.2 \times 10^4\ \text{g m}^{-3} = 12\ \text{g l}^{-1}$$

The maximum cell concentration supported by oxygen transfer in the fermenter is 12 g l^{-1}.

(b) Assume that addition of copper sulphate does not affect C^*_{AL} or k_La.

$$x_{max} = \frac{0.17\ \text{s}^{-1}\,(8 \times 10^{-3}\ \text{kg m}^{-3})}{\dfrac{3\ \text{mmol}}{\text{g h}} \cdot \left|\dfrac{1\ \text{h}}{3600\ \text{s}}\right| \cdot \left|\dfrac{1\ \text{gmol}}{1000\ \text{mmol}}\right| \cdot \left|\dfrac{32\ \text{g}}{1\ \text{gmol}}\right| \cdot \left|\dfrac{1\ \text{kg}}{1000\ \text{g}}\right|}$$

$$x_{max} = 5.0 \times 10^4\ \text{g m}^{-3} = 50\ \text{g l}^{-1}$$

The maximum cell concentration supported by oxygen transfer in the fermenter after addition of copper sulphate is 50 g l^{-1}.

To assess the oxygen transfer capability of a particular fermenter and for application of Eqs. (10.42) and (10.43), it is important that the actual $k_L a$ developed in the fermenter vessel be known. Methods for measuring $k_L a$ in bioprocesses are outlined in Section 10.10. Application of Eqs. (10.42) and (10.43) also requires knowledge of the oxygen solubility C^*_{AL} and the specific oxygen uptake rate q_O. Evaluation of these parameters is described in Sections 10.8 and 10.11.

10.6 FACTORS AFFECTING OXYGEN TRANSFER IN FERMENTERS

The rate of oxygen transfer in fermentation broths is influenced by several physical and chemical factors that change the value of k_L, the value of a, or the driving force for mass transfer ($C^*_{AL} - C_{AL}$). As a general rule of thumb, k_L in fermentation liquids is about 3 to 4×10^{-4} m s^{-1} for bubbles greater than 2 to 3 mm diameter; this can be reduced to 1×10^{-4} m s^{-1} for smaller bubbles depending on bubble rigidity. Once the bubbles are above 2 to 3 mm in size, k_L is relatively constant and insensitive to conditions. If substantial improvement in mass transfer rates is required, it is usually more productive to focus on increasing the interfacial area a. Operating values of the combined coefficient $k_L a$ span a wide range in bioreactors over about three orders of magnitude; this is due mainly to the large variation in a. In production-scale fermenters, the value of $k_L a$ is typically in the range 0.02 s^{-1} to 0.25 s^{-1}.

In this section, several aspects of fermenter design and operation are discussed in terms of their effect on oxygen mass transfer.

10.6.1 Bubbles

The efficiency of gas–liquid mass transfer depends to a large extent on the characteristics of the bubbles dispersed in the liquid medium. Bubble behaviour exerts a strong influence on the value of $k_L a$: some properties of bubbles affect mainly the magnitude of k_L, whereas others change the interfacial area a.

Large-scale aerobic cultures are carried out most commonly in stirred fermenters. In these vessels, oxygen is supplied to the medium by sparging swarms of air bubbles underneath the impeller. The action of the impeller then creates a dispersion of gas throughout the vessel. In small laboratory-scale fermenters, all of the liquid is close to the impeller; therefore, bubbles in these systems are subjected frequently to severe distortions as they interact with turbulent liquid currents in the vessel. In contrast, bubbles in most industrial stirred tanks spend a large proportion of their time floating relatively free and unimpeded through the liquid after initial dispersion at the impeller. Liquid in large fermenters away from the impeller does not possess sufficient energy for continuous break-up of bubbles. This is a consequence of scale; most laboratory fermenters operate with stirrer power between 10 and 20 kW m^{-3}, whereas large agitated vessels operate at 0.5 to 5 kW m^{-3}. The result is that virtually all large commercial-size stirred tank reactors operate mostly in the free-bubble-rise regime [20].

The most important property of air bubbles in fermenters is their size. For a given volume of gas, more interfacial area a is provided if the gas is dispersed into many small bubbles

rather than a few large ones; therefore a major goal in bioreactor design is a high level of gas dispersion. However, there are other important benefits associated with small bubbles. Small bubbles have correspondingly slow bubble-rise velocities; consequently they stay in the liquid longer, allowing more time for oxygen to dissolve. Small bubbles therefore create high *gas hold-up*, which is defined as the fraction of the working volume of the reactor occupied by entrained gas:

$$\varepsilon = \frac{V_G}{V_T} = \frac{V_G}{V_L + V_G} \tag{10.44}$$

where ε is the gas hold-up, V_T is the total fluid volume (gas + liquid), V_G is the volume of gas bubbles in the reactor, and V_L is the volume of liquid. Because the total interfacial area for oxygen transfer depends on the total volume of gas in the system as well as on the average bubble size, high mass transfer rates are achieved at high gas hold-ups.

Gas hold-up values are very difficult to predict and may be anything from very low (0.01) up to a maximum in commercial-scale stirred fermenters of about 0.2. Under normal operating conditions, a significant fraction of the oxygen in fermentation vessels is contained in the gas hold-up. For example, if the culture is sparged with air and the broth saturated with dissolved oxygen, for a gas hold-up of only 0.03, about half the total oxygen in the system is in the gas phase.

While it is desirable to have small bubbles, there are practical limits. Bubbles $\ll 1$ mm diameter can become a nuisance in bioreactors. The oxygen concentration in these bubbles equilibrates with that in the medium within seconds, so that the gas hold-up no longer reflects the capacity of the system for mass transfer [21]. Problems with very small bubbles are exacerbated in viscous non-Newtonian broths: tiny bubbles remain lodged in these fluids for long periods of time because their rise velocity is reduced. As a rule of thumb, relatively large bubbles must be employed in viscous cultures.

Bubble size also affects the value of k_L. In most fermentation broths, if the bubbles have diameters less than 2 to 3 mm, surface tension effects dominate the behaviour of the bubble surface. As a result, the bubbles behave as rigid spheres with immobile surfaces and no internal gas circulation. A rigid bubble surface gives lower k_L values; k_L decreases with decreasing bubble diameter below about 2 to 3 mm. In contrast, depending on the liquid properties, bubbles in fermentation media with sizes greater than about 3 mm develop internal circulation and relatively mobile surfaces. Bubbles with mobile surfaces are able to wobble and move in spirals during free rise; this behaviour has a marked beneficial effect on k_L and the rate of mass transfer.

To summarise the influence of bubble size on oxygen transfer, small bubbles are generally beneficial because they provide higher gas hold-ups and greater interfacial surface area compared with large bubbles. However, k_L for bubbles less than about 2 to 3 mm in diameter is reduced due to surface effects. Very small bubbles $\ll 1$ mm should be avoided, especially in viscous broths.

10.6.2 Sparging, Stirring, and Medium Properties

In this section we consider the physical processes in fermenters and system properties that affect bubble size and the value of $k_L a$.

Bubble Formation

In fermenters, air bubbles are formed at the sparger. Several types of sparger are in common use. *Porous spargers* of sintered metal, glass, or ceramic are applied mainly in small-scale systems; gas throughput is limited because the sparger poses a high resistance to flow. Cells growing through the fine holes and blocking the sparger can also be a problem. *Orifice spargers*, also known as perforated pipes, are constructed by making small holes in piping that is then fashioned into a ring or cross and placed in the reactor. The individual holes on orifice spargers should be large enough to minimise blockages. *Point* or *nozzle spargers* are used in many agitated fermenters from laboratory to production scale. These spargers consist of a single open pipe or partially closed pipe providing a point-source stream of air bubbles. Advantages compared with other sparger designs include low resistance to gas flow and small risk of blockage.

Bubbles leaving the sparger usually fall within a relatively narrow size range depending on the sparger type. This size range is a significant parameter in the design of air-driven fermenters such as bubble and airlift columns (Section 14.2 in Chapter 14) because there is no other mechanism for bubble dispersion in these reactors. However in stirred vessels, design of the sparger and the mechanics of bubble formation are of secondary importance compared with the effects of the impeller. As a result of continual bubble break-up and dispersion by the impeller and coalescence from bubble collisions, the bubble sizes in stirred reactors often bear little relation to those formed at the sparger.

Gas Dispersion

The two-phase flow patterns set up in stirred vessels with gassing have been described in Chapter 8 (Sections 8.3.4 and 8.4). The effectiveness of bubble break-up and dispersion depends on the relative rates of stirring and gas flow; the balance between these operating parameters determines whether *impeller flooding*, *impeller loading*, or *complete gas dispersion* occurs. Flooding should be avoided because an impeller surrounded by gas no longer contacts the liquid properly, resulting in poor mixing and gas dispersion. At stirrer speeds above that required to prevent flooding, gas is increasingly recirculated around the tank.

Gas dispersion in stirred vessels takes place mainly in the immediate vicinity of the impeller. The formation and function of *ventilated cavities* behind the impeller blades are discussed in Section 8.4. Gas from the sparger together with a large fraction of the recirculating gas in the system is entrained in these cavities. As the impeller blades rotate at high speed, small gas bubbles are thrown out from the back of the cavities into the bulk liquid. Because bubbles formed at the sparger are immediately drawn into the impeller zone, dispersion of gas in stirred vessels is largely independent of sparger design. As long as the sparger is located under the stirrer, it has been shown that sparger type does not affect mass transfer significantly.

Bubble Coalescence

Coalescence of small bubbles into bigger bubbles is generally undesirable for oxygen transfer because the total interfacial area and gas hold-up are reduced. The frequency of bubble coalescence depends mainly on the liquid properties. In *coalescing liquids* such as pure water, a large fraction of bubble collisions results in the formation of bigger bubbles.

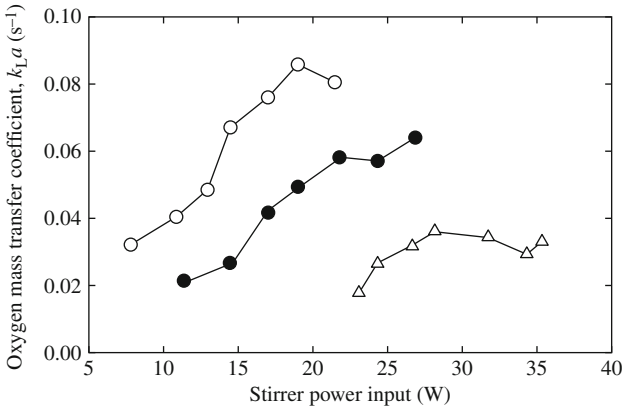

FIGURE 10.9 Effect of solution composition on k_La in a stirred tank at constant gas flow rate: (●) water (coalescing); (○) 5% Na_2SO_4 in water (noncoalescing); and (△) 0.7% w/w carboxymethyl cellulose in water (viscous, pseudoplastic).
Data from S.J. Arjunwadkar, K. Sarvanan, P.R. Kulkarni, and A.B. Pandit, 1998, Gas–liquid mass transfer in dual impeller bioreactor. Biochem. Eng. J. *1, 99–106.*

In contrast, in *noncoalescing liquids*, colliding bubbles tend to bounce off each other due to surface tension effects and do not coalesce readily. In noncoalescing liquids in stirred vessels, the bubbles sizes remain close to those produced at the back of the ventilated cavities behind the impeller blades.

The coalescence properties of liquids depend on the liquid composition. Compared with pure water, the presence of salts and ions suppresses coalescence; therefore, simple fermentation media are usually noncoalescing to some extent depending on composition. This is an advantage for oxygen transfer. The addition of ions to water in sparged vessels markedly reduces the average bubble size and increases the gas hold-up, so much so that the interfacial area a in water containing salts may be up to 10 times greater than that obtained without salts [22].

Experimental results for the effect of solution composition on k_La are shown in Figure 10.9. The presence of solutes has a significant impact on the rate of oxygen transfer. The results for water and 5% Na_2SO_4 salt in water illustrate the effect of liquid coalescence properties: k_La is lower in water than in noncoalescing salt solution. Because the composition and therefore the coalescence properties of fermentation broths vary with time during cell cultures, k_La can also be expected to vary accordingly.

Viscosity

The rheology of fluids has a significant effect on bubble size, gas hold-up, and k_La. With increasing viscosity, the thickness of the fluid boundary layers surrounding the bubbles increases, thus increasing the resistance to oxygen transfer. High viscosity also dampens turbulence, changes the size and structure of the ventilated cavities at the impeller blades, and reduces the effectiveness of gas dispersion. Except in low-viscosity fluids where these effects are negligible, k_La decreases with increasing liquid viscosity. As an example, as shown in Figure 10.9, k_La in pseudoplastic carboxymethyl cellulose solution is significantly lower than in water or salt solution at the same fermenter power input. In non-Newtonian fluids, sharp reductions in k_La have been found to occur at apparent viscosities above 10 to 2000 mPa s [23].

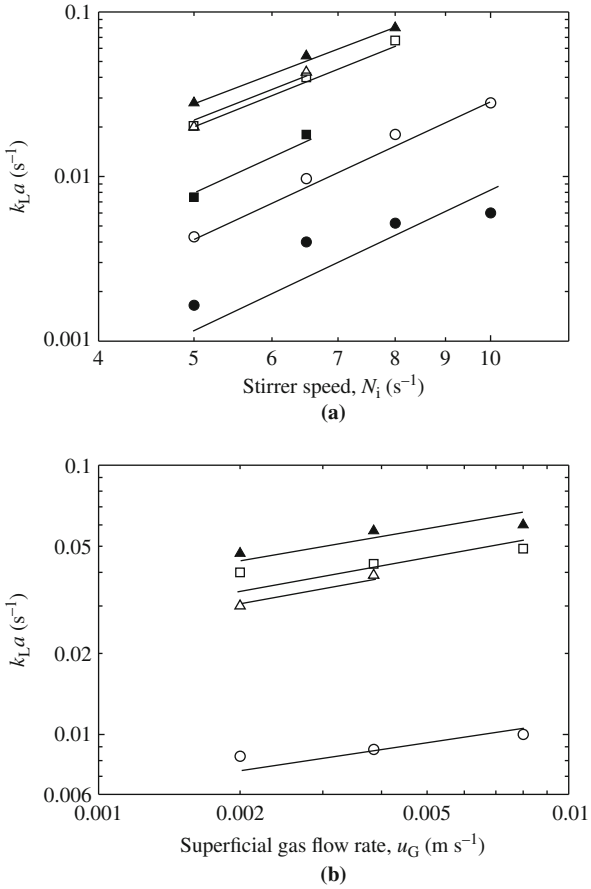

FIGURE 10.10 Dependence of k_La on operating conditions in a stirred tank. The data are plotted using logarithmic coordinates. (a) Effect of stirrer speed N_i at constant gas velocity. (b) Effect of gas flow rate u_G at constant stirrer speed. The symbols represent Newtonian fluids with viscosities: (△) 0.91 mPa s; (▲) 1.3 mPa s; (□) 2.1 mPa s; (■) 5.1 mPa s; (○) 13.3 mPa s; and (●) 70.2 mPa s.
From H. Yagi and F. Yoshida, 1975, Gas absorption by Newtonian and non-Newtonian fluids in sparged agitated vessels. Ind. Eng. Chem. Process Des. Dev. *14, 488–493.*

Stirrer Speed and Gas Flow Rate

Under normal fermenter operating conditions, increasing the stirrer speed and gas flow rate improves the value of k_La. Typical data for k_La in Newtonian fluids of varying viscosity are shown in Figure 10.10. The strong dependence of k_La on stirrer speed is evident from Figure 10.10(a): in this system, doubling the stirrer speed N_i resulted in an average 4.6-fold increase in k_La. Increasing the gas flow rate is a less effective strategy for improving k_La: for example, in the system represented in Figure 10.10(b), doubling the gas flow rate increased k_La by only about 20%. Moreover, in most systems there is limited practical scope for increasing k_La by increasing the gas flow: as discussed in Sections 8.3.4 and 8.4, impeller flooding occurs at high gas flow rates unless the impeller is able to disperse all the gas impinging on it. At very high gassing rates, the liquid contents can be blown out of the fermenter. In viscous non-Newtonian fluids, the dependence of k_La on stirrer speed is generally weaker than in low-viscosity systems while the effect of gas velocity is similar.

10.6.3 Antifoam Agents

Most cell cultures produce a variety of foam-producing and foam-stabilising agents, such as proteins, polysaccharides, and fatty acids. Foam build-up in fermenters is very common, particularly in aerobic systems. Foaming causes a range of reactor operating problems; foam control is therefore an important consideration in fermentation design. Excessive foam overflowing from the top of the fermenter provides an entry route for contaminating organisms and causes blockage of outlet gas lines. Liquid and cells trapped in the foam represent an effective loss of bioreactor volume, as conditions in the foam may not be favourable for metabolic activity. To make matters worse, fragile cells can be damaged by collapsing foam. To accommodate foam layers as well as the increase in fluid volume in aerated vessels due to gas hold-up, a space of 20 to 30% of the tank volume must be left between the top of the liquid and the vessel headplate when setting up fermenters. Foaming is exacerbated by high gas flow rates and high stirrer speeds.

Addition of special antifoam compounds to the medium is the most common method of reducing foam build-up in fermenters. However, antifoam agents affect the surface chemistry of bubbles and their tendency to coalesce, and have a significant effect on $k_L a$. Most antifoam agents are strong surface-tension-lowering substances. Decrease in surface tension reduces the average bubble diameter, thus producing higher values of a. However, this is countered by a reduction in the mobility of the gas–liquid interface, which lowers the value of k_L. With most silicon-based antifoams, the decrease in k_L is generally larger than the increase in a so that, overall, $k_L a$ is reduced [24, 25]. Typical data for surface tension and $k_L a$ as a function of antifoam concentration are shown in Figure 10.11. In this experiment, a reduction in $k_L a$ of almost 50% occurred after addition of only a small amount of antifoam. In some cases, the decrease in the rate of oxygen transfer is dramatic, by up to a factor of 5 to 10.

To maintain the noncoalescing character of the medium and high $k_L a$ values, mechanical rather than chemical methods of disrupting foam are preferred because the properties of the liquid are not changed. Mechanical foam breakers, such as high-speed discs rotating at the top of the vessel and centrifugal foam destroyers, are suitable when foam development is moderate. However, some of these devices need large quantities of power to operate in commercial-scale vessels; in addition, their limited foam-destroying capacity is a problem with highly foaming cultures. In many cases, use of chemical antifoam agents is unavoidable.

10.6.4 Temperature

The temperature of aerobic fermentations affects both the solubility of oxygen C^*_{AL} and the mass transfer coefficient k_L. Increasing the temperature causes C^*_{AL} to drop, so that the driving force for mass transfer $(C^*_{AL} - C_{AL})$ is reduced. At the same time, the diffusivity of oxygen in the liquid film surrounding the bubbles is increased, resulting in an increase in k_L. The net effect of temperature on oxygen transfer depends on the range of temperature considered. For temperatures between 10°C and 40°C, which includes the operating range for most fermentations, an increase in temperature is more likely to increase the rate of

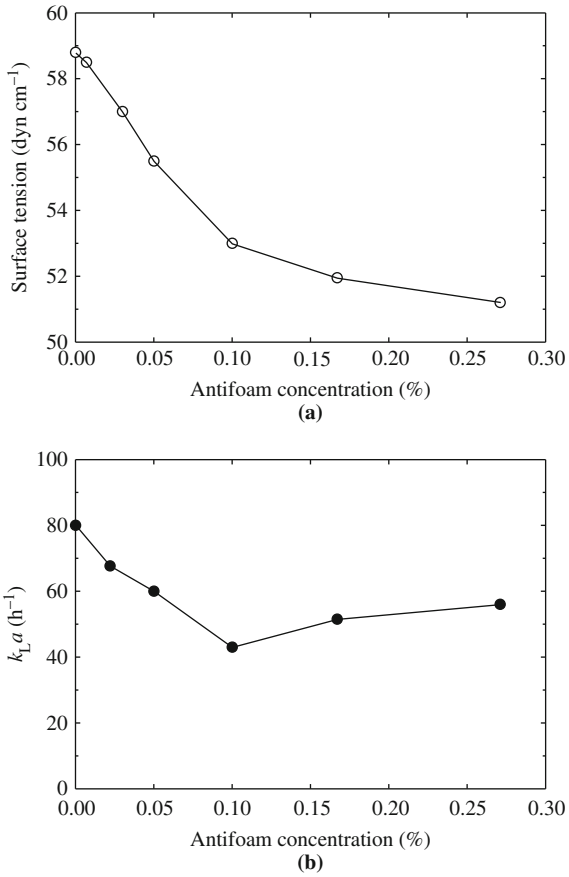

FIGURE 10.11 Effect of antifoam concentration on: (a) surface tension, and (b) $k_L a$, in a *Penicillium chrysogenum* fermentation broth.
Data from F.H. Deindoerfer and E.L. Gaden, 1955, Effects of liquid physical properties on oxygen transfer in penicillin fermentation. Appl. Microbiol. *3, 253–257; with unit conversion from R.K. Finn, 1954, Agitation–aeration in the laboratory and in industry.* Bact. Rev. *18, 254–274.*

oxygen transfer. Above 40°C, the solubility of oxygen drops significantly, adversely affecting the driving force and rate of mass transfer.

10.6.5 Gas Pressure and Oxygen Partial Pressure

The pressure and oxygen partial pressure of the gas used to aerate fermenters affect the value of C^*_{AL}. The equilibrium relationship between these parameters for dilute liquid solutions is given by *Henry's law*:

$$p_{AG} = p_T\, y_{AG} = H C^*_{AL} \tag{10.45}$$

where p_{AG} is the *partial pressure* of component A in the gas phase, p_T is the total gas pressure, y_{AG} is the mole fraction of A in the gas phase, and C^*_{AL} is the solubility of component A in the liquid. H is *Henry's constant*, which is a function of temperature. From Eq. (10.45), if the total gas pressure p_T or the concentration of oxygen in the gas y_{AG} is increased at constant temperature, C^*_{AL} and therefore the mass transfer driving force $(C^*_{AL} - C_{AL})$ also increase.

In some cell cultures, oxygen-enriched air or pure oxygen may be used instead of air to improve oxygen transfer. The effect on oxygen solubility can be determined using Henry's law. At a fixed temperature so that H remains constant, if p_T and y_{AG} are varied from condition 1 to condition 2, from Eq. (10.45):

$$\frac{C^*_{AL2}}{C^*_{AL1}} = \frac{p_{AG2}}{p_{AG1}} = \frac{p_{T2}\, y_{AG2}}{p_{T1}\, y_{AG1}} \tag{10.46}$$

According to the *International Critical Tables* [26], the mole fraction y_{AG1} of oxygen in air is 0.2099. If pure oxygen is used instead of air, y_{AG2} is 1. From Eq. (10.46), if the gases are applied at the same total pressure:

$$\frac{C^*_{AL2}}{C^*_{AL1}} = \frac{1}{0.2099} = 4.8 \tag{10.47}$$

Therefore, sparging pure oxygen instead of air at the same total pressure and temperature increases the solubility of oxygen by a factor of 4.8. Alternatively, the solubility can be increased by sparging compressed air at higher total pressure p_T. Both these strategies increase the operating cost of the fermenter; it is also possible in some cases that the culture will suffer inhibitory effects from exposure to very high oxygen concentrations.

10.6.6 Presence of Cells and Macromolecules

Oxygen transfer is influenced by the presence of cells in fermentation broths. The effect depends on the morphology of the organism and the cell concentration. Cells with complex morphology, such as branched hyphae, generally lead to lower oxygen transfer rates by interfering with bubble break-up and promoting coalescence. Cells, proteins, and other molecules that adsorb at gas–liquid interfaces also cause *interfacial blanketing*, which reduces the effective contact area between gas and liquid. Macromolecules and very small particles accumulating at the bubble surface reduce the mobility of the interface, thus lowering k_L, but may also decrease coalescence, thereby increasing a. The quantitative effect of interfacial blanketing is highly system-specific.

Because cell, substrate, and product concentrations, and therefore the viscosity and coalescence properties of the fluid, change during batch fermentations, the value of k_La also varies. An example of change in k_La as a result of these combined factors is shown in Figure 10.12.

10.7 MEASURING DISSOLVED OXYGEN CONCENTRATION

The concentration of dissolved oxygen C_{AL} in fermenters is normally measured using a *dissolved oxygen electrode*. There are two types in common use: *galvanic electrodes* and *polarographic electrodes*. Details of the construction and operating principles of oxygen probes can be found in the literature (e.g., [27, 28]). In both designs, a membrane permeable to oxygen separates the fermentation fluid from the electrode. As illustrated in Figure 10.13, oxygen

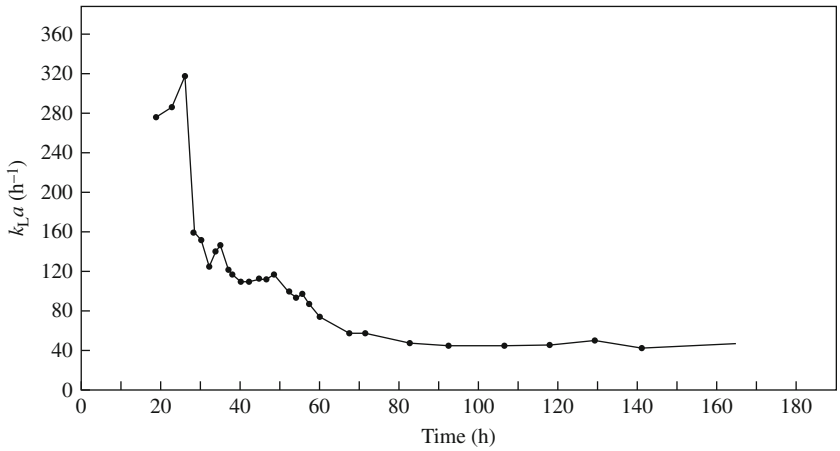

FIGURE 10.12 Variation in k_La during a batch 300-1 streptomycete fermentation.
From C.M. Tuffile and F. Pinho, 1970, Determination of oxygen transfer coefficients in viscous streptomycete fermentations. Biotechnol. Bioeng. *12, 849–871.*

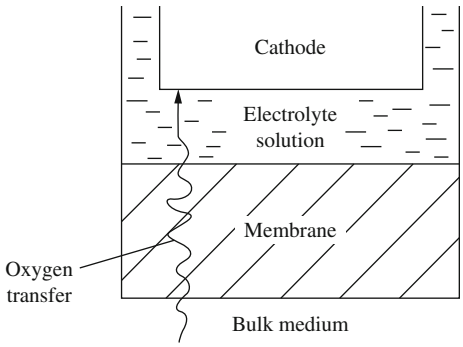

FIGURE 10.13 Diffusion of oxygen from the bulk liquid to the cathode of an oxygen electrode.

diffuses through the membrane to the cathode, where it reacts to produce a current between the anode and cathode proportional to the oxygen partial pressure in the fermentation broth. An electrolyte solution in the electrode supplies ions that take part in the reaction and must be replenished at regular intervals. Steam-sterilisable or autoclavable probes are available commercially and are inserted directly into fermentation vessels for online monitoring of dissolved oxygen. The probe should be located to avoid the direct impingement of bubbles on the electrode membrane as this distorts the probe signal. Repeated calibration of dissolved oxygen probes is necessary; fouling by cells attaching to the membrane surface, electronic noise due to air bubbles passing close to the membrane, and signal drift are the main operating problems.

As indicated in Figure 10.13, the supply of oxygen from the bulk medium to the cathode in oxygen probes is a mass transfer process. Because there is no bulk fluid motion in

the membrane or electrolyte solution, operation of the probe relies on diffusion of oxygen across these thicknesses. This takes time, so the response of an electrode to sudden changes in dissolved oxygen level is subject to delay. This does not affect many applications of oxygen probes in fermenters, as changes in dissolved oxygen tension during cell culture are normally relatively slow. However, as described in more detail in Section 10.10.2 (Electrode Response Time and Liquid Boundary Layers subsection), electrode dynamics can have a significant influence on the measurement of oxygen uptake rates and $k_L a$ in culture broths. Microprobes for dissolved oxygen measurement are also available. The smaller cathode size and lower oxygen consumption by these instruments means that their response is much quicker than the more robust devices used in fermentation vessels.

Both galvanic and polarographic electrodes measure the *oxygen tension* or partial pressure of dissolved oxygen in the fermentation broth, not the dissolved oxygen concentration. To convert oxygen tension to dissolved oxygen concentration, it is necessary to know the solubility of oxygen in the liquid at the temperature and pressure of measurement. For example, if the dissolved oxygen tension measured using an oxygen electrode is 60% air saturation and the solubility of oxygen in the solution under air is 8.0×10^{-3} kg m^{-3}, the dissolved oxygen concentration is $(0.6 \times 8.0 \times 10^{-3})$ kg m^{-3} $= 4.8 \times 10^{-3}$ kg m^{-3}.

10.8 ESTIMATING OXYGEN SOLUBILITY

The concentration difference $(C^*_{AL} - C_{AL})$ is the driving force for oxygen mass transfer. Because this difference is usually very small, it is important that the solubility C^*_{AL} be known accurately. Otherwise, small errors in C^*_{AL} will result in large errors in $(C^*_{AL} - C_{AL})$.

Air is used to provide oxygen in most industrial fermentations. Values for the solubility of oxygen in water at various temperatures and 1 atm air pressure are listed in Table 10.2. However, fermentations are not carried out using pure water, and the gas composition and pressure can be varied. Because the presence of dissolved material in the liquid and the oxygen partial pressure in the gas phase affect oxygen solubility, the values in Table 10.2 may not be directly applicable to bioprocessing systems.

10.8.1 Effect of Oxygen Partial Pressure

As indicated in Henry's law, Eq. (10.45), oxygen solubility is directly proportional to the total gas pressure and the mole fraction of oxygen in the gas phase. The solubility of oxygen in water as a function of these variables can be determined using Eq. (10.45) and the values for Henry's constant listed in Table 10.2.

10.8.2 Effect of Temperature

The variation of oxygen solubility with temperature is shown in Table 10.2 for water in the range 0 to 40°C. Oxygen solubility falls with increasing temperature. The solubility of

TABLE 10.2 Solubility of Oxygen in Water under 1 atm Air Pressure

Temperature (°C)	Oxygen solubility under 1 atm air pressure (kg m^{-3})	Henry's constant (m^3 atm gmol^{-1})
0	1.48×10^{-2}	0.454
10	1.15×10^{-2}	0.582
15	1.04×10^{-2}	0.646
20	9.45×10^{-3}	0.710
25	8.69×10^{-3}	0.774
26	8.55×10^{-3}	0.787
27	8.42×10^{-3}	0.797
28	8.29×10^{-3}	0.810
29	8.17×10^{-3}	0.822
30	8.05×10^{-3}	0.835
35	7.52×10^{-3}	0.893
40	7.07×10^{-3}	0.950

Calculated from data in International Critical Tables, *1928, vol. III, McGraw-Hill, New York, p. 257.*

oxygen from air in pure water between 0°C and 36°C has been correlated using the following equation [29]:

$$C^*_{AL} = 14.161 - 0.3943\,T + 0.007714\,T^2 - 0.0000646\,T^3 \tag{10.48}$$

where C^*_{AL} is oxygen solubility in units of mg l^{-1}, and T is temperature in °C.

10.8.3 Effect of Solutes

The presence of solutes such as salts, acids, and sugars affects the solubility of oxygen in water as indicated in Tables 10.3 and 10.4. These data show that the solubility of oxygen is reduced by the addition of ions and sugars that are normally required in fermentation media. Quicker et al. [30] have developed an empirical correlation to correct values of oxygen solubility in water for the effects of cations, anions, and sugars:

$$\log_{10}\left(\frac{C^*_{AL0}}{C^*_{AL}}\right) = 0.5\sum_i H_i z_i^2 C_{iL} + \sum_j K_j C_{jL} \tag{10.49}$$

where

C^*_{AL0} = oxygen solubility at zero solute concentration (mol m^{-3})
C^*_{AL} = oxygen solubility in the presence of solutes (mol m^{-3})
H_i = constant for ionic component i (m^3 mol^{-1})
z_i = charge (valence) of ionic component i

TABLE 10.3 Solubility of Oxygen in Aqueous Solutions at 25°C under 1 atm Oxygen Pressure

	Oxygen solubility at 25°C under 1 atm oxygen pressure (kg m^{-3})		
Concentration (M)	**HCl**	**½ H_2SO_4**	**NaCl**
0	4.14×10^{-2}	4.14×10^{-2}	4.14×10^{-2}
0.5	3.87×10^{-2}	3.77×10^{-2}	3.43×10^{-2}
1.0	3.75×10^{-2}	3.60×10^{-2}	2.91×10^{-2}
2.0	3.50×10^{-2}	3.28×10^{-2}	2.07×10^{-2}

Calculated from data in International Critical Tables, *1928, vol. III, McGraw-Hill, New York, p. 271.*

TABLE 10.4 Solubility of Oxygen in Aqueous Solutions of Sugars under 1 atm Oxygen Pressure

Sugar	Concentration (gmol per kg H_2O)	Temperature (°C)	Oxygen solubility under 1 atm oxygen pressure (kg m^{-3})
Glucose	0	20	4.50×10^{-2}
	0.7	20	3.81×10^{-2}
	1.5	20	3.18×10^{-2}
	3.0	20	2.54×10^{-2}
Sucrose	0	15	4.95×10^{-2}
	0.4	15	4.25×10^{-2}
	0.9	15	3.47×10^{-2}
	1.2	15	3.08×10^{-2}

Calculated from data in International Critical Tables, *1928, vol. III, McGraw-Hill, New York, p. 272.*

C_{iL} = concentration of ionic component i in the liquid (mol m^{-3})
K_j = constant for nonionic component j (m^3 mol^{-1})
C_{jL} = concentration of nonionic component j in the liquid (mol m^{-3})

Values of H_i and K_j for use in Eq. (10.49) are listed in Table 10.5. In a typical fermentation medium, the oxygen solubility is between 5% and 25% lower than in water as a result of solute effects.

10.9 MASS TRANSFER CORRELATIONS FOR OXYGEN TRANSFER

In general, there are two approaches to evaluating mass transfer coefficients: calculation using empirical correlations, and experimental measurement. In both cases, for gas–liquid mass transfer, separate determination of k_L and a is laborious and sometimes impossible. It is convenient, therefore, to evaluate k_La as a combined term. In this section we consider

TABLE 10.5 Values of H_i and K_j in Eq. (10.49) at 25°C

Cation	$H_i \times 10^3$ (m^3 mol^{-1})	Anion	$H_i \times 10^3$ (m^3 mol^{-1})	Sugar	$K_j \times 10^3$ (m^3 mol^{-1})
H^+	−0.774	OH^-	0.941	Glucose	0.119
K^+	−0.596	Cl^-	0.844	Lactose	0.197
Na^+	−0.550	CO_3^{2-}	0.485	Sucrose	0.149*
NH_4^+	−0.720	SO_4^{2-}	0.453		
Mg^{2+}	−0.314	NO_3^-	0.802		
Ca^{2+}	−0.303	HCO_3^-	1.058		
Mn^{2+}	−0.311	$H_2PO_4^-$	1.037		
		HPO_4^{2-}	0.485		
		PO_4^{3-}	0.320		

Approximately valid for sucrose concentrations up to about 200 g l^{-1}.
From A. Schumpe, I. Adler, and W.-D. Deckwer, 1978, Solubility of oxygen in electrolyte solutions. Biotechnol. Bioeng. *20, 145–150; and G. Quicker, A. Schumpe, B. König, and W.-D. Deckwer, 1981, Comparison of measured and calculated oxygen solubilities in fermentation media.* Biotechnol. Bioeng. *23, 635–650.*

calculation of k_La using published correlations. Experimental methods for measuring k_La are described later in Section 10.10.

The value of k_La in fermenters depends on the fluid properties and the prevailing hydrodynamic conditions. Relationships between k_La and parameters such as liquid density, viscosity, oxygen diffusivity, bubble diameter, and fluid velocity have been investigated extensively. The results of these studies in the form of empirical correlations between mass transfer coefficients and important operating variables are available in the literature. Theoretically, these correlations allow prediction of mass transfer coefficients based on information gathered from a large number of previous experiments. In practice, however, the accuracy of published correlations for k_La applied to biological systems is generally poor.

The main reason is that oxygen transfer is strongly affected by the additives present in fermentation media. Because fermentation liquids contain varying levels of substrates, products, salts, surface-active agents, and cells, the surface chemistry of bubbles, and therefore the mass transfer situation, become very complex. Most available correlations for oxygen transfer coefficients were determined using air in pure water; however, the presence of additives in water affects the value of k_La significantly and it is very difficult to make corrections for different liquid compositions. The effective mass transfer area a is also subject to interfacial blanketing of the bubble–liquid surface by cells and other components of the broth. Prediction of k_La under these conditions is problematic.

When mass transfer coefficients are required for large-scale equipment, another factor related to hydrodynamic conditions limits the applicability of published correlations. Most studies of oxygen transfer have been carried out in laboratory-scale stirred reactors, which are characterised by high turbulence throughout most of the vessel. In contrast, intense

turbulence in large-scale fermenters is limited to the impeller region; flow in the remainder of the tank is much slower. As a result, because of the different hydrodynamic regimes present in small- and large-scale vessels, mass transfer correlations developed in the laboratory tend to overestimate the oxygen transfer capacity of commercial-scale systems.

Although published mass transfer correlations cannot be applied directly to fermentation systems, there is a general consensus in the literature about the form of the equations and the relationship between k_La and reactor operating conditions. The most successful correlations are dimensional equations of the form [22]:

$$k_La = A\left(\frac{P_T}{V_L}\right)^{\alpha} u_G^{\beta} \tag{10.50}$$

In Eq. (10.50), k_La is the oxygen transfer coefficient, P_T is the total power dissipated, and V_L is the liquid volume. u_G is the *superficial gas velocity*, which is defined as the volumetric gas flow rate divided by the cross-sectional area of the fermenter. All of the hydrodynamic effects of flow and turbulence on bubble dispersion and the mass transfer boundary layer are represented by the power term, P_T. The total power dissipated is calculated as the sum of the power input by stirring under gassed conditions (Section 8.5.3) and, if it makes a significant contribution, the power associated with isothermal expansion of the sparged gas (Section 8.6).

Note that correlations of the type represented by Eq. (10.50) are independent of the sparger or stirrer design: the power input determines k_La independent of stirrer type. A, α, and β are constants. The values of α and β are largely insensitive to broth properties and usually fall within the range 0.2 to 1.0. In contrast, the dimensional parameter A varies significantly with liquid composition and is sensitive to the coalescing properties and cell content of culture broths. Because both exponents α and β are typically <1 in value, increasing k_La by raising either the air flow rate or power input becomes progressively less efficient and more costly as the inputs increase.

For viscous and non-Newtonian fluids, a modified form of Eq. (10.50) can be used to incorporate explicitly the effect of viscosity on the mass transfer coefficient:

$$k_La = B\left(\frac{P_T}{V_L}\right)^{\alpha} u_G^{\beta}\, \mu_a^{-\delta} \tag{10.51}$$

where B is a modified constant reflecting the properties of the liquid other than viscosity, μ_a is the apparent viscosity (Section 7.5), and δ is a constant typically in the range 0.5 to 1.3.

10.10 MEASUREMENT OF k_La

Because of the difficulties associated with using correlations to predict k_La in bioreactors (Section 10.9), oxygen transfer coefficients are routinely determined experimentally. This is not without its own problems however, as discussed below. Whichever method is used to measure k_La, the measurement conditions should match those applied in the fermenter. Techniques for measuring k_La have been reviewed in the literature [22, 31, 32].

10.10.1 Oxygen Balance Method

The steady-state oxygen balance method is the most reliable procedure for estimating $k_L a$, and allows determination from a single-point measurement. An important advantage is that the method can be applied to fermenters during normal operation. It is strongly dependent, however, on accurate measurement of the inlet and outlet gas composition, flow rate, pressure, and temperature. Large errors as high as ±100% can be introduced if the measurement techniques are inadequate. Considerations for the design and operation of laboratory equipment to ensure accurate results are described by Brooks et al. [33].

To determine $k_L a$, the oxygen contents of the gas streams flowing to and from the fermenter are measured. From a mass balance at steady state:

$$N_A = \frac{1}{V_L}\left[(F_g C_{AG})_i - (F_g C_{AG})_o\right] \tag{10.52}$$

where N_A is the volumetric rate of oxygen transfer, V_L is the volume of liquid in the fermenter, F_g is the volumetric gas flow rate, C_{AG} is the gas-phase concentration of oxygen, and subscripts i and o refer to the inlet and outlet gas streams, respectively. The first bracketed term on the right side represents the rate at which oxygen enters the fermenter in the inlet gas stream; the second term is the rate at which oxygen leaves. The difference between them is the rate at which oxygen is transferred out of the gas into the liquid. Because gas concentrations are generally measured as partial pressures, the ideal gas law Eq. (2.35) can be incorporated into Eq. (10.52) to obtain an alternative expression:

$$N_A = \frac{1}{R V_L}\left[\left(\frac{F_g p_{AG}}{T}\right)_i - \left(\frac{F_g p_{AG}}{T}\right)_o\right] \tag{10.53}$$

where R is the ideal gas constant (Appendix B), p_{AG} is the oxygen partial pressure in the gas, and T is the absolute temperature. Because there is often not a great difference between the amounts of oxygen in the gas streams entering and leaving fermenters, especially in small-scale systems, application of Eq. (10.53) involves subtracting two numbers of similar magnitude. To minimise the associated error, p_{AG} is usually measured using mass spectrometry or similar high-sensitivity technique. The temperature and flow rate of the gases must also be measured carefully to determine an accurate value of N_A. Once N_A is known, if C_{AL} in the fermentation broth is measured using a dissolved oxygen electrode and C^*_{AL} is evaluated as described in Section 10.8, $k_L a$ can then be determined from Eq. (10.39). The value of $k_L a$ will vary depending on the stirrer speed and air flow rate used during the measurement and the properties of the culture broth.

There are several assumptions inherent in the equations used in the oxygen balance method:

1. The liquid phase is well mixed.
2. The gas phase is well mixed.
3. The pressure is constant throughout the vessel.

These assumptions relate to application of Eq. (10.39) to determine $k_L a$ from the measured results for N_A. Assumption (1) allows us to use a single C_{AL} value to represent the

concentration of dissolved oxygen in the fermentation broth. It applies reasonably well in small vessels where there is a relatively high stirrer power input per unit volume. However, the liquid phase in large-scale fermenters may not be well mixed, particularly if the culture broth is viscous. Assumptions (2) and (3) are required for evaluation of the oxygen solubility, C^*_{AL}. Because solubility depends on the gas-phase composition and pressure, we assume that these properties are the same throughout the tank. Assumption (2) is valid when the bubble gas composition is uniform throughout the vessel and the same as that in the outlet gas stream. This occurs most readily in small, intensely agitated vessels with high levels of gas recirculation; accordingly, assumption (2) applies generally in laboratory-scale fermenters. In contrast, the higher bubble residence times and lower gas recirculation levels in large vessels mean that the gas phase is less likely to be well mixed. Assumption (3) is also generally valid in small-scale vessels. However, in large, tall fermenters, there may be a considerable difference in hydrostatic pressure between the top and bottom of the tank due to the liquid weight. Issues affecting the analysis of oxygen transfer in large fermenters are considered in more detail in Section 10.12.

EXAMPLE 10.2 STEADY-STATE $k_L a$ MEASUREMENT

A 20-litre stirred fermenter containing *Bacillus thuringiensis* is used to produce a microbial insecticide. The oxygen balance method is applied to determine $k_L a$. The fermenter operating pressure is 150 kPa and the culture temperature is 30°C. The oxygen tension in the broth is measured as 82% using a probe calibrated to 100% in situ using water and air at 30°C and 150 kPa. The solubility of oxygen in the culture fluid is the same as in water. Air is sparged into the vessel; the inlet gas flow rate measured outside the fermenter at 1 atm pressure and 22°C is 0.23 l s^{-1}. The exit gas from the fermenter contains 20.1% oxygen and has a flow rate of 8.9 l min^{-1}.

(a) Calculate the volumetric rate of oxygen uptake by the culture.
(b) What is the value of $k_L a$?

Solution

(a) From Table A.5 in Appendix A, the fermenter operating pressure is:

$$150 \times 10^3 \text{ Pa} \cdot \left| \frac{1 \text{ atm}}{1.013 \times 10^5 \text{ Pa}} \right| = 1.48 \text{ atm}$$

The oxygen partial pressure in the inlet air at 1 atm is 0.2099 atm (Section 10.6.5). From Appendix B, $R = 0.082057$ l atm K^{-1} gmol^{-1}. Using Eq. (10.53):

$$N_A = \frac{1}{0.082057 \text{ l atm K}^{-1} \text{ gmol}^{-1} (20 \text{ l})} \left[\left(\frac{0.23 \text{ l s}^{-1} (0.2099 \text{ atm})}{(22 + 273.15) \text{ K}} \right) - \left(\frac{8.9 \text{ l min}^{-1} \cdot \left| \frac{1 \text{ min}}{60 \text{ s}} \right| \cdot (0.201)(1.48 \text{ atm})}{(30 + 273.15) \text{ K}} \right) \right]$$

$$N_A = \frac{1}{0.082057\ \text{l atm K}^{-1}\ \text{gmol}^{-1}\ (20\ \text{l})}\left[(1.636\times10^{-4}) - (1.456\times10^{-4})\right]\text{l atm K}^{-1}\ \text{s}^{-1}$$

$$N_A = 1.1\times10^{-5}\ \text{gmol l}^{-1}\ \text{s}^{-1}$$

Because, at steady state, the rate of oxygen transfer is equal to the rate of oxygen uptake by the cells, the volumetric rate of oxygen uptake by the culture is 1.1×10^{-5} gmol l^{-1} s^{-1}.

(b) Assume that the gas phase is well mixed so that the oxygen concentration in the bubbles contacting the liquid is the same as in the outlet gas, that is, 20.1%. As the difference in oxygen concentration between the inlet and outlet gas streams is small, we can also consider the composition of the gas phase to be constant throughout the fermenter. From Table 10.2, the solubility of oxygen in water at 30°C and 1 atm air pressure is 8.05×10^{-3} kg m^{-3} = 8.05×10^{-3} g l^{-1}. Using Eq. (10.46) to determine the solubility at the fermenter operating pressure of 1.48 atm and gas-phase oxygen mole fraction of 0.201:

$$C^*_{AL2} = \frac{p_{T2}\ y_{AG2}}{p_{T1}\ y_{AG1}} C^*_{AL1} = \frac{(1.48\ \text{atm})\ 0.201}{(1\ \text{atm})\ 0.2099}\ 8.05\times10^{-3}\ \text{g l}^{-1} = 0.0114\ \text{g l}^{-1}$$

C_{AL} in the fermenter is 82% of the oxygen solubility at 30°C and 1.48 atm air pressure. From Eq. (10.45), solubility is proportional to total pressure; therefore:

$$C_{AL} = 0.82\ \frac{1.48\ \text{atm}}{1\ \text{atm}}\ 8.05\times10^{-3}\ \text{g l}^{-1} = 9.77\times10^{-3}\ \text{g l}^{-1}$$

Applying these results in Eq. (10.39):

$$k_L a = \frac{1.1\times10^{-5}\ \text{gmol l}^{-1}\ \text{s}^{-1}\cdot\left|\dfrac{32\ \text{g}}{1\ \text{gmol}}\right|}{0.0114\ \text{g l}^{-1} - 9.77\times10^{-3}\ \text{g l}^{-1}}$$

$$k_L a = 0.22\ \text{s}^{-1}$$

The value of $k_L a$ is 0.22 s^{-1}.

Even when high-sensitivity gas measuring equipment is used, the oxygen balance method is not readily applicable to cultures with low cell growth and oxygen uptake rates, for example, plant and animal cell cultures and aerobic waste treatment systems. When oxygen uptake is slow, the difference in oxygen content between the inlet and outlet gas streams can become diminishingly small, resulting in unacceptable levels of error. In these circumstances, other methods for measuring $k_L a$ must be considered.

10.10.2 Dynamic Method

In this method for estimating $k_L a$, changes in dissolved oxygen tension are measured using an oxygen electrode after a step change in aeration conditions in the fermenter. The results are interpreted using unsteady-state mass balance equations to obtain the value of

k_La. The main advantage of the dynamic method over the steady-state technique is the comparatively low cost of the analytical equipment needed. The measurement is also independent of the oxygen solubility and can be carried out even if C^*_{AL} is unknown. In practice, the dynamic method is best suited for measuring k_La in relatively small vessels. It is used commonly with laboratory-scale fermenters.

Although the dynamic method is simple and easy to perform experimentally, it can give very inaccurate results unless several aspects of the measurement system are examined and characterised. These include the response time of the dissolved oxygen electrode, the effect of liquid boundary layers at the probe surface, and gas-phase dynamics in the vessel. These features of the measurement system should be assessed in conjunction with the dynamic method.

Simple Dynamic Method

The simplest version of the dynamic method will be described here. This method gives reasonable results for k_La only if the following assumptions are valid:

1. The liquid phase is well mixed.
2. The response time of the dissolved oxygen electrode is much smaller than $1/k_La$ (see Section 10.10.2, Electrode Response Time and Liquid Boundary Layers subsection).
3. The measurement is performed at sufficiently high stirrer speed to eliminate liquid boundary layers at the surface of the oxygen probe (see Section 10.10.2, Electrode Response Time and Liquid Boundary Layers subsection).
4. Gas-phase dynamics can be ignored (see Section 10.10.2, Gas-Phase Dynamics subsection).

Assumption (1) is required for C_{AL} measurements at a fixed position in the reactor to represent the dissolved oxygen concentration throughout the vessel, so that results for k_La are not dependent on electrode location. This is relatively easy to achieve in small, vigorously agitated fermenters but may not occur in large vessels containing viscous broths. Assumptions (2) and (3) refer to the results of test experiments that should be carried out in conjunction with the simple dynamic method. These assumptions are more likely to hold using fast oxygen electrodes in vigorously agitated, low-viscosity fluids when the value of k_La is relatively low. Assumption (4) refers to the properties of the gas phase during the measurement period. Gas hold-up and gas mixing have a significant influence in most applications of the dynamic method; however, we neglect these effects here for simplicity. Gas-phase dynamics are discussed later in more detail (Section 10.10.2, Gas-Phase Dynamics subsection). Assumption (4) is likely to be valid only in small vessels containing low-viscosity fluids with low gas hold-up, low levels of gas recirculation, and relatively high gas throughput. If any of the above four assumptions do not hold, the simple dynamic method will not provide an accurate indication of k_La and alternative procedures should be considered.

To measure k_La using the simple dynamic method, the fermenter containing culture broth is stirred and sparged at fixed rates so that the dissolved oxygen concentration C_{AL} is constant. At time t_0, the broth is deoxygenated, either by sparging nitrogen into the vessel or, as indicated in Figure 10.14, by stopping the air flow and allowing the culture to

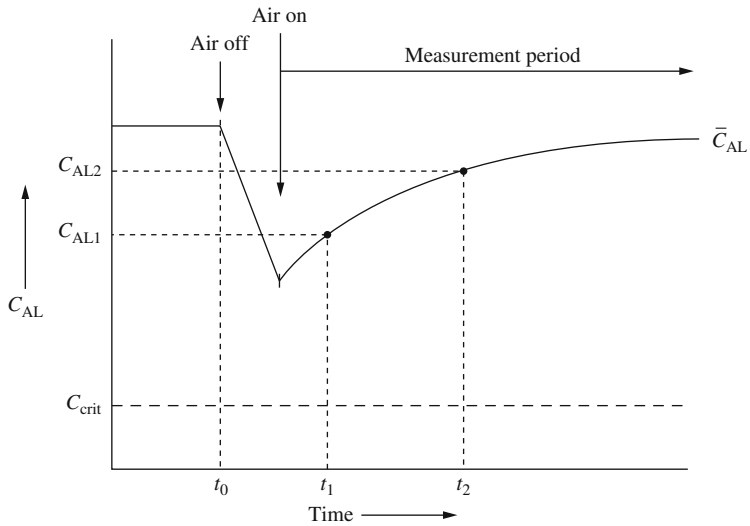

FIGURE 10.14 Variation of dissolved oxygen concentration for the dynamic measurement of k_La.

consume the available oxygen in solution. Air is then pumped into the broth at a constant flow rate and the increase in C_{AL} is measured using a dissolved oxygen probe as a function of time. It is important that the oxygen concentration remains above the critical level C_{crit} so that the rate of oxygen uptake by the cells remains independent of the dissolved oxygen tension. Assuming that reoxygenation of the broth is fast relative to cell growth, the dissolved oxygen level will soon reach a steady-state value $\overline{C}_{AL}$, which reflects a balance between oxygen supply and oxygen consumption in the system. C_{AL1} and C_{AL2} are two oxygen concentrations measured during reoxygenation at times t_1 and t_2, respectively. We can develop an equation for k_La in terms of these experimental data.

During the reoxygenation step, the system is not at steady state. The rate of change in dissolved oxygen concentration is equal to the rate of oxygen transfer from the gas to the liquid, minus the rate of oxygen consumption by the cells:

$$\frac{dC_{AL}}{dt} = k_La\,(C^*_{AL} - C_{AL}) - q_O\,x \tag{10.54}$$

where $q_O x$ is the rate of oxygen consumption. We can determine an expression for $q_O x$ by considering the final steady-state dissolved oxygen concentration, $\overline{C}_{AL}$. When $C_{AL} = \overline{C}_{AL}$, $dC_A/dt = 0$ because there is no change in C_{AL} with time. Therefore, from Eq. (10.54):

$$q_O\,x = k_La\,(C^*_{AL} - \overline{C}_{AL}) \tag{10.55}$$

Substituting this result into Eq. (10.54) and cancelling the $k_La\,C^*_{AL}$ terms gives:

$$\frac{dC_{AL}}{dt} = k_La\,(\overline{C}_{AL} - C_{AL}) \tag{10.56}$$

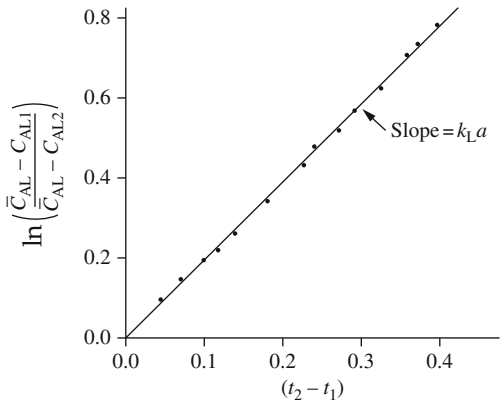

FIGURE 10.15 Evaluating k_La from data measured using the dynamic method.

Assuming k_La is constant with time, we can integrate Eq. (10.56) between t_1 and t_2 using the integration rules described in Appendix E. The resulting equation for k_La is:

$$k_La = \frac{\ln\left(\dfrac{\overline{C}_{AL} - C_{AL1}}{\overline{C}_{AL} - C_{AL2}}\right)}{t_2 - t_1} \tag{10.57}$$

Using Eq. (10.57), k_La can be estimated using two points from Figure 10.14 or, more accurately, from several values of (C_{AL1}, t_1) and (C_{AL2}, t_2). When $\ln\left(\frac{\overline{C}_{AL} - C_{AL1}}{\overline{C}_{AL} - C_{AL2}}\right)$ is plotted against $(t_2 - t_1)$ as shown in Figure 10.15, the slope is k_La. The value obtained for k_La reflects the operating stirrer speed, the air flow rate during the reoxygenation step, and the properties of the culture broth. Equation (10.57) can be applied to actively respiring cultures or to systems without oxygen uptake. In the latter case, $\overline{C}_{AL} = C^*_{AL}$ and nitrogen sparging is required for the deoxygenation step of the procedure.

Before we accept the value of k_La determined using this technique, the validity of assumptions (1) through (4) during the measurement must be checked. Assumption (1) can be verified by repeating the k_La measurement using different probe locations. The remaining three assumptions are addressed in the following sections.

Electrode Response Time and Liquid Boundary Layers

The dynamic method relies on the measurement of changes in dissolved oxygen tension after a step change in fermenter aeration conditions. Problems can arise with this approach if the oxygen electrode is slow to respond to the increase in liquid-phase oxygen levels as the culture broth is reoxygenated. As described in Section 10.7, because several mass transfer steps are involved in the operation of oxygen probes, it may be impossible to achieve a fast electrode response to changes in dissolved oxygen tension. If the electrode response is slower than the actual increase in oxygen concentration, the measured values of C_{AL} will reflect the response characteristics of the probe rather than the change in oxygen

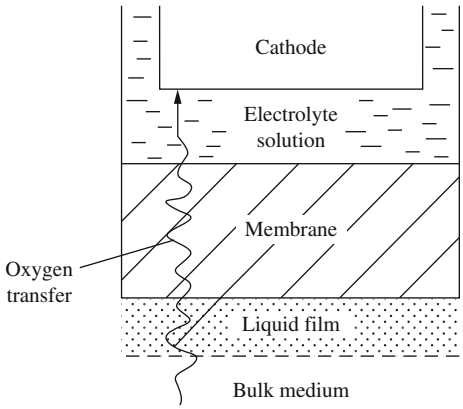

FIGURE 10.16 Development of a liquid film at the surface of an oxygen probe.

concentration in the fermenter. Therefore, the *electrode response time* should always be measured as part of the dynamic method for determining $k_L a$.

As well as the mass transfer resistances represented in Figure 10.13, development of a liquid boundary layer at the membrane–liquid interface, as illustrated in Figure 10.16, may also affect the response time of the electrode. Whether or not a boundary layer is present depends on the flow conditions, liquid properties, and rate of oxygen consumption at the probe cathode. Boundary layer development can be negligible for probes with small cathodes applied in well-mixed, low-viscosity liquids such as water. In some cases, for example, when using microprobes, boundary layers do not develop even in unagitated liquids. However, in most applications, particularly if the liquid is a viscous fermentation broth, liquid films at the probe surface are of concern. When a liquid film is present, the response of the probe is slower than in its absence and the dissolved oxygen readings will vary with stirrer speed. Both these outcomes are undesirable and reduce the accuracy of the dynamic method.

The electrode response time and liquid boundary layer effects can be measured in test experiments. These experiments should be carried out under conditions as close as possible to those applied for $k_L a$ measurement. The same gas flow rate and culture broth are used. The fermenter is prepared by sparging with air to give a constant dissolved oxygen tension, $\overline{C}_{AL}$. The oxygen electrode is equilibrated in a separate, vigorously agitated, nitrogen-sparged vessel providing a 0% oxygen environment. The probe is then transferred quickly from the nitrogen-sparged vessel to the fermenter: this procedure exposes the probe to a step change in dissolved oxygen tension from 0% to $\overline{C}_{AL}$. The response of the probe is recorded. The procedure is repeated using a range of stirrer speeds in the fermenter.

Typical results from the test experiments in low-viscosity fluid are shown in Figure 10.17. The electrode is transferred to the fermenter at time zero. After being at 0% oxygen, the probe takes some time to record a steady new signal corresponding to $\overline{C}_{AL}$. The response of the probe becomes faster as the stirrer speed N_i is increased, reflecting a progressive reduction in the thickness of the liquid boundary layer at the probe surface. At sufficiently high stirrer speed, no further change in electrode response is observed with additional increase in agitation rate, indicating that the boundary layer has been

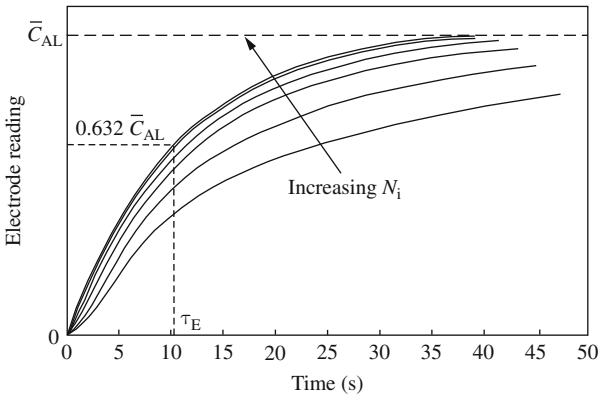

FIGURE 10.17 Typical electrode response curves after a step change in dissolved oxygen tension at different stirrer speeds, N_i. In this example, the electrode response time is just over 10 s.

eliminated. Under these conditions, the response curve represents the dynamics of the electrode itself, independent of external liquid velocity.

The response of dissolved oxygen electrodes is usually assumed to follow first-order kinetics. Accordingly, the *electrode response time* τ_E is defined as the time taken for the probe to indicate 63.2% of the total step change in dissolved oxygen level. As shown in Figure 10.17, the response time can be obtained from the response curves measured at high stirrer speeds in the absence of liquid films. For commercially available steam-sterilisable electrodes, response times are usually in the range of 10 to 100 s. However, faster nonautoclavable electrodes with response times of 2 to 3 s are also available, as are microelectrodes that respond even more rapidly. Some oxygen electrodes have responses that deviate substantially from first-order (e.g., the electrode may have a tailing response so that it slows excessively as the new dissolved oxygen level is approached), or there may be a significant difference between the response times for upward and downward step changes. Such electrodes are not suitable for dynamic k_La measurements.

In viscous fermentation broths, it may be impossible to eliminate liquid boundary layers in the test experiments, even at high stirrer speeds. This makes estimation of the electrode response time difficult using fermentation fluid. Instead, τ_E may be evaluated using water, with the assumption that the electrode response does not depend on the measurement fluid. Experiments in water at different stirrer speeds are still required to ensure that τ_E is determined in the absence of boundary layer effects. Although the value of τ_E may be obtained in water, because the development of liquid films depends strongly on the properties of the fluid, measurements in water do not provide information about the elimination of boundary layers in the actual fermentation broth.

The results from the test experiments are used to check the validity of two of the assumptions involved in the simple dynamic method. Assumption (2) (Section 10.10.2, Simple Dynamic Method subsection) is valid if the electrode response time is small compared with the rate of oxygen transfer; this is checked by comparing the value of τ_E with $1/k_La$. The error in k_La has been estimated to be <6% for $\tau_E \leq 1/k_La$ and <3% for $\tau_E \leq 0.2/k_La$, so that commercial electrodes with response times between 2 and 3 s can be used to measure k_La values up to about 0.1 s^{-1} [22]. For assumption (3) to be valid, only stirrer speeds above that eliminating liquid boundary layers at the probe surface in culture broth

can be used to determine $k_L a$. If either assumption (2) or (3) does not hold, the simple dynamic method cannot be used to measure $k_L a$. Factors involved in assumption (4) are outlined in the following section.

Gas-Phase Dynamics

The term *gas-phase dynamics* refers to changes with time in the properties of a gas dispersion, including the number and size of the bubbles and the gas composition. Gas-phase dynamics can have a substantial influence on the results of $k_L a$ measurement. Because of the complexity and uncertainty associated with gas flow patterns, it is difficult to accurately account for these effects except in the simplest situations. Problems associated with gas-phase behaviour can make the dynamic method an impractical technique for determining $k_L a$. As the average residence time of bubbles in the liquid increases, so does the influence of gas dynamics on measured $k_L a$ values.

In the dynamic method, a change in aeration conditions is used as the basis for evaluating $k_L a$. However, although the inlet gas flow rate and composition may be altered quickly, this does not necessarily result in an immediate change in the gas hold-up and composition of the bubbles dispersed in the liquid. Depending on system variables such as the extent of gas recirculation, coalescence properties of the liquid, and fluid viscosity, some time is required for a new gas hold-up and gas-phase composition to be established. Therefore, because the driving force for oxygen transfer depends on the gas-phase oxygen concentration, and as $k_L a$ varies with the volume of gas hold-up through its dependence on the interfacial area a, the oxygen transfer conditions and $k_L a$ itself are likely to be changing during the measurement period. Until a new steady state is established within the dispersed gas phase, the measured values of C_{AL} represent not only the kinetics of oxygen transfer but also the gas-phase dynamics in the fermenter.

Let us consider the two methods commonly used to deoxygenate the culture broth for dynamic $k_L a$ measurement. Both these procedures affect the state of the gas dispersion at the start of the measurement period.

- *Nitrogen sparging*. In this version of the simple dynamic method, nitrogen is sparged into the broth at t_0 to achieve an initial reduction in dissolved oxygen tension. Depending on the duration of nitrogen sparging, at the end of the deoxygenation step we can assume at least that the gas hold-up contains more nitrogen and less oxygen than in air. In the presence of an active cell culture, the bubbles will also contain carbon dioxide and, depending on the humidity of the inlet gas, water vapour. If, at the commencement of the measurement period, the gas supply is suddenly switched to air at the same flow rate, the gas hold-up volume, and therefore the gas−liquid interfacial area a, will remain roughly the same, but the composition of gas in the bubbles will start to change. As a result of gas mixing and dispersion at the impeller, bubble coalescence, and gas recirculation, the incoming air mixes with the preexisting nitrogen-rich hold-up until all the excess nitrogen from the deoxygenation step is flushed out of the system. Until this process is complete, the measured C_{AL} values will be influenced by the changing gas-phase composition.
- *De-gassing*. An alternative procedure for deoxygenation of active broth is to switch off the normal air supply to the fermenter at t_0 (Figure 10.14), thus allowing oxygen

consumption by the cells to reduce the dissolved oxygen tension. Depending on the extent of gas recirculation and the time required for bubbles to escape the liquid, the gas hold-up volume will be reduced during the deoxygenation step. When aeration is recommenced, the gas hold-up and gas–liquid interfacial area a must be reestablished before k_La becomes constant. Until this occurs, the measured C_{AL} values will be affected by changes in the gas hold-up.

Transient gas-phase conditions are created using both strategies commonly applied for deoxygenation during dynamic k_La measurement. Even if the fermenter is relatively small, gas-phase transitions may continue to occur for a substantial proportion of the measurement period, thus compromising the accuracy of measured k_La values. If nitrogen sparging is used, the high-nitrogen hold-up is more readily flushed out of the liquid if the hold-up volume is low, the gas flow rate is high, and the liquid has a low viscosity so that bubbles disengage quickly and are not trapped in the fluid. Bubble recirculation from the bulk liquid back to the impeller should also be minimal to allow nitrogen-rich bubbles to escape quickly from the vessel. As gas recirculation occurs to a greater extent in intensely agitated tanks, the effect of gas-phase dynamics after nitrogen sparging is more significant in systems operated with high stirrer power per unit volume. If the de-gassing procedure is used instead, a new steady-state gas hold-up is established more quickly if the hold-up volume is low.

As nitrogen sparging and switching off the air supply leave the gas phase in significantly different states after culture deoxygenation, a comparison of k_La values determined using both deoxygenation methods under otherwise identical conditions may show whether gas dynamics are important. If the k_La values are similar, this suggests that changes in gas composition and hold-up occur rapidly relative to the rate of gas–liquid oxygen transfer, giving us more confidence in the measurement technique. However, the limitations imposed by gas-phase dynamics are difficult to overcome and it is possible that the simple dynamic method will be unable to provide reliable k_La results in particular applications.

EXAMPLE 10.3 ESTIMATING k_La USING THE SIMPLE DYNAMIC METHOD

A stirred fermenter is used to culture haematopoietic cells isolated from umbilical cord blood. The liquid volume is 15 litres. The simple dynamic method is used to determine k_La. The air flow is shut off for a few minutes and the dissolved oxygen level drops; the air supply is then reconnected at a flow rate of 0.25 l s^{-1}. The following results are obtained at a stirrer speed of 50 rpm.

Time (s)	5	20
Oxygen tension (% air saturation)	50	66

When steady state is established, the dissolved oxygen tension is 78% air saturation. In separate test experiments, the electrode response to a step change in oxygen tension did not vary with stirrer speed above 40 rpm. The probe response time under these conditions was 2.8 s. When the

$k_L a$ measurement was repeated using nitrogen sparging to deoxygenate the culture, the results for oxygen tension as a function of time were similar to those listed. Estimate $k_L a$.

Solution

$\overline{C}_{AL} = 78\%$ air saturation. Let us define $t_1 = 5$ s, $C_{AL1} = 50\%$, $t_2 = 20$ s, and $C_{AL2} = 66\%$. From Eq. (10.57):

$$k_L a = \frac{\ln\left(\frac{78-50}{78-66}\right)}{(20-5)\,\mathrm{s}} = 0.056\,\mathrm{s}^{-1}$$

Before we can be confident about this value for $k_L a$, we must consider the electrode response time, the presence of liquid films at the surface of the probe, and the influence of gas-phase dynamics. The results from the test experiments indicate that there are no liquid film effects at 50 rpm. For $\tau_E = 2.8$ s and $1/k_L a = 17.9$ s, $\tau_E = 0.16/k_L a$. From Section 10.10.2 (Electrode Response Time and Liquid Boundary Layers subsection), as $\tau_E < 0.2/k_L a$, τ_E is small enough that the error associated with the electrode response can be neglected. Because the measured results for oxygen tension were similar using two different deoxygenation methods, the effect of gas-phase dynamics can also be neglected. Therefore, $k_L a$ is 0.056 s^{-1}.

Modified Dynamic Methods

When the electrode response is slow, if liquid boundary layers at the probe surface cannot be eliminated, or if the effects of gas-phase dynamics are significant, the simple dynamic method (Section 10.10.2, Simple Dynamic Method subsection) is not suitable for estimating $k_L a$. Sterilisable dissolved oxygen electrodes used in fermenters typically have relatively long response times, and measuring $k_L a$ under nonsterile conditions with a fast, nonautoclavable electrode is not always practical. It is also sometimes impossible to eliminate liquid boundary layers during $k_L a$ measurement, particularly in viscous fluids; moreover, stirrer speeds may be restricted in some cultures to avoid cell damage. In general, unless there is evidence to the contrary, gas-phase dynamics are expected to influence dynamic $k_L a$ measurements and often cannot be neglected. Large errors greater than 100% have been found to occur when the simple dynamic method is applied without correction for these effects.

Several modified procedures have been developed to account for the experimental factors that affect the results of the simple dynamic method. Equations describing the mass transfer processes responsible for electrode lag and liquid film resistance can be included in the models used to evaluate $k_L a$ [34]. Alternatively, after applying moment analysis of the response curves, the data for dissolved oxygen tension can be normalised based on empirical observation of any electrode, liquid film, or gas mixing effects [35]. Accounting for gas-phase dynamics and imperfections in gas mixing is the most challenging correction required. Gas-phase oxygen concentrations estimated as a function of time and location have been incorporated into the model equations [36]; the experimental methods can also be modified to alleviate the uncertainty about gas-phase properties [37].

A useful variation of the dynamic methods discussed so far is the *dynamic pressure method*. In this technique, a step change in aeration conditions is achieved, not by altering the composition of the inlet gas stream, but by imposing a step change in fermenter pressure. Temporarily closing and then constricting the gas outlet during sparging is an effective method for inducing the required pressure change, including in large-scale vessels. A relatively small pressure increase of about 20% is sufficient. The k_La value is evaluated from measurements of the dissolved oxygen tension as the system moves towards steady state at the new pressure. The advantage of this approach is that the oxygen concentration is changed in all the bubbles in the vessel simultaneously, thus avoiding the problems of transient gas-phase composition or loss of gas hold-up that occur with the simple dynamic method. However, the expansion or shrinkage of bubbles immediately after a sudden pressure change can cause difficulties if the bubble sizes are slow to restabilise; the oxygen probe must also be unaffected by pressure variation. Further details of this method are available [38, 39]. The dynamic pressure method applied in conjunction with equations to correct for electrode and liquid film effects is widely considered to be the most reliable approach for dynamic k_La measurement.

10.10.3 Sulphite Oxidation

This method is based on oxidation of sodium sulphite to sulphate in the presence of a catalyst such as Cu^{2+} or Co^{2+}. Although the sulphite method has been used extensively, the results appear to depend on operating conditions in an unknown way and usually give higher k_La values than other techniques. Accordingly, its application is discouraged [22]. Because salt solutions are used, the average bubble size is affected by changes in the coalescence properties of the liquid and the results obtained have limited applicability to real fermentation broths.

10.11 MEASUREMENT OF THE SPECIFIC OXYGEN UPTAKE RATE, q_O

Application of Eqs. (10.42) and (10.43) for analysis of the mass transfer performance of fermenters requires knowledge of the specific oxygen uptake rate, q_O. This parameter reflects the intrinsic requirement of an organism for oxygen to support growth and product synthesis. It can be measured using several experimental techniques.

The oxygen balance method for measuring k_La (Section 10.10.1) also allows us to evaluate q_O. At steady state, the volumetric rate of oxygen uptake by the cells is equal to the volumetric rate of gas–liquid oxygen transfer, N_A (Section 10.5.2). Once N_A is determined using Eq. (10.53), q_O is found by dividing N_A by the cell concentration x. For example, for N_A with units of gmol l^{-1} s^{-1} and x with units of g l^{-1}, q_O is obtained with units of gmol g^{-1} s^{-1}. As discussed in Section 10.10.1, the accuracy of this technique depends strongly on accurate measurement of the inlet and outlet gas composition, flow rate, pressure, and temperature, and on the validity of the assumptions used to derive the mass transfer equations.

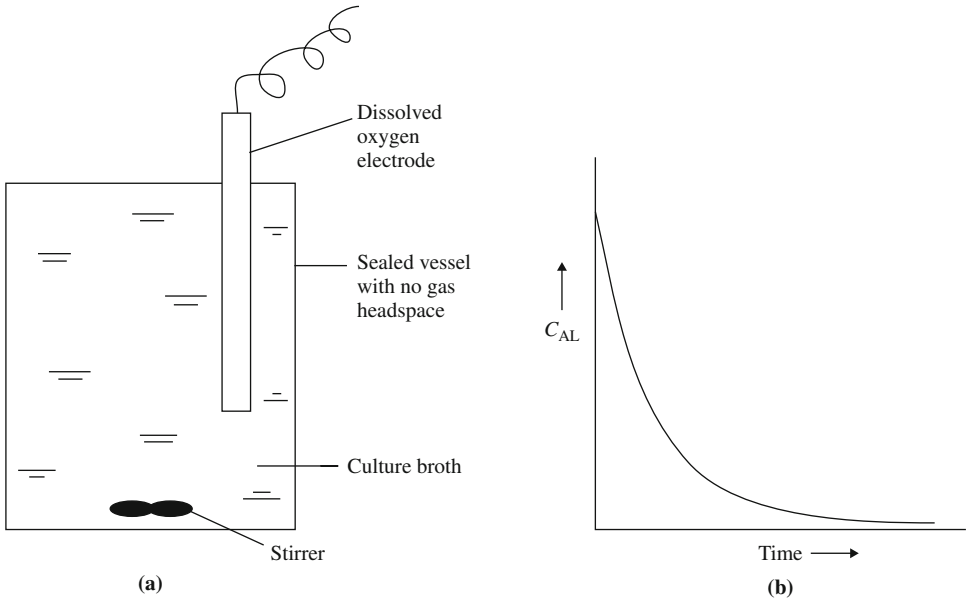

FIGURE 10.18 Dynamic method for measurement of q_O. (a) Sealed experimental chamber equipped with an oxygen electrode and stirrer and containing culture broth. (b) Measured data for dissolved oxygen concentration C_{AL} versus time.

Dynamic methods can also be used to measure q_O. A sample of culture broth containing a known cell concentration x is placed in a small chamber equipped with an oxygen electrode and stirrer as shown in Figure 10.18(a). The broth is sparged with air: at the commencement of the measurement period, the air flow is stopped and the vessel sealed to make it airtight. The decline in dissolved oxygen concentration C_{AL} due to oxygen uptake by the cells is recorded using the oxygen electrode as shown in Figure 10.18(b). The initial slope of the curve of C_{AL} versus time gives the volumetric rate of oxygen uptake by the cells, Q_O. Dividing Q_O by the cell concentration x gives the specific rate of oxygen uptake, q_O. All gas bubbles must be removed from the liquid before the measurements are started; the sealed chamber must also be airtight without any gas headspace so that additional oxygen cannot enter the liquid during data collection.

Factors similar to those outlined in Section 10.10.2 for dynamic measurement of k_La also affect the accuracy of q_O obtained using this technique. The electrode response must be relatively fast and liquid boundary layers at the probe surface must be eliminated by operating the stirrer at a sufficiently high speed. Fortunately, unlike for k_La measurement, the concentration of cells in the chamber can be adjusted to make it easier to comply with these requirements. If necessary, a relatively dilute cell suspension can be used to reduce the speed of oxygen uptake so that a relatively slow electrode response does not affect the results and any liquid boundary layers are more readily removed. The size of the vessel is also typically very small to minimise the effects of gas-phase dynamics and mixing characteristics.

10.12 PRACTICAL ASPECTS OF OXYGEN TRANSFER IN LARGE FERMENTERS

Special difficulties are associated with measuring oxygen transfer rates and $k_L a$ in large fermenters. These problems arise mainly because significant gradients of liquid- and gas-phase composition and other properties develop with increasing scale.

10.12.1 Liquid Mixing

In our discussion of oxygen transfer so far, we have assumed that the liquid phase is perfectly mixed and that $k_L a$ is constant throughout the entire reactor. This requires that turbulence and rates of turbulence kinetic energy dissipation are uniformly distributed. These conditions occur reasonably well in laboratory-scale stirred reactors, which are characterised by high turbulence throughout most of the vessel. In contrast, as discussed in Section 8.11, perfect mixing is difficult to achieve in commercial-scale reactors and, as illustrated in Figures 8.16 and 8.23, turbulence is far from uniformly distributed. Most of the oxygen transfer in industrial-scale fermenters takes place in the region near the impeller. In much of the rest of the vessel, the bubbles are in free rise and the liquid velocity is significantly reduced, especially if the viscosity is high. The composition of the liquid phase, which has a strong influence on bubble interfacial properties and $k_L a$, can also vary significantly within large vessels.

Imperfect mixing in large-scale fermenters has a number of consequences for the quantification of oxygen transfer. First, different values of $k_L a$ and a range of oxygen uptake rates could be determined depending on where in the tank the dissolved oxygen concentration C_{AL} is measured. Accordingly, $k_L a$ values from a particular measurement location may not be representative of overall oxygen transfer conditions. Moreover, it may be possible to increase oxygen transfer significantly by improving bulk mixing conditions. Although relationships such as Eq. (10.50) predict that $k_L a$ will be the same as long as the power and gas flow rate remain constant, if different degrees of mixing are achieved for the same power input, a change in measured $k_L a$ values could be observed as conditions in the vessel become more homogeneous.

Equations (10.50) and (10.51) apply to well-mixed systems. For production-scale bioreactors, a better representation of oxygen transfer may be achieved using a two-compartment model of the vessel, with different correlations applied to the mixed zone close to the impeller and the bubble zone away from the impeller [40].

10.12.2 Gas Mixing

In analysis of oxygen transfer, it is often assumed that the gas phase is well mixed—that is, the gas composition is uniform and equal to that in the outlet gas stream. In large fermenters, these conditions may not be met due to substantial depletion of oxygen in the gas phase during passage of the bubbles from the bottom to the top of the tank. This creates an axial gradient of gas-phase concentration down the height of the vessel. Differences in composition between the inlet and outlet gas streams are greater in large

tanks than at small scales. Modified mass transfer models that include the effects of plug flow or plug flow with axial dispersion in the gas phase have been used to better represent the gas mixing conditions in large-scale fermenters [36, 41].

10.12.3 Pressure Effects

Even when there is rapid mixing in large-scale fermenters, variations in gas-phase pressure occur due to static pressure changes down the height of the vessel. The pressure at the bottom of tall vessels is higher than at the top due to the weight of the liquid. The static pressure difference p_s is given by the equation:

$$p_s = \rho g H_L \tag{10.58}$$

where ρ is the liquid density, g is gravitational acceleration, and H_L is the liquid height. As the solubility of oxygen is sensitive to gas-phase pressure and oxygen partial pressure, significant variation in these conditions between the top and bottom of the vessel affects the value of C^*_{AL} used in mass transfer calculations. Allowance can be made for this in models of the mass transfer process [42]; alternatively, an average concentration-difference driving force $(C^*_{AL} - C_{AL})$ across the system can be determined. A suitable average is the *logarithmic-mean concentration difference*, $(C^*_{AL} - C_{AL})_{lm}$:

$$(C^*_{AL} - C_{AL})_{lm} = \frac{(C^*_{AL} - C_{AL})_o - (C^*_{AL} - C_{AL})_i}{\ln\left[\dfrac{(C^*_{AL} - C_{AL})_o}{(C^*_{AL} - C_{AL})_i}\right]} \tag{10.59}$$

In Eq. (10.59), subscripts i and o represent conditions at the inlet and outlet ends of the vessel, respectively.

10.12.4 Interaction between Oxygen Transfer and Heat Transfer

As discussed in Chapter 9, heat transfer is a critical function in bioreactors. In large-scale vessels, the fermentation broth must be cooled to remove the heat generated by metabolism and thus prevent the culture temperature rising to deleterious levels. Because the rate of metabolic heat generation in aerobic cultures is directly proportional to the rate of oxygen consumption by the cells (Section 5.9.2), oxygen transfer and heat transfer are closely related. Rapid oxygen uptake can create major heat removal problems. For highly aerobic cultures in large fermenters that deliver high oxygen transfer rates, heat transfer can become the limiting factor affecting the maximum feasible rate of reaction.

The heat transfer situation is usually most severe towards the end of the culture cycle when the volumetric rate of oxygen uptake, Q_O, is greatest. In some cases, it may be sensible to slow down the rate of oxygen consumption by the culture to avoid the necessity of installing expensive heat transfer equipment and processes. Therefore, if strategies such as increasing the stirrer speed, gas flow rate, pressure, and oxygen partial pressure (Section 10.6) are undertaken to improve k_La and the oxygen transfer driving force, the consequent extra heat burden must be borne in mind. Heat and oxygen transfer are linked and should be considered together, especially in large-scale operations.

10.13 ALTERNATIVE METHODS FOR OXYGENATION WITHOUT SPARGING

In small-scale bioreactors or when shear-sensitive organisms such as animal cells are being cultured, alternative methods for providing oxygen are sometimes used. As outlined in Section 8.16.1 (Cell Damage from Bursting Bubbles subsection), the large forces generated by bubbles bursting at the surface of sparged cell cultures can cause very high rates of animal cell damage. For that reason, aeration by other means may be required or preferred.

An alternative to gas sparging is *surface aeration*. Using this approach, gas containing oxygen is flushed through the headspace of the reactor above the liquid; oxygen is then transferred to the liquid through the upper surface of the culture broth. Surface aeration contributes to oxygen transfer even when the liquid is aerated by sparging; however, in vigorously agitated systems, its contribution is small compared with the high oxygenation rates achieved using entrained bubbles. The rate of oxygen transfer during surface aeration can be described using the equations in Section 10.4.3, with $k_L a$ in Eq. (10.39) representing the conditions in the liquid boundary layer at the liquid−headspace interface. The value of $k_L a$ and the rate of surface aeration increase with stirrer speed. The height of the impeller above the vessel floor may also be important because it affects the fluid velocity at the liquid surface.

Even though animal cell cultures have relatively low oxygen requirements as indicated earlier in Table 10.1, surface aeration can be inadequate for supporting growth to high cell densities. For suspension culture of baby hamster kidney cells, $k_L a$ values for surface aeration have been reported in the range 2.8×10^{-5}–$1.1 \times 10^{-3}\ s^{-1}$, whereas $k_L a$ for aeration of the same cultures by sparging is 2.8×10^{-4}–$6.9 \times 10^{-3}\ s^{-1}$ [43]. Because mild agitation and reduced air flow rates are used with animal cells in sparged systems to avoid hydrodynamic and bubble damage, these $k_L a$ values with sparging are significantly lower than the range of 0.02 to $0.25\ s^{-1}$ typically found in production-scale fermenters used for microbial culture. Relative to the liquid volume, the area available for oxygen transfer by surface aeration declines significantly as the size of the fermenter increases. As a result, surface aeration is unsuitable for large-scale operations or must be supplemented by other techniques.

Membrane tubing aeration is another bubble-free option for oxygenation of cultures. Aeration is achieved by gas exchange through silicone or microporous polypropylene or Teflon tubing immersed in the culture broth. Gas flowing in the tube diffuses through the tube walls and into the medium under a concentration-difference driving force; air or oxygen-enriched air may be used in the tubing. For bubble-free aeration, the gas pressure inside the tubing must remain below the bubble point to avoid bubbles forming on the outside of the tube walls. In membrane aeration, the main resistances to oxygen transfer are the tube wall itself and the liquid film surrounding the outside of the tubing. To prevent the cells from settling and to promote mixing, the tubing assembly may be kept in motion as an effective stirrer; this also enhances oxygen transfer through the liquid boundary layer at the tube surface. Membrane aeration is used mainly for small-scale animal cell culture.

10.14 OXYGEN TRANSFER IN SHAKE FLASKS

Shake flasks, *conical flasks*, or *Erlenmeyer flasks* are employed commonly in laboratories for microbial and plant cell culture. Their application for animal cell culture is less frequent. Shake flasks with capacity from 25 ml to 5 litres are used for a wide range of experimental purposes, including screening and assessing cell lines, testing the effects of culture conditions, and bioprocess development.

A typical shake flask is shown in Figure 10.19. Shake flasks have flat bottoms and sloping sides and can be made of glass, plastic, or metal. The flask opening is of variable width and is fitted with a porous cap or plug closure. Gases are exchanged through the closure without the introduction of contaminating organisms. Flasks containing culture broth are placed on shaking tables or in incubator–shakers; the shaking movement is responsible for mixing and mass transfer in the flask. Shaking can be performed using either an *orbital* motion, which is also called *rotary* or *gyratory shaking*, or a linear *reciprocating* (back-and-forth) motion. Orbital shakers are becoming more common than reciprocating machines.

10.14.1 Oxygen Transfer through the Flask Closure

The first mass transfer resistance encountered in the delivery of oxygen to shake-flask cultures is the flask closure. A variety of porous materials is used to stopper shake flasks, including cotton, cotton wool bound with cheesecloth, and silicone sponge. Aluminium foil may also be used to cover the stopper and upper neck of the flask. The rate of oxygen transfer through the closure depends on the diffusion coefficient for oxygen in the material, the width of the neck opening, and the stopper depth. The diffusion coefficient varies with the porosity or bulk density of the stopper material. Wetting the stopper increases significantly the resistance to gas transfer as well as the risk of culture contamination, and can be a problem when flasks are shaken vigorously.

The flask closure affects the composition of gas in the headspace of the flask. In addition to impeding oxygen transfer into the culture, the closure prevents rapid escape of carbon dioxide and other gases generated by the cells. Volatile substances such as ethanol may also build up in the gas phase.

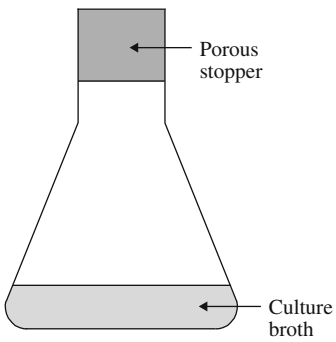

FIGURE 10.19 Typical shake flask for cell culture.

Although several types of flask stopper have been investigated for their oxygen transfer characteristics, it is unclear which type of closure gives the best results. In some cases, for example with large flasks or if the liquid is shaken very vigorously, the flask closure becomes the dominant resistance for oxygen transfer to the cells.

10.14.2 Oxygen Transfer within the Flask

The culture broth in shake flasks is supplied with oxygen by surface aeration from the gas atmosphere in the flask. Within the flask, the main resistance to oxygen transfer is the liquid-phase boundary layer at the gas–liquid interface. The rate of oxygen transfer from the gas phase is represented by Eq. (10.39) and depends on the area available for oxygen transfer, the liquid velocity, the viscosity, diffusion coefficient, and surface mobility at the phase boundary, and the concentration-difference driving force ($C^*_{AL} - C_{AL}$). Although oxygen transfer in shake flasks does not depend on the coalescing properties of the liquid because of the absence of bubbles, electrolytes and other components in the broth may affect the oxygen solubility and surface properties at the interface.

The area available for oxygen transfer in shake flasks is not simply equal to the surface area of the resting fluid as represented in Figure 10.19. When a flask is shaken on an orbital shaker, the liquid is distributed within the flask as shown in Figure 10.20: liquid is thrown up onto the walls due to the centrifugal forces associated with flask rotation. As the liquid swirls around the flask, a thin film is deposited on the flask wall and is replaced with each rotation. Because this film is available for oxygen transfer into the liquid, the mass transfer area a at any given time includes the surface area of liquid film on the flask wall. The overall rate of oxygen transfer depends on the rate of generation of fresh liquid surface, or the frequency with which the liquid film is replenished.

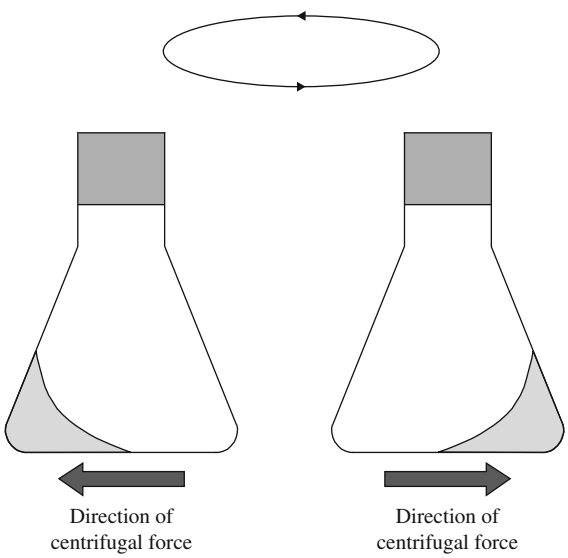

FIGURE 10.20 Distribution and movement of liquid in a shake flask on an orbital shaker.

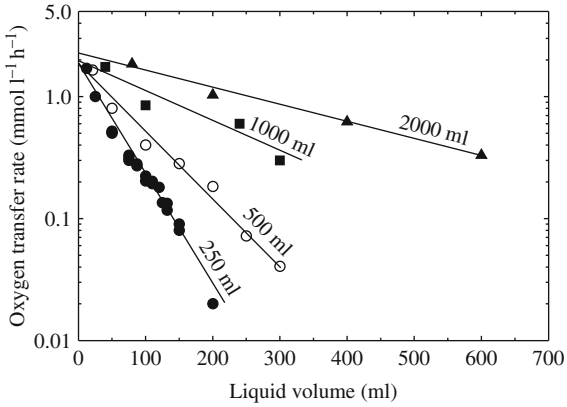

FIGURE 10.21 Effect of flask size and liquid volume on the rate of oxygen transfer. Shake flasks of nominal size—(●) 250 ml, (○) 500 ml, (■) 1000 ml, and (▲) 2000 ml—were tested on a reciprocating shaker with amplitude 3 in. operated at 96 rpm. The data are plotted using semi-logarithmic coordinates.
Data from M.A. Auro, H.M. Hodge, and N.G. Roth, 1957, Oxygen absorption rates in shaken flasks. Ind. Eng. Chem. *49, 1237–1238.*

Oxygen transfer in shake flasks is sensitive to operating conditions that affect the development of liquid films at the flask wall. Factors influencing the value of *a* include:

- Flask shape
- Flask size
- Surface properties of the flask walls (e.g., hydrophilic or hydrophobic)
- Shaking speed
- Flask displacement during shaking
- Liquid volume
- Liquid properties (e.g., viscosity)

The area of liquid film per unit volume of fluid is enhanced using large flasks with small liquid volumes on shakers with large displacement distance per rotation operated at high speed. As indicated in Figure 10.21, the rate of oxygen transfer is strongly dependent on flask size and liquid volume. The importance of limiting the liquid volume in shake flasks is evident in Figure 10.21; for example, using >100 ml of medium in a 250-ml flask reduces the mass transfer coefficient substantially compared with 50 ml. It is also important that the flask material support the development of a liquid film on the walls; hydrophobic materials such as plastic are therefore not recommended when oxygen transfer is critical. The difference between oxygen transfer rates in hydrophilic and hydrophobic flasks is illustrated in Figure 10.22. When the culture's oxygen requirements are high, gas–liquid mass transfer can be enhanced in shake flasks by the use of baffles, creases, or dimples in the flask walls. These indentations break up the swirling motion of the liquid, increase the level of liquid splashing onto the flask walls, and thus improve aeration. A disadvantage of using baffles is the increased risk of wetting the flask closure.

Because surface-to-volume ratios decrease with increasing liquid volume, shake-flask culture and surface aeration are practical only at relatively small scales. For some cultures, the maximum rate of oxygen transfer in shake flasks is not sufficient to meet the cellular oxygen demand. In these cases, shake flasks offer insufficient oxygen supply and the culture performance is limited by oxygen transfer.

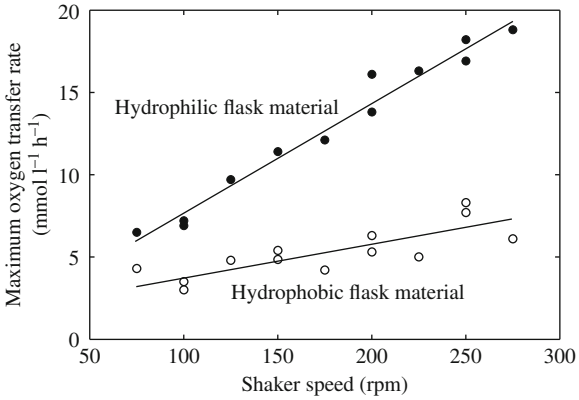

FIGURE 10.22 Effect of flask material properties on the rate of oxygen transfer in 250-ml shake flasks on an orbital shaker.
Data from U. Maier and J. Büchs, 2001, Characterisation of the gas–liquid mass transfer in shaking bioreactors. Biochem. Eng. J. *7, 99–106.*

SUMMARY OF CHAPTER 10

At the end of Chapter 10 you should:

- Be able to describe the *two-film theory* of mass transfer between phases
- Know *Fick's law* in terms of the *binary diffusion coefficient*, $\mathscr{D}_{AB}$
- Be able to describe in simple terms the mathematical analogy between mass, heat, and momentum transfer
- Know the equation for the rate of gas–liquid oxygen transfer in terms of the *mass transfer coefficient* $k_L a$ and the *concentration-difference driving force*
- Understand the importance of the *critical oxygen concentration*
- Be able to identify the steps that are most likely to present major resistances to oxygen transfer from bubbles to cells
- Understand how oxygen transfer and $k_L a$ can limit the biomass density in fermenters
- Understand the mechanisms of *gas dispersion* and *coalescence* in stirred fermenters and the importance of bubble size in determining *gas hold-up* and $k_L a$
- Know how $k_L a$ depends on bioreactor operating conditions such as the stirrer speed, power input, gas flow rate, and liquid properties such as viscosity
- Know how temperature, total pressure, oxygen partial pressure, and the presence of dissolved and suspended material affect the rate of oxygen transfer and the solubility of oxygen in fermentation broths
- Be able to apply the *oxygen balance method* and the *simple dynamic method* for experimental determination of $k_L a$, with understanding of their advantages and limitations
- Know how the specific oxygen uptake rate q_O can be measured in cell cultures
- Understand the particular problems affecting assessment of oxygen transfer in large fermenters
- Be familiar with techniques for culture aeration that do not involve gas sparging
- Understand the mechanisms of oxygen transfer in shake flasks

PROBLEMS

10.1 Rate-controlling processes in fermentation

Serratia marcescens bacteria are used for the production of threonine. The maximum specific oxygen uptake rate of *S. marcescens* in batch culture is 5 mmol O_2 g^{-1} h^{-1}. It is planned to operate the fermenter to achieve a maximum cell density of 40 g l^{-1}. At the fermentation temperature and pressure, the solubility of oxygen in the culture liquid is 8×10^{-3} kg m^{-3}. At a particular stirrer speed, $k_L a$ is 0.15 s^{-1}. Under these conditions, will the rate of cell metabolism be limited by mass transfer or depend solely on metabolic kinetics?

10.2 Test for oxygen limitation

An 8-m^3 stirred fermenter is used to culture *Agrobacterium* sp. ATCC 31750 for production of curdlan. The liquid medium contains 80 g l^{-1} sucrose. Under optimal conditions, 1.0 g dry weight of cells is produced for every 4.2 g of sucrose consumed. The fermenter is sparged with air at 1.5 atm pressure, and the specific oxygen demand is 7.5 mmol per g dry weight per h. To achieve the maximum yield of curdlan, the fermentation temperature is held constant at 32°C. The solubility of oxygen in the fermentation broth is 15% lower than in water due to solute effects. If the maximum $k_L a$ that can be achieved is 0.10 s^{-1}, does the fermenter's mass transfer capacity support complete consumption of substrate?

10.3 $k_L a$ required to maintain critical oxygen concentration

A genetically engineered strain of yeast is cultured in a bioreactor at 30°C for production of heterologous protein. The oxygen requirement is 80 mmol l^{-1} h^{-1}; the critical oxygen concentration is 0.004 mM. The solubility of oxygen in the fermentation broth is estimated to be 10% lower than in water due to solute effects.

(a) What is the minimum mass transfer coefficient necessary to sustain this culture with dissolved oxygen levels above critical if the reactor is sparged with air at approximately 1 atm pressure?

(b) What mass transfer coefficient is required if pure oxygen is used instead of air?

10.4 Oxygen transfer with different impellers

A 10-m^3 stirred fermenter with liquid height 2.3 m is used to culture *Trichoderma reesei* for production of cellulase. The density of the culture fluid is 1000 kg m^{-3}. An equation for the oxygen transfer coefficient as a function of operating variables has been developed for *T. reesei* broth:

$$k_L a = 2.5 \times 10^{-3} \left(\frac{P_T}{V_L}\right)^{0.7} u_G^{0.3}$$

where $k_L a$ has units of s^{-1}, P_T is the total power input in W, V_L is the liquid volume in m^3, and u_G is the superficial gas velocity in m s^{-1}. The fermenter is sparged using a gas flow rate of 0.6 vvm (vvm means volume of gas per volume of liquid per minute). The vessel is stirred with a single impeller but two alternative impeller designs, a Rushton turbine and a curved-blade disc turbine, are available. Both impellers are sized and operated so that their ungassed power draw is 9 kW.

(a) If the power loss with gassing is 50% for the Rushton and 5% for the curved-blade turbine, compare the $k_L a$ values achieved using each impeller.

(b) What is the percentage contribution to P_T from gassing with the two different impellers?

(c) If the cell concentration is limited to 15 g l^{-1} using the Rushton turbine because of mass transfer effects, estimate the maximum possible cell concentration with the curved-blade disc turbine.

It is decided to install the Rushton turbine, but to compensate for the effect on k_La of its loss of power with gassing by increasing the gas flow rate.

(d) Estimate the gas flow rate required to obtain the same maximum cell concentration using the Rushton turbine as that achieved with the curved-blade disc turbine. Express your answer in vvm. What are your assumptions? (Iterative solution may be required.)

10.5 Foam control and oxygen transfer

Foaming is controlled routinely in fermenters using a foam sensor and pump for automatic addition of antifoam agent. As shown in Figure 10P5.1, the foam sensor is located at the top of the vessel above the liquid surface. When a head of foam builds up so that foam contacts the lower tip of the sensor, an electrical signal is sent to the pump to add antifoam. The antifoam agent destroys the foam, the foam height is therefore reduced, contact with the foam sensor is broken, and the pump supplying the antifoam agent is switched off. Further build-up of foam reactivates the control process.

If the position of the foam sensor is fixed, when the gap between the liquid surface and sensor is reduced by raising the liquid height, a smaller foam build-up is tolerated before antifoam agent is added. Therefore, antifoam addition will be triggered more often if the working volume of the vessel is increased. Although a greater fermenter working volume means that more cells and/or product are formed, addition of excessive antifoam

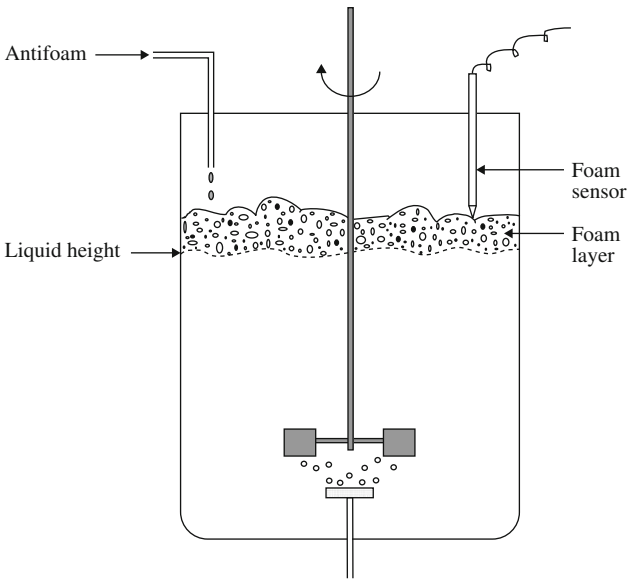

FIGURE 10P5.1 Stirred fermenter with automatic foam control system.

agent could reduce $k_L a$ significantly, thereby increasing the likelihood of mass transfer limitations.

A stirred fermenter of diameter 1.5 m is used to culture *Bacillus licheniformis* for production of serine alkaline protease. The fermenter is operated five times with automatic antifoam addition using five different liquid heights. The position of the foam sensor is the same in each fermentation. The volume of antifoam added and the $k_L a$ at the end of the culture period are recorded.

Liquid height (m)	Antifoam added (l)	$k_L a$ (s^{-1})
1.10	0.16	0.016
1.29	0.28	0.013
1.37	1.2	0.012
1.52	1.8	0.012
1.64	2.4	0.0094

Under ideal conditions, the maximum specific oxygen uptake rate for *B. licheniformis* is 2.6 mmol g^{-1} h^{-1}. When glucose is used as the carbon source at an initial concentration of 20 g l^{-1}, a maximum of 0.32 g of cells are produced for each g of glucose consumed, and 0.055 g of protease is produced per g of biomass formed. The solubility of oxygen in the broth is estimated as 7.8 g m^{-3}.

(a) Using the $k_L a$ values associated with each level of antifoam addition, estimate the maximum cell concentrations supported by oxygen transfer as a function of liquid height. Assume that antifoam exerts a much stronger influence on $k_L a$ than on other properties of the system such as oxygen solubility and specific oxygen uptake rate.

(b) Calculate the maximum mass of cells and maximum mass of protease that can be produced based on the oxygen transfer capacity of the fermenter as a function of liquid height.

(c) Is protease production limited by oxygen transfer at any of the liquid heights tested?

(d) What operating liquid height would you recommend for this fermentation process? Explain your answer.

10.6 Improving the rate of oxygen transfer

Rifamycin is produced in a 17-m^3 stirred fermenter using a mycelial culture, *Nocardia mediterranei*. The fermenter is sparged with air under slight pressure so the solubility of oxygen in the broth is 10.7 g m^{-3}. Data obtained during operation of the fermenter are shown in Figure 10P6.1. After about 147 hours of culture, vegetable oil is added to the broth to disperse a thick build-up of foam. This has a severe effect on the oxygen transfer coefficient and reduces the dissolved oxygen tension.

(a) Calculate the steady-state oxygen transfer rate before and after addition of the vegetable oil.

(b) The relationship between $k_L a$ and the fermenter operating conditions is:

$$k_L a \propto \left(\frac{P_T}{V_L}\right)^{0.5} u_G{}^{0.3}$$

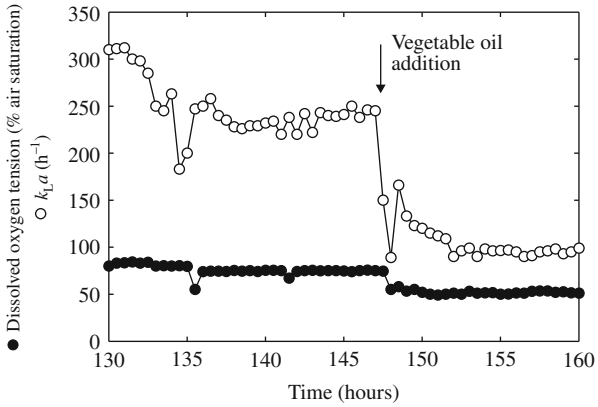

FIGURE 10P6.1 Online time-course data from a stirred fermenter used for rifamycin production.

Because increasing the gas flow rate would aggravate the problems with foaming, it is decided to restore the value of k_La by increasing the power input by stirring. If the power contribution from gas sparging is negligible, by how much does the stirrer power need to be increased to overcome the effects of the vegetable oil on k_La?

(c) To save the cost of increasing the power input, instead of (b), it is decided to improve oxygen transfer by sparging the fermenter with oxygen-enriched air. The total gas flow rate and pressure are unchanged. To restore the rate of oxygen transfer after vegetable oil addition to that before oil was added, what volume percentage of oxygen is required in the sparge gas if the desired dissolved oxygen concentration in the broth is 6.2×10^{-3} kg m^{-3}?

10.7 Oxygen transfer for different cell types

The specific oxygen demands and critical oxygen concentrations for typical microbial, plant, and animal cell cultures are listed below.

Cell culture	q_O	C_{crit} (mmol l^{-1})
Escherichia coli	8.5 mmol (g dry weight)$^{-1}$ h^{-1}	0.0082
Vitis vinifera (grape)	0.60 mmol (g dry weight)$^{-1}$ h^{-1}	0.055
Chinese hamster ovary (CHO)	3.0×10^{-10} mmol cell^{-1} h^{-1}	0.020

(a) Estimate the k_La required to achieve cell concentrations of 25 g dry weight l^{-1} for *E. coli* and *V. vinifera* and 3.0×10^9 cells l^{-1} for CHO cells, while maintaining the dissolved oxygen concentration above critical. The oxygen solubility in the media used for the cultures is 7.2×10^{-3} kg m^{-3}.

(b) The relationship between k_La and the power input to a 1-m^3 stirred bioreactor is:

$$k_La \propto \left(\frac{P_T}{V_L}\right)^{0.5}$$

Compare the bioreactor power requirements for culture of the three different cell types under the conditions described in (a).

10.8 Single-point $k_L a$ determination using the oxygen balance method

A 200-litre stirred fermenter contains a batch culture of *Bacillus subtilis* bacteria at 28°C. Air at 20°C is pumped into the vessel at a rate of 1 vvm (vvm means volume of gas per volume of liquid per minute). The average pressure in the fermenter is 1 atm. The volumetric flow rate of off-gas from the fermenter is measured as 189 l min^{-1}. The exit gas stream is analysed for oxygen and is found to contain 20.1% O_2. The dissolved oxygen concentration in the broth is measured using an oxygen electrode as 52% air saturation. The solubility of oxygen in the fermentation broth at 28°C and 1 atm air pressure is 7.8×10^{-3} kg m^{-3}.

(a) Calculate the oxygen transfer rate.

(b) Determine the value of $k_L a$ for the system.

(c) The oxygen analyser used to measure the exit gas composition was incorrectly calibrated. If the oxygen content has been overestimated by 10%, what error is associated with the result for $k_L a$?

10.9 Steady-state $k_L a$ measurement

Escherichia coli bacteria are cultured at 35°C and 1 atm pressure in a 500-litre fermenter using the following medium:

Component	Concentration (g l^{-1})
glucose	20
sucrose	8.5
$CaCO_3$	1.3
$(NH_4)_2SO_4$	1.3
Na_2HPO_4	0.09
KH_2PO_4	0.12

Air at 25°C and 1 atm is sparged into the vessel at a rate of 0.4 m^3 min^{-1}. The dissolved oxygen tension measured using a polarographic electrode calibrated in situ in sterile culture medium is 45% air saturation. The gas flow rate leaving the fermenter is measured using a rotary gas meter as 6.3 l s^{-1}. The oxygen concentration in the off-gas is 19.7%.

(a) Estimate the solubility of oxygen in the fermentation broth. What are your assumptions?

(b) What is the oxygen transfer rate?

(c) Determine the value of $k_L a$.

(d) Estimate the maximum cell concentration that can be supported by oxygen transfer in this fermenter if the specific oxygen demand of the *E. coli* strain is 5.4 mmol g^{-1} h^{-1}.

(e) If the biomass yield from the combined sugar substrates is 0.5 g g^{-1}, is growth in the culture limited by oxygen transfer or substrate availability?

10.10 Oxygen transfer in a pressure vessel

A fermenter of diameter 3.6 m and liquid height 6.1 m is used for production of ustilagic acid by *Ustilago zeae*. The pressure at the top of the fermenter is 1.4 atma. The vessel is

stirred using dual Rushton turbines and the fermentation temperature is 29°C. The dissolved oxygen tension is measured using two electrodes: one electrode is located near the top of the tank, the other is located near the bottom. Both electrodes are calibrated in situ in sterile culture medium. The dissolved oxygen reading at the top of the fermenter is 50% air saturation; the reading at the bottom is 65% air saturation. The fermenter is sparged with air at 20°C at a flow rate of 30 $m^3\ min^{-1}$ measured at atmospheric pressure. Off-gas leaving the vessel at a rate of 20.5 $m^3\ min^{-1}$ contains 17.2% oxygen. The solubility of oxygen in the fermentation broth is not significantly different from that in water. The density of the culture broth is 1000 kg m^{-3}.

(a) What is the oxygen transfer rate?

(b) Estimate the pressure at the bottom of the tank.

(c) The gas phase in large fermenters is often assumed to exhibit plug flow. Under these conditions, no gas mixing occurs so that the gas composition at the bottom of the tank is equal to that in the inlet gas stream, while the gas composition at the top of the tank is equal to that in the outlet gas stream. For the gas phase in plug flow, estimate the oxygen solubility at the top and bottom of the tank.

(d) What is the value of $k_L a$?

(e) If the cell concentration is 16 g l^{-1}, what is the specific oxygen demand?

(f) Industrial fermentation vessels are rated for operation at elevated pressures so they can withstand steam sterilisation. Accordingly, the fermenter used for ustilagic acid production can be operated safely at a maximum pressure of 2.7 atma. Assuming that respiration by *U. zeae* and the value of $k_L a$ are relatively insensitive to pressure, what maximum cell concentration can be supported by oxygen transfer in the fermenter after the pressure is raised?

10.11 Dynamic $k_L a$ measurement

The simple dynamic method is used to measure $k_L a$ in a fermenter operated at 30°C and 1 atm pressure. Data for the dissolved oxygen concentration as a function of time during the reoxygenation step are as follows.

Time (s)	C_{AL} (% air saturation)
10	43.5
15	53.5
20	60.0
30	67.5
40	70.5
50	72.0
70	73.0
100	73.5
130	73.5

(a) Calculate the value of $k_L a$.

(b) What additional experiments are required to check the reliability of this $k_L a$ result?

10.12 $k_L a$ measurement using the dynamic pressure method

The dynamic pressure method is applied for measurement of $k_L a$ in a 3000-l stirred fermenter containing a suspension culture of *Micrococcus glutamicus*. The stirrer is operated at 60 rpm and the gas flow rate is fixed at 800 l min^{-1}. The following dissolved oxygen concentrations are measured using a polarographic dissolved oxygen electrode after a step increase in fermenter pressure.

Time (s)	C_{AL} (% air saturation)
6	50.0
10	56.1
25	63.0
40	64.7

The steady-state dissolved oxygen tension at the end of the dynamic response is 66% air saturation.

(a) Estimate the value of $k_L a$.

(b) An error is made determining the steady-state oxygen level, which is taken as 70% instead of 66% air saturation. What effect does this 6% error in $\overline{C}_{AL}$ have on the result for $k_L a$?

(c) At the end of the $k_L a$ experiment, the electrode response time is measured by observing the output after a step change in dissolved oxygen tension from 0 to 100% air saturation. The stirrer speeds tested are 40, 50, and 60 rpm. Figure 10P12.1 at the bottom of page shows a chart recording of the results at 60 rpm; the results at 50 rpm are not significantly different. From this information, how much confidence do you have in the $k_L a$ measurements? Explain your answer.

10.13 Surface versus bubble aeration

Hematopoietic cells used in cancer treatment are cultured at 37°C in an 8.5-cm diameter bioreactor with working volume 500 ml. The culture fluid is mixed using a stirrer speed of 30 rpm. The reactor is operated at ambient pressure.

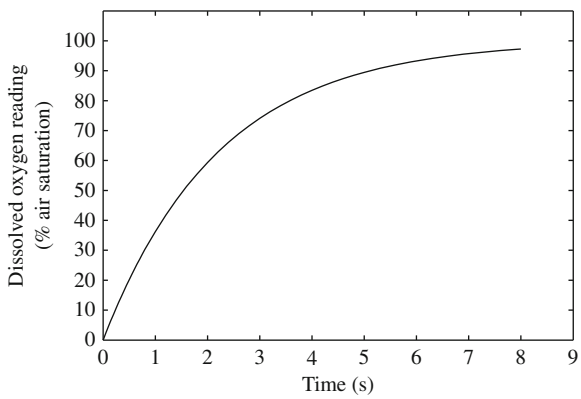

FIGURE 10P12.1 Chart recording of the electrode response at 60 rpm to a step change in dissolved oxygen tension.

(a) The dissolved oxygen tension is controlled at 50% air saturation using surface aeration only. A 50:20:30 mixture of air, oxygen, and nitrogen is passed at a fixed flow rate through the headspace. The specific oxygen uptake rate for hematopoietic cells is 7.7×10^{-12} g cell^{-1} h^{-1} and the cell concentration is 1.1×10^{9} cells l^{-1}. Estimate the value of $k_L a$ for surface aeration.

(b) Instead of surface aeration, the bioreactor is sparged gently with air. When the dissolved oxygen tension is maintained at the critical level of 8% air saturation, the cell concentration is 3.9×10^{9} cells l^{-1}. What is the $k_L a$ for bubble aeration?

(c) Surface aeration is preferred for this shear-sensitive culture, but the surface $k_L a$ needs improvement. For the gassing conditions applied in (a), estimate the vessel diameter required for surface aeration to achieve the same $k_L a$ obtained with sparging. What are your assumptions?

10.14 Shake-flask aeration

A mixed culture of heterotrophic microorganisms isolated from the Roman baths at Bath is prepared for bioleaching of manganese ore. One hundred ml of molasses medium is used in 300-ml flasks with 4-cm-long silicone sponge stoppers. The width of the flask opening is 3.2 cm. The cultures are incubated at 30°C on an orbital shaker operated at 80 rpm.

(a) With the flask closure removed, $k_L a$ for gas–liquid mass transfer is estimated using the dynamic method. During the reoxygenation step, the dissolved oxygen tension measured using a small, rapid-response electrode is 65% air saturation after 5 s and 75% after 30 s. The steady-state oxygen tension is 90% air saturation. What is the resistance to oxygen transfer in the flask? What are your assumptions?

(b) An expression for the mass transfer coefficient K_c for the flask closure is:

$$K_c = \frac{\mathscr{D}_e A_c}{L_c V_G}$$

where $\mathscr{D}_e$ is the effective diffusion coefficient of oxygen in the closure material, A_c is the cross-sectional area of the closure, L_c is the closure length, and V_G is the volume of gas in the flask. If $\mathscr{D}_e$ for silicone sponge is 20.8 cm^2 s^{-1}, what resistance to oxygen transfer is provided by the flask closure?

(c) What proportion of the total resistance to oxygen transfer does the flask closure represent?

(d) It is decided to improve the rate of gas–liquid oxygen transfer so that the resistance to oxygen transfer within the flask is approximately equal to that of the flask closure. A study of the dependence of $k_L a$ on shake-flask operating parameters yields the relationship:

$$k_L a \propto N^{1.2} \left(\frac{V_F}{V_L}\right)^{0.85}$$

where N is the shaker speed in rpm, V_F is the flask size in ml, and V_L is the liquid volume in ml. If the shaker speed can be increased to a maximum of 150 rpm:

(i) What size flask is needed if the culture volume remains at 100 ml?

(ii) If 300-ml flasks are the only shake flasks available, what culture volume should be used?

References

[1] R.E. Treybal, Mass-Transfer Operations, third ed., McGraw-Hill, 1980.
[2] Perry's Chemical Engineers' Handbook, eighth ed., McGraw-Hill, 2008.
[3] T.K. Sherwood, R.L. Pigford, C.R. Wilke, Mass Transfer, McGraw-Hill, 1975.
[4] J.M. Coulson, J.F. Richardson, J.R. Backhurst, J.H. Harker, Coulson and Richardson's Chemical Engineering, vol. 1, sixth ed., Butterworth-Heinemann, 1999 (Chapters 10 and 12).
[5] M.J. Johnson, Metabolism of penicillin-producing molds, Ann. N.Y. Acad. Sci. 48 (1946) 57–66.
[6] C.E. Clifton, A comparison of the metabolic activities of *Aerobacter aerogenes, Eberthella typhi* and *Escherichia coli*, J. Bacteriol. 33 (1937) 145–162.
[7] G.C. Paul, M.A. Priede, C.R. Thomas, Relationship between morphology and citric acid production in submerged *Aspergillus niger* fermentations, Biochem. Eng. J. 3 (1999) 121–129.
[8] O. Rahn, G.L. Richardson, Oxygen demand and oxygen supply, J. Bacteriol. 41 (1941) 225–249.
[9] P. Gikas, A.G. Livingston, Use of specific ATP concentration and specific oxygen uptake rate to determine parameters of a structured model of biomass growth, Enzyme Microb. Technol. 22 (1998) 500–510.
[10] E.B. Chain, G. Gualandi, G. Morisi, Aeration studies. IV. Aeration conditions in 3000-liter submerged fermentations with various microorganisms, Biotechnol. Bioeng. 8 (1966) 595–619.
[11] A.H.E. Bijkerk, R.J. Hall, A mechanistic model of the aerobic growth of *Saccharomyces cerevisiae*, Biotechnol. Bioeng. 19 (1977) 267–296.
[12] A.L. Jensen, J.S. Schultz, P. Shu, Scale-up of antibiotic fermentations by control of oxygen utilization, Biotechnol. Bioeng. 8 (1966) 525–537.
[13] K. Ozergin-Ulgen, F. Mavituna, Oxygen transfer and uptake in *Streptomyces coelicolor* A3(2) culture in a batch bioreactor, J. Chem. Technol. Biotechnol. 73 (1998) 243–250.
[14] W.H. Bartholomew, E.O. Karow, M.R. Sfat, R.H. Wilhelm, Oxygen transfer and agitation in submerged fermentations, Ind. Eng. Chem. 42 (1950) 1801–1809.
[15] A. Pinches, L.J. Pallent, Rate and yield relationships in the production of xanthan gum by batch fermentations using complex and chemically defined growth media, Biotechnol. Bioeng. 28 (1986) 1484–1496.
[16] P.A. Bond, M.W. Fowler, A.H. Scragg, Growth of *Catharanthus roseus* cell suspensions in bioreactors: on-line analysis of oxygen and carbon dioxide levels in inlet and outlet gas streams, Biotechnol. Lett. 10 (1988) 713–718.
[17] A. Kato, S. Nagai, Energetics of tobacco cells, *Nicotiana tabacum* L., growing on sucrose medium, Eur. J. Appl. Microbiol. Biotechnol. 7 (1979) 219–225.
[18] P. Ducommun, P.-A. Ruffieux, M.-P. Furter, I. Marison, U. von Stockar, A new method for on-line measurement of the volumetric oxygen uptake rate in membrane aerated animal cell cultures, J. Biotechnol. 78 (2000) 139–147.
[19] S. Tatiraju, M. Soroush, R. Mutharasan, Multi-rate nonlinear state and parameter estimation in a bioreactor, Biotechnol. Bioeng. 63 (1999) 22–32.
[20] S.P.S. Andrew, Gas–liquid mass transfer in microbiological reactors, Trans. IChemE 60 (1982) 3–13.
[21] J.J. Heijnen, K. van't Riet, A.J. Wolthuis, Influence of very small bubbles on the dynamic $k_L A$ measurement in viscous gas–liquid systems, Biotechnol. Bioeng. 22 (1980) 1945–1956.
[22] K. van't Riet, Review of measuring methods and results in nonviscous gas–liquid mass transfer in stirred vessels, Ind. Eng. Chem. Process Des. Dev. 18 (1979) 357–364.
[23] A. Ogut, R.T. Hatch, Oxygen transfer into Newtonian and non-Newtonian fluids in mechanically agitated vessels, Can. J. Chem. Eng. 66 (1988) 79–85.
[24] Y. Kawase, M. Moo-Young, The effect of antifoam agents on mass transfer in bioreactors, Bioprocess Eng. 5 (1990) 169–173.
[25] A. Prins, K. van't Riet, Proteins and surface effects in fermentation: foam, antifoam and mass transfer, Trends Biotechnol. 5 (1987) 296–301.
[26] International Critical Tables (1926–1930) McGraw-Hill; first electronic ed., International Critical Tables of Numerical Data, Physics, Chemistry and Technology (2003), Knovel.
[27] Y.H. Lee, G.T. Tsao, Dissolved oxygen electrodes, Adv. Biochem. Eng. 13 (1979) 35–86.
[28] V. Linek, J. Sinkule, V. Vacek, Dissolved oxygen probes, in: M. Moo-Young (Ed.), Comprehensive Biotechnology, vol. 4, Pergamon Press, 1985, pp. 363–394.

[29] G.A. Truesdale, A.L. Downing, G.F. Lowden, The solubility of oxygen in pure water and sea-water, J. Appl. Chem. 5 (1955) 53–62.
[30] G. Quicker, A. Schumpe, B. König, W.-D. Deckwer, Comparison of measured and calculated oxygen solubilities in fermentation media, Biotechnol. Bioeng. 23 (1981) 635–650.
[31] P.R. Gogate, A.B. Pandit, Survey of measurement techniques for gas–liquid mass transfer coefficient in bioreactors, Biochem. Eng. J. 4 (1999) 7–15.
[32] M. Sobotka, A. Prokop, I.J. Dunn, A. Einsele, Review of methods for the measurement of oxygen transfer in microbial systems, Ann. Rep. Ferm. Proc. 5 (1982) 127–210.
[33] J.D. Brooks, D.G. Maclennan, J.P. Barford, R.J. Hall, Design of laboratory continuous-culture equipment for accurate gaseous metabolism measurements, Biotechnol. Bioeng. 24 (1982) 847–856.
[34] V. Linek, V. Vacek, Oxygen electrode response lag induced by liquid film resistance against oxygen transfer, Biotechnol. Bioeng. 18 (1976) 1537–1555.
[35] N.D.P. Dang, D.A. Karrer, I.J. Dunn, Oxygen transfer coefficients by dynamic model moment analysis, Biotechnol. Bioeng. 19 (1977) 853–865.
[36] M. Nocentini, Mass transfer in gas–liquid, multiple-impeller stirred vessels, Trans. IChemE 68 (1990) 287–294.
[37] V. Linek, V. Vacek, P. Beneš, A critical review and experimental verification of the correct use of the dynamic method for the determination of oxygen transfer in aerated agitated vessels to water, electrolyte solutions and viscous liquids, Chem. Eng. J. 34 (1987) 11–34.
[38] V. Linek, P. Beneš, V. Vacek, Dynamic pressure method for k_La measurement in large-scale bioreactors, Biotechnol. Bioeng. 33 (1989) 1406–1412.
[39] V. Linek, T. Moucha, M. Doušová, J. Sinkule, Measurement of k_La by dynamic pressure method in pilot-plant fermentor, Biotechnol. Bioeng. 43 (1994) 477–482.
[40] N.M.G. Oosterhuis, N.W.F. Kossen, Oxygen transfer in a production scale bioreactor, Chem. Eng. Res. Des. 61 (1983) 308–312.
[41] S. Shioya, I.J. Dunn, Model comparisons for dynamic k_La measurements with incompletely mixed phases, Chem. Eng. Commun. 3 (1979) 41–52.
[42] K. Petera, P. Ditl, Effect of pressure profile on evaluation of volumetric mass transfer coefficient in k_La bioreactors, Biochem. Eng. J. 5 (2000) 23–27.
[43] R.E. Spier, B. Griffiths, An examination of the data and concepts germane to the oxygenation of cultured animal cells, Develop. Biol. Standard. 55 (1984) 81–92.

Suggestions for Further Reading

Mass Transfer Theory

See also references 1, 3, and 4.

McCabe, W. L., Smith, J. C., & Harriott, P. (2005). *Unit Operations of Chemical Engineering* (7th ed., Chapter 17). McGraw-Hill.

Oxygen Transfer in Fermenters

van't Riet, K. (1983). Mass transfer in fermentation. *Trends Biotechnol.*, *1*, 113–119.

Measurement of $\mathbf{k_La}$ *and* $\mathbf{q_O}$

See also references 31–42.

Linek, V., Sinkule, J., & Beneš, P. (1991). Critical assessment of gassing-in methods for measuring k_La in fermentors. *Biotechnol. Bioeng.*, *38*, 323–330.
Pouliot, K., Thibault, J., Garnier, A., & Acuña Leiva, G. (2000). K_La evaluation during the course of fermentation using data reconciliation techniques. *Bioprocess Eng.*, *23*, 565–573.
Ruffieux, P.-A., von Stockar, U., & Marison, I. W. (1998). Measurement of volumetric (OUR) and determination of specific (qO_2) oxygen uptake rates in animal cell cultures. *J. Biotechnol.*, *63*, 85–95.
Tobajas, M., & García-Calvo, E. (2000). Comparison of experimental methods for determination of the volumetric mass transfer coefficient in fermentation processes. *Heat Mass Transfer*, *36*, 201–207.

Oxygen Transfer in Shake Flasks

Maier, U., & Büchs, J. (2001). Characterisation of the gas–liquid mass transfer in shaking bioreactors. *Biochem. Eng. J.*, *7*, 99–106.

Mrotzek, C., Anderlei, T., Henzler, H.-J., & Büchs, J. (2001). Mass transfer resistance of sterile plugs in shaking bioreactors. *Biochem. Eng. J.*, *7*, 107–112.

Schultz, J. S. (1964). Cotton closure as an aeration barrier in shaken flask fermentations. *Appl. Microbiol.*, *12*, 305–310.

van Suijdam, J. C., Kossen, N.W.F., & Joha, A. C. (1978). Model for oxygen transfer in a shake flask. *Biotechnol. Bioeng.*, *20*, 1695–1709.

CHAPTER

11

Unit Operations

Bioprocesses treat raw materials and generate useful products. Individual operations or steps in the process that alter the properties of materials are called unit operations. Although the specific objectives of bioprocesses vary from factory to factory, each processing scheme can be viewed as a series of component operations that appear again and again in different systems. For example, most bioprocesses involve one or more of the following unit operations: adsorption, centrifugation, chromatography, crystallisation, dialysis, distillation, drying, evaporation, filtration, flocculation, flotation, homogenisation, humidification, microfiltration, milling, precipitation, sedimentation, solvent extraction, and ultrafiltration.

As an illustration, the sequence of unit operations used for the manufacture of particular enzymes is shown in the flow sheet of Figure 11.1. Although the same operations are involved in other processes, the order in which they are carried out, the conditions used, and the materials handled account for the differences in final results. However, the engineering principles for design of unit operations are independent of specific industries or applications.

In a typical fermentation process, raw materials are altered most significantly by the reactions occurring in the fermenter. However physical changes before and after fermentation are also important to prepare the substrates for reaction and to extract and purify the desired product from the culture broth. The term 'unit operation' usually refers to processes that cause physical modifications to materials, such as a change of phase or component concentration. Chemical or biochemical transformations are the subject of reaction engineering, which is considered in detail in Chapters 12 through 14.

11.1 OVERVIEW OF DOWNSTREAM PROCESSING

In fermentation broths, the desired product is present within a complex mixture of many components. Any treatment of the culture broth after fermentation to concentrate and purify the product is known as *downstream processing*. In most cases, downstream processing requires only physical modification of the broth material rather than further

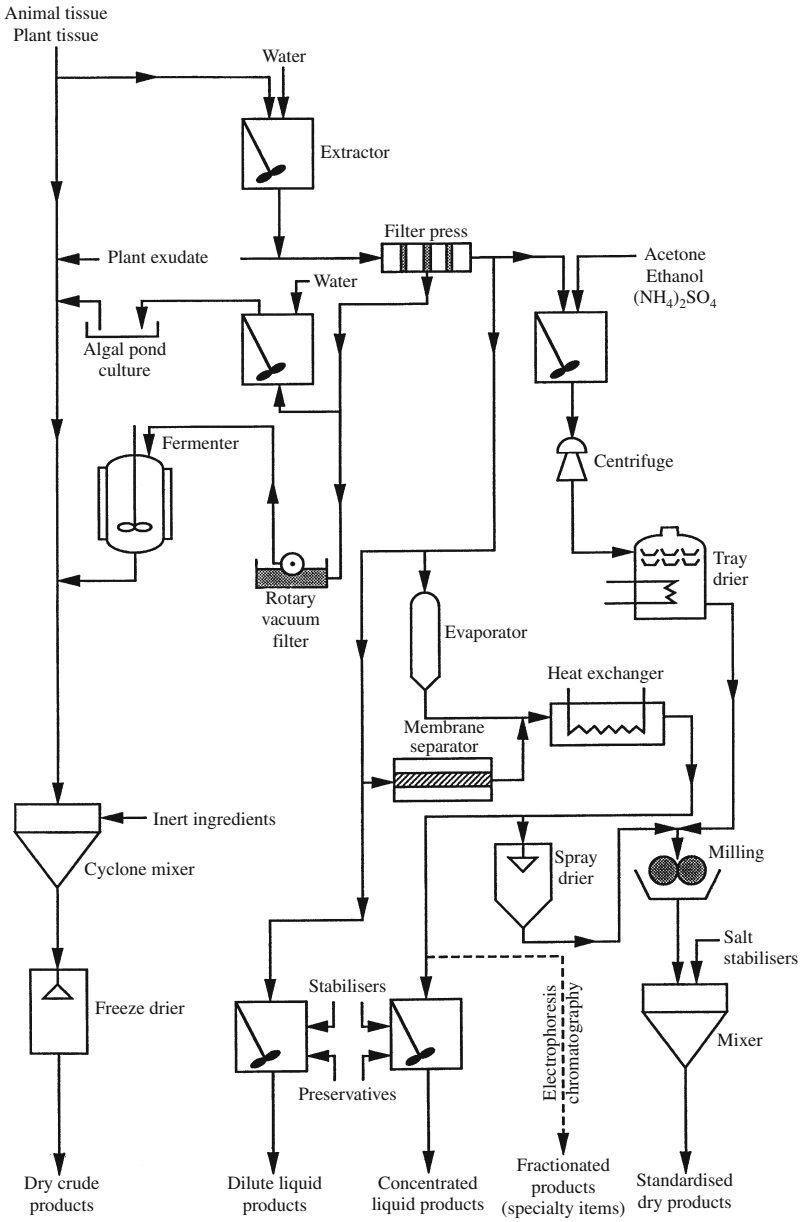

FIGURE 11.1 Typical unit operations used in the manufacture of enzymes. *From B. Atkinson, and F. Mavituna, 1991,* Biochemical Engineering and Biotechnology Handbook, *2nd ed., Macmillan, Basingstoke; and W.T. Faith, C.E. Neubeck, and E.T. Reese, 1971, Production and applications of enzymes.* Adv. Biochem. Eng. *1, 77–111.*

chemical or biochemical transformation. Nevertheless, there are several reasons why downstream processing is often technically very challenging.

- *Fermentation products are formed in dilute solution*. Water is the main component of cell culture media and, therefore, of harvested fermentation broth. Many other components are also present in the broth mixture, providing a wide range of contaminating

substances that must be removed to isolate the desired product. In general, purification from dilute solutions involves more recovery steps and higher costs than when the product is available in a concentrated form with fewer impurities.

- *Biological products are labile*. Products produced in fermentations are sensitive to temperature and can be degraded by exposure to solvents, strong acids and bases, and high salt concentrations. This restricts the range of downstream processing operations that can be applied for product recovery.
- *Harvested fermentation broths are susceptible to contamination*. Typically, once the broth is removed from the controlled environment of the fermenter, aseptic conditions are no longer maintained and the material is subject to degradation by the activity of contaminating organisms. Unless downstream processing occurs rapidly and without delay, product quality can deteriorate significantly.

Although each recovery scheme will be different, the sequence of steps in downstream processing can be generalised depending on whether the biomass itself is the desired product (e.g., bakers' yeast), whether the product is contained within the cells (e.g., enzymes and recombinant proteins), or whether the product accumulates outside the cells in the fermentation liquor (e.g., ethanol, antibiotics, and monoclonal antibodies). General schemes for these three types of downstream processing operation are represented in Figure 11.2 and involve the following major steps.

1. *Cell removal*. A common first step in product recovery is the removal of cells from the fermentation liquor. If the cells are the product, little or no further downstream processing is required. If the product is contained within the biomass, harvesting the cells from the large volume of fermentation liquid removes many of the impurities present and concentrates the product substantially. Removal of the cells can also assist the recovery of products from the liquid phase. Filtration, microfiltration, and centrifugation are typical unit operations for cell removal.
2. *Cell disruption and cell debris removal*. These downstream processing steps are required when the product is located inside the cells. Unit operations such as high-pressure homogenisation are used to break open the cells and release their contents for subsequent purification. The cell debris generated during cell disruption is separated from the product by filtration, microfiltration, or centrifugation.
3. *Primary isolation*. A wide variety of techniques is available for primary isolation of fermentation products from cell homogenate or cell-free broth. The methods used depend on the physical and chemical properties of the product and surrounding material. The aim of primary isolation is to remove components with properties that are substantially different from those of the product. Typically, processes for primary isolation are relatively nonselective; however significant increases in product quality and concentration can be accomplished. Unit operations such as solvent extraction, aqueous two-phase liquid extraction, adsorption, precipitation, and ultrafiltration are used for primary isolation.

   There are special challenges associated with the design and operation of primary isolation processes in large-scale production systems. When the product is extracellular, large volumes of culture liquid must be treated at this stage. As intermediate storage of this liquid is impractical and disposal expensive, the processes and equipment used for

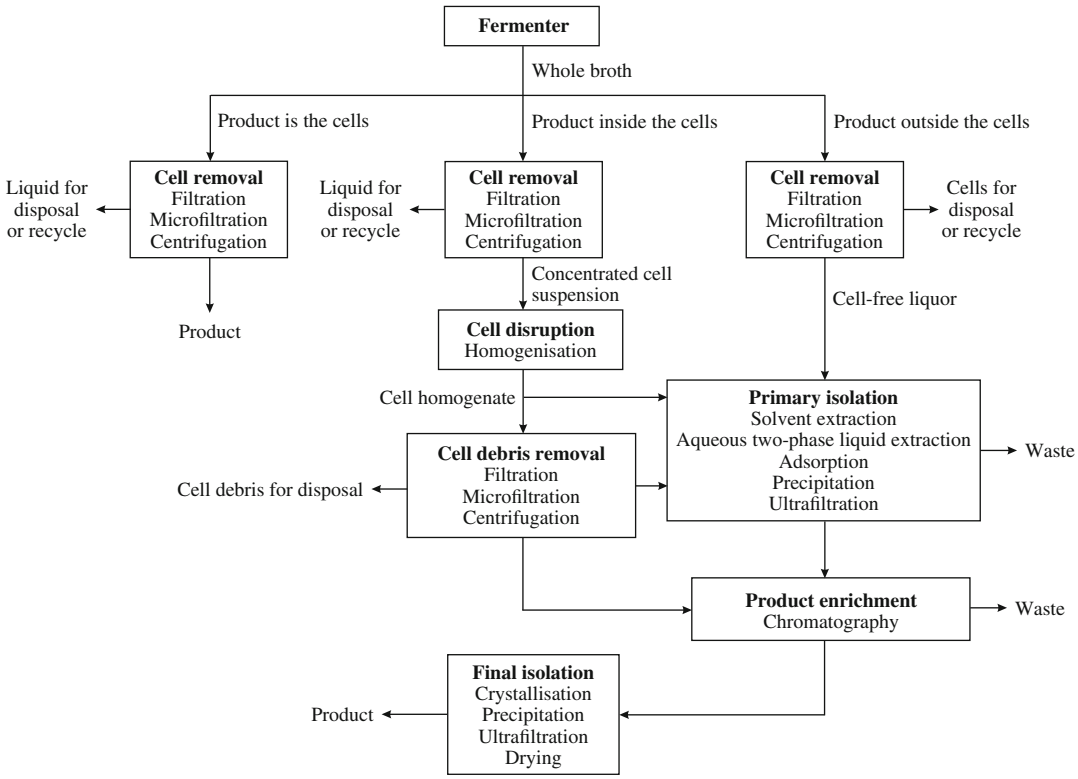

FIGURE 11.2 Generalised downstream processing schemes for cells as product, products located inside the cells, and products located outside the cells in the fermentation liquor.

primary isolation must be robust and reliable to minimise broth spoilage and product deterioration in the event of equipment breakdown or process malfunction. It is essential that the operations used for primary isolation be able to treat the fermentation liquor at the rate it is generated. The large liquid volumes involved also mean that low-energy, low-cost processes are required. A desirable feature of primary isolation processes is that a significant reduction in liquid volume is achieved. This reduces the equipment size and operating costs associated with subsequent recovery steps.

4. *Product enrichment*. Processes for product enrichment are highly selective and are designed to separate the product from impurities with properties close to those of the product. Chromatography is a typical unit operation used at this stage of product resolution.
5. *Final isolation*. The form of the product and final purity required vary considerably depending on the product application. Ultrafiltration for liquid products, and crystallisation followed by centrifugation or filtration and drying for solid products, are typical operations used for final processing of high-quality materials such as pharmaceuticals.

TABLE 11.1 Typical Profile of Product Quality during Downstream Processing

Step	Typical Unit Operation	Product Concentration (g l^{-1})	Product Quality (%)
Harvest broth	–	0.1–5	0.1–1
Cell removal	Filtration	1–5	0.2–2
Primary isolation	Extraction	5–50	1–10
Product enrichment	Chromatography	50–200	50–80
Final isolation	Crystallisation	50–200	90–100

Adapted from P.A. Belter, E.L. Cussler, and W.-S. Hu, 1988, Bioseparations: Downstream Processing For Biotechnology, *John Wiley, New York.*

A typical profile of product concentration and quality through the various stages of downstream processing is given in Table 11.1.

The performance of downstream processing operations can be characterised quantitatively using two parameters, the *concentration factor* δ and the *separation factor* α. These parameters are defined as:

$$\delta = \frac{\text{concentration of product after treatment}}{\text{concentration of product before treatment}} \tag{11.1}$$

and

$$\alpha = \frac{\left(\dfrac{\text{concentration of product}}{\text{concentration of contaminant}}\right)_{\text{after treatment}}}{\left(\dfrac{\text{concentration of product}}{\text{concentration of contaminant}}\right)_{\text{before treatment}}} \tag{11.2}$$

A concentration factor of >1 indicates that the product is enriched during the treatment process. The separation factor differs from the concentration factor by representing the change in product concentration relative to that of some key contaminating compound. Individual downstream processing operations may achieve high concentration factors even though separation of the desired product from a particular contaminant remains relatively poor. On the other hand, highly selective recovery methods give high values of α, but this may be accompanied by only a modest increase in product concentration.

Downstream processing can account for a substantial proportion of the total production cost of a fermentation product. For example, the ratio of fermentation cost to product recovery cost is approximately 60:40 for antibiotics such as penicillin. For newer antibiotics this ratio is reversed; product recovery is more costly than fermentation. Many modern products of biotechnology such as recombinant proteins and monoclonal antibodies require expensive downstream processing that can account for 80 to 90% of the total process cost. Starting product levels before recovery have a strong influence on downstream costs; purification is more expensive when the initial concentration of product in the biomass or fermentation broth is low. As illustrated in Figure 11.3 for several products of bioprocessing, the higher the starting concentration, the cheaper is the final material.

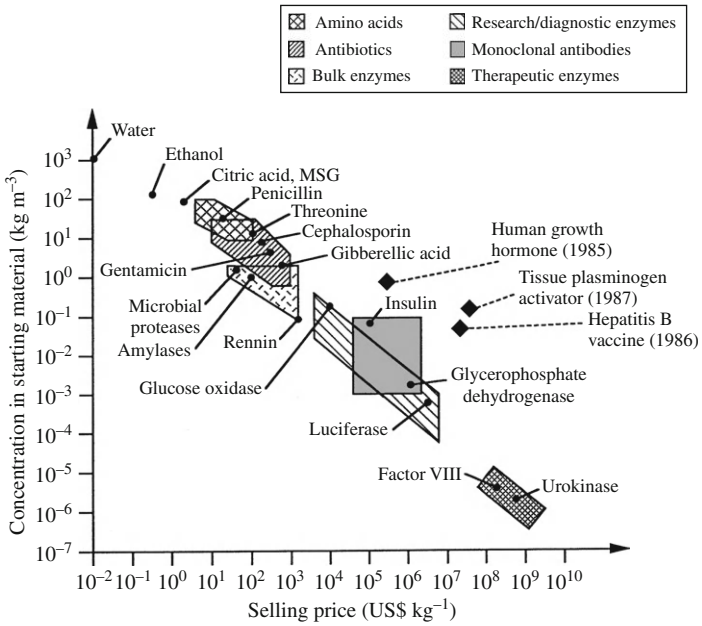

FIGURE 11.3 Relationship between selling price and concentration before downstream recovery for several products of bioprocessing. *From J.L. Dwyer, 1984, Scaling up bioproduct separation with high performance liquid chromatography.* Bio/Technology *2, 957–964; and J. van Brunt, 1988,* How big is big enough? Bio/Technology *6, 479–485.*

Because each downstream processing step involves some loss of product, total losses can be substantial for multistep procedures. For example, if 80% of the product is retained at each purification step, after a six-step process only $(0.8)^6$ or about 26% of the initial product remains. If the starting concentration is very low, more recovery stages are required with higher attendant losses and costs. This situation can be improved either by enhancing the synthesis of product during fermentation or by developing better downstream processing techniques that minimise product loss.

There is an extensive literature on downstream processing, much of it dealing with recent advances. To cover thoroughly all unit operations used in bioprocessing is beyond the scope of this book. Rather than attempt such treatment, this chapter considers the engineering principles of a selection of unit operations commonly applied for recovery of fermentation products. Information about other unit operations can be found in the references listed at the end of the chapter.

11.2 OVERVIEW OF CELL REMOVAL OPERATIONS

One of the first steps in downstream processing is the removal of cells from the culture liquid. This is the case if the cells themselves are the product, or if the product is an intra- or extracellular metabolite. Although whole broth processing without cell removal is possible, it is not commonly pursued.

The major process options for cell removal are *filtration*, *microfiltration*, and *centrifugation*. Broadly, separations using filtration and microfiltration are based on particle size, whereas centrifugation relies on particle density. However, other factors such as the shape,

compressibility, and surface charge of the cells and the density and viscosity of the broth also exert a considerable influence on the performance of these operations. Cell removal from microbial fermentation broths can be technically very challenging because of the small size, low density, and gelatinous nature of many industrial microorganisms. In contrast, due mainly to the low numbers of cells generated, cell removal after mammalian cell culture is comparatively straightforward.

Prior to filtration or centrifugation, it may be necessary to pretreat or *precondition* the fermentation broth to improve the efficiency of cell separation. Heating is used to denature proteins and enhance the filterability of mycelial broths, such as in penicillin production. Pretreatments that reduce the viscosity of the broth are beneficial for both filtration and centrifugation. Alternatively, electrolytes or polymeric flocculants may be added to promote aggregation of cells and colloids into larger, denser particles that are easier to filter or centrifuge. Filter aids, which are solid particles used to increase the speed of filtration, are often applied to fermentation broths prior to filtering (Section 11.3.1). Changing the duration or conditions of the fermentation can sometimes assist subsequent cell removal by modifying the composition and viscosity of the medium and properties of the cells.

The general features of unit operations used for cell removal are described here.

- *Filtration*. In conventional filtration, cell solids are retained on a filter cloth to form a porous cake while liquid filtrate passes through the cloth. The process generates a relatively dry, friable cake of packed cells; however, the liquid filtrate usually contains a small proportion of solids that escape through the filter cloth. This is reflected in the filtrate clarity, which generally decreases if filter aids are used to improve the rate of filtration. Large-scale filtration is difficult to perform under sterile conditions. Filtration is not a practical option for cell removal if filter aid is required to achieve an acceptable filtration rate and the product is intracellular or the cells themselves are the fermentation product. This is because contamination of the filtered cells with foreign particles is inappropriate unless the cells are waste by-products; the presence of filter aid can also cause equipment problems if the cells must be disrupted mechanically to release intracellular material. Microfiltration and centrifugation are better options for cell removal under these circumstances.
- *Microfiltration*. Microfiltration uses microporous membranes and cross-flow filtration methods to recover the cells as a fluid concentrate. The maximum cell concentrations generated range from about 10% w/v for gelatinous solids up to 60 to 70% w/v for more rigid particles. It is generally not necessary to precondition broths treated using microfiltration techniques. Because filter aids are also not required, microfiltration is an attractive option for harvesting cells containing intracellular products or cells as product. Because cell recovery using microfiltration is typically close to 100%, the liquid filtrate or permeate produced by microfiltration is of much greater clarity than that generated by conventional filtration using filter aids. This is an advantage when the product is extracellular, as the filtrate contains minimal contaminating components. A potential disadvantage is that unacceptably high amounts of extracellular product may be entrained in the cell concentrate stream. Microfiltration can be carried out under sterile conditions. In many cases, microfiltration is less expensive than filtration or centrifugation, although exact cost comparisons depend on the particular process.

- *Centrifugation*. This can be an effective strategy for cell recovery when the cells are too small and difficult to filter using conventional filtration. In principle, centrifugation is suitable for recovery of cells as product and for preprocessing of both intracellular and extracellular components. Centrifugation of fermentation broths produces a thick, concentrated cell sludge or cream that contains more extracellular liquid than is produced in conventional filtration. The liquid supernatant may be either cloudy or clear depending on the operating conditions. The use of flocculants and other broth-conditioning agents improves the performance of centrifuges; however, the presence of these additives in either the cell concentrate or liquid discharge may be undesirable for particular products. Steam-sterilisable centrifuges are available for separations that must be carried out under aseptic conditions. Aerosol generation associated with the operation of high-speed centrifuges can create health and safety problems depending on the organism and products being separated. The equipment costs for centrifugation tend to be greater than for filtration and microfiltration.
- *Other operations*. Although filtration, microfiltration, and centrifugation account for the vast majority of cell separations in bioprocessing, other methods are also available. *Gravity settling* or *sedimentation* is suitable for cells that form aggregates or flocs of sufficient size and density to settle quickly under gravity. Polyvalent agents and polymers may be added to increase particle coagulation and improve the rate of sedimentation. Gravity settling is used typically in large-scale waste treatment processes for liquid clarification, and in beer brewing processes with flocculent strains of yeast. Another cell recovery process is *foam flotation*, which relies on the selective adsorption or attachment of cells to gas bubbles rising through liquid. Surfactants may be used to increase the number of cells associated with the bubbles. The cells are recovered by skimming the foam layers that collect on top of the liquid. The effectiveness of foam flotation has been reported for a range of different microorganisms [1].

Filtration and centrifugation operations are considered in greater detail in Sections 11.3 and 11.4. As one of a group of similar membrane processes, microfiltration is discussed further in Section 11.10. Decisions about which type of cell removal operation to use for a particular application are usually made after a considerable amount of experimental testing.

11.3 FILTRATION

In conventional filtration, solid particles are separated from a fluid−solid mixture by forcing the fluid through a *filter medium* or *filter cloth* that retains the particles. Solids are deposited on the filter and, as the deposit or *filter cake* increases in depth, pose a resistance to further filtration. Filtration can be performed using either vacuum or positive-pressure equipment. The pressure difference exerted across the filter to separate fluid from the solids is called the filtration *pressure drop*.

The ease of filtration depends on the properties of the solid and fluid. Filtration of crystalline, incompressible solids in low-viscosity liquids is relatively straightforward. In contrast, fermentation broths can be difficult to filter because of the small size and gelatinous nature of the cells and the viscous non-Newtonian behaviour of the broth. Most microbial

filter cakes are *compressible*, that is, the porosity of the cake declines as the pressure drop across the filter increases. This can be a major problem causing reduced filtration rates and product loss. Filtration of fermentation broths is carried out typically under nonaseptic conditions; therefore, the process must be efficient and reliable to avoid undue contamination and the degradation of labile products.

11.3.1 Filter Aids

Filter aids such as diatomaceous earth have found widespread use in the fermentation industry to improve the efficiency of filtration. Diatomaceous earth, also known as kieselguhr, is the fused skeletal remains of diatoms. Packed beds of granulated kieselguhr have very high porosity; as little as 15% of the total volume of packed kieselguhr is solid, the rest is empty space. Such high porosity facilitates liquid flow around the particles and improves the rate of filtration. Kieselguhr with average particle sizes of 10 to 25 μm are used with fermentation broths.

Filter aids are applied in two ways. As shown in Figure 11.4, filter aid can be used as a precoat on the filter medium to prevent blockage or 'blinding' of the filter by solids that

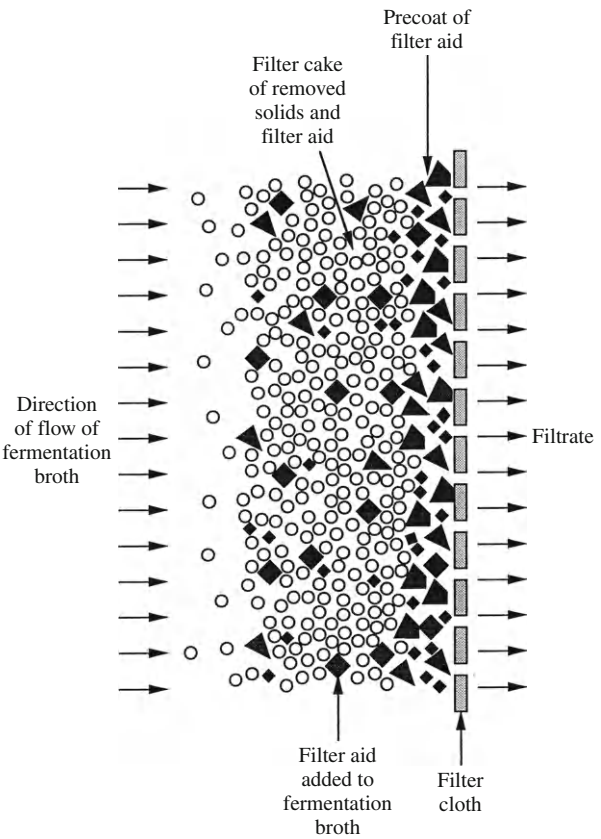

FIGURE 11.4 Use of filter aid in filtration of fermentation broth.

would otherwise wedge themselves into the pores of the cloth. Filter aid can also be added to the fermentation broth, typically at concentrations of 1 to 5% w/w, to increase the porosity of the cake as it forms. Filter aids add to the cost of filtration; the minimum quantity needed to achieve the desired result must be established experimentally. Kieselguhr absorbs liquid; therefore, if the fermentation product is in the liquid phase, some will be lost. Another disadvantage is that filtrate clarity is reduced when the rate of filtration is increased using filter aid. Disposal of waste cell material is more difficult if it contains kieselguhr; for example, biomass cannot be used as animal feed unless the filter aid is removed. Use of filter aids is not appropriate if the cells themselves are the product of the fermentation or when the cells require further processing after filtration for recovery of intracellular material.

11.3.2 Filtration Equipment

Plate filters are suitable for filtration of small fermentation batches; this type of filter gradually accumulates biomass and must be periodically opened and cleared of filter cake. Larger processes require continuous filters. *Rotary drum vacuum filters*, such as that shown in Figure 11.5, are the most widely used filtration devices in the fermentation

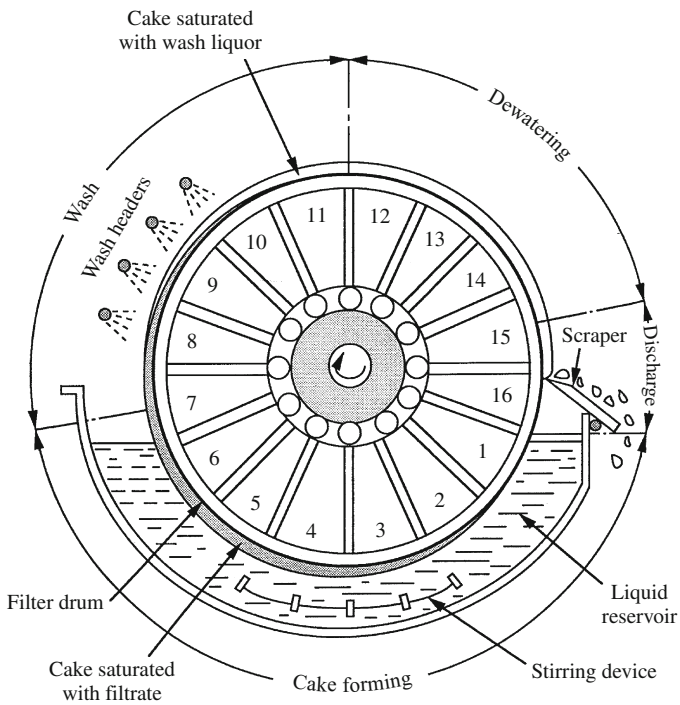

FIGURE 11.5 Continuous rotary drum vacuum filter.
From G.G. Brown, A.S. Foust, D.L. Katz, R. Schneidewind, R.R. White, W.P. Wood, G.M. Brown, L.E. Brownell, J.J. Martin, G.B. Williams, J.T. Banchero, and J.L. York, 1950, Unit Operations, *John Wiley, New York.*

industry. A horizontal drum 0.5 to 3 m in diameter is covered with filter cloth and rotated slowly at 0.1 to 2 rpm. The cloth is partially immersed in an agitated reservoir containing material to be filtered. As a section of drum enters the liquid, a vacuum is applied from the interior of the drum. A cake forms on the face of the cloth while liquid is drawn through internal pipes to a collection tank. As the drum rotates out of the reservoir, the surface of the filter is sprayed with wash liquid, which is drawn through the cloth and collected in a separate holding tank. After washing, the cake is dewatered by continued application of the vacuum. The vacuum is turned off as the drum reaches the discharge zone where the cake is removed by means of a scraper, knife, or strings. Air pressure may be applied at this stage to help dislodge the filter cake from the cloth. After the cake is removed, the drum reenters the reservoir for another filtration cycle.

11.3.3 Filtration Theory

Filtration theory is used to estimate the rate of filtration. For a given pressure drop across the filter, the rate of filtration is greatest just as filtering begins. This is because the resistance to filtration is at a minimum when there are no deposited solids. The orientation of particles in the initial cake deposit is very important and can influence significantly the structure and permeability of the whole filter bed. Excessive pressure drops and high initial rates of filtration cause plugging of the filter cloth and a very high subsequent resistance to flow. Flow resistance due to the filter cloth can be considered constant if particles do not penetrate the material; however, the resistance due to the cake increases with cake thickness.

The rate of filtration is usually measured as the rate at which liquid filtrate is collected. The filtration rate depends on the area of the filter cloth, the viscosity of the fluid, the pressure difference across the filter, and the resistance to filtration offered by the cloth and deposited solids. At any instant during filtration, the rate of filtration is given by the equation:

$$\frac{1}{A}\frac{\mathrm{d}V_\mathrm{f}}{\mathrm{d}t} = \frac{\Delta p}{\mu_\mathrm{f}\left[\alpha\left(\dfrac{M_\mathrm{c}}{A}\right) + R_\mathrm{m}\right]} \tag{11.3}$$

where A is the filter area, V_f is the volume of filtrate, t is the filtration time, Δp is the pressure drop across the filter, μ_f is the filtrate viscosity, M_c is the total mass of solids in the cake, α is the average *specific cake resistance*, and R_m is the *filter medium resistance*. R_m includes the effect of the filter cloth and any particles wedged in it during the initial stages of filtration. α has dimensions LM^{-1}; R_m has dimensions L^{-1}. $\mathrm{d}V_\mathrm{f}/\mathrm{d}t$ is the filtrate flow rate or *volumetric rate of filtration*. The capital cost of the filter depends on A; the bigger the area required to achieve a given filtration rate, the larger are the equipment and related investment. α is a measure of the resistance of the filter cake to flow; its value depends on the shape and size of the particles, the size of the interstitial spaces between them, and the mechanical stability of the cake. Resistance due to the filter medium is often negligible compared with the cake resistance, which is represented by the term $\alpha(M_\mathrm{c}/A)$.

If the filter cake is incompressible, the specific cake resistance α does not vary with the pressure drop across the filter. However, cakes from fermentation broths are seldom

incompressible; as cell cakes compress with increasing Δp, filtration rates decline. For a compressible cake, α can be related to Δp empirically as follows:

$$\alpha = \alpha'(\Delta p)^s \tag{11.4}$$

where s is the cake *compressibility* and α' is a constant dependent largely on the size and morphology of the particles in the cake. The value of s is zero for rigid incompressible solids; for highly compressible material s is close to unity. α is also related to the average properties of the particles in the cake as follows:

$$\alpha = \frac{K_v a^2 (1-\varepsilon)}{\varepsilon^3 \rho_p} \tag{11.5}$$

where K_v is a factor dependent on the shape of the particles, a is the particle specific surface area:

$$a = \frac{\text{surface area of a single particle}}{\text{volume of a single particle}} \tag{11.6}$$

ε is the *porosity* of the cake:

$$\varepsilon = \frac{\text{total volume of the cake} - \text{volume of solids in the cake}}{\text{total volume of the cake}} \tag{11.7}$$

and ρ_p is the density of the particles. For compressible cakes, both ε and K_v depend on the filtration pressure drop.

It is useful to consider methods for improving the rate of filtration. A number of strategies can be deduced from the relationship between the variables in Eq. (11.3).

- *Increase the filter area A*. When all other parameters remain constant, the rate of filtration is improved if A is increased. However, this requires installation of larger filtration equipment and greater capital cost.
- *Increase the filtration pressure drop* Δp. The problem with this approach for compressible cakes is that α increases with Δp as indicated in Eq. (11.4), and higher α results in lower filtration rates. In practice, pressure drops are usually kept below about 0.5 atm to minimise cake resistance. Improving the filtration rate by increasing the pressure drop can only be achieved by reducing s, the compressibility of the cake. Addition of filter aid to the broth may reduce s to some extent.
- *Reduce the cake mass* M_c. This is achieved in continuous rotary filtration by reducing the thickness of the cake deposited per revolution of the drum, and ensuring that the scraper leaves minimal cake residue on the filter cloth.
- *Reduce the liquid viscosity* μ_f. Material to be filtered is sometimes diluted if the starting viscosity is very high.
- *Reduce the specific cake resistance* α. From Eq. (11.5), possible methods of reducing α for compressible cakes are as follows:
  - *Increase the porosity* ε. Cake porosity usually decreases as cells are filtered. Application of filter aid reduces this effect.

- *Reduce the shape factor of the particles K_v*. In the case of mycelial broths, it may be possible to change the morphology of the cells by manipulating the fermentation conditions.
- *Reduce the specific surface area of the particles a*. Increasing the average size of the particles and minimising variations in particle size reduce the value of a. Changes in fermentation conditions and broth pretreatment are used to achieve these effects.

Integration of Eq. (11.3) allows us to calculate the time required to filter a given volume of material. Before carrying out the integration, let us substitute an expression for the mass of solids in the cake as a function of the filtrate volume:

$$M_c = c\,V_f \tag{11.8}$$

In Eq. (11.8), c is the mass of solids deposited per volume of filtrate; this term is related to the concentration of solids in the material to be filtered. Substituting Eq. (11.8) into Eq. (11.3), the expression for the rate of filtration becomes:

$$\frac{1}{A}\frac{dV_f}{dt} = \frac{\Delta p}{\mu_f\left[\alpha\left(\frac{cV_f}{A}\right) + R_m\right]} \tag{11.9}$$

Equation (11.9) can be interpreted according to the *general rate principle*, which equates the rate of a process to the ratio of the driving force and the resistance. As Δp is the driving force for filtration, the resistances offered by the filter cake and filter medium are represented by the terms summed together in the denominator of Eq. (11.9). The relative contributions of these two resistances can be estimated using the equations:

$$\text{Proportion of the total resistance due to the filter cake} = \frac{\alpha\left(\frac{cV_f}{A}\right)}{\alpha\left(\frac{cV_f}{A}\right) + R_m} \tag{11.10}$$

$$\text{Proportion of the total resistance due to the filter medium} = \frac{R_m}{\alpha\left(\frac{cV_f}{A}\right) + R_m} \tag{11.11}$$

A filter can be operated in two different ways. If the pressure drop across the filter is kept constant, the filtration rate will become progressively smaller as resistance due to the cake increases. Alternatively, in constant-rate filtration, the flow rate is maintained by gradually increasing the pressure drop. Filtrations are most commonly carried out at constant pressure. When this is the case, Eq. (11.9) can be integrated directly because V_f and t are the only variables: for a given filtration device and material to be filtered, each of the remaining parameters is constant.

It is convenient for integration to write Eq. (11.9) in its reciprocal form:

$$A\frac{dt}{dV_f} = \mu_f \alpha c \frac{V_f}{A\,\Delta p} + \frac{\mu_f R_m}{\Delta p} \tag{11.12}$$